4-2-2009

Characterization of PET samples processed in an RF oxygen discharge

Russell L. Rhoton

Characterization of PET Samples

Processed in an RF Oxygen Discharge

by

Russell L. Rhoton

Thesis

Submitted to the College of Technology
in partial fulfillment of the requirements
for the Degree of

Master of Science

in

Manufacturing Processing

Thesis Committee:

Erik Lokensgard, PhD. Chair

Mary L. Brake, PhD.

Pamela Speelman, PhD.

April 2, 2009

Ypsilanti, Michigan

ABSTRACT

A radio frequency plasma (13.56 MHz) was used to modify the surface of a poly (ethylene terepthalate) (PET) sample. The plasma was generated in a pure oxygen process atmosphere at pressures of 100 mTorr, and 2.0 Torr at output powers of 250 Watts and 500 Watts.

Optical emission spectroscopy (OES) was used to characterize the plasma/sample interaction. Spectra were measured from 250 nm to 900 nm during each of the processing sessions.

The spectra showed changes depending upon the pressure of the plasma. Molecules of OH and atomic oxygen were observed at low pressures (100 mTorr), whereas CO and atomic hydrogen were observed at high pressures (2.0 Torr).

The sessile drop method was used to determine the relative change in the wettability of the sample surface along a continuum from hydrophobic to hydrophilic.

The measured angles were compared to the initial readings (Figure 18) and showed a decrease of 40-50% in contact angle after treatment.

There was an observable change in the PET samples after processing; in particular, the surface was visibly degraded.

TABLE OF CONTENTS

Chapter 1 Introduction 1

Overview 1
Purpose and Objectives of the Study 3
Research Questions 4
Summary 5

Chapter 2 Review of Literature 6

Overview 6
Polymers 8
Plasma Processing 10
Diagnostics 13
Contact Angle 15
Summary 16

Chapter 3 Experimental Methodology 17

Overview 17
Materials and Methods 17
Processing System Design 17
Process Diagnostics 19
Contact Angle 21

Chapter 4 Experimental Results 22

Overview 22
Optical Emission Spectroscopy 22
Contact Angle 29
Visual Comparison of Samples 31

Chapter 5 Conclusions (Summary) and Suggestions for Further Work 33

Overview 33
Further Work 35

References 36

Appendix A Contact angle video captures 40

Appendix B Process Spectra 54

LIST OF FIGURES

Figure1. Poly(ethylene-terepthalate) monomer 9

Figure 2. PET Polymer chain. 9

Figure 3. Polyester Sheet Manufacturing Process (HIFI Industrial Films, UK) 10

Figure 4. Experimental Plasma Discharge System. 11

Figure 5. SpectraSense post processing screen. 15

Figure 6. Experimental Chamber Setup. 18

Figure 7. Spectrum Analyzer 1.6 software. 20

Figure 8. FTA Analysis software showing contact angle calculation screen. 21

Figure 9. Spectrum of process reactor prior to introduction of sample. 23

Figure 10. Spectrum showing increase in OH after processing (100 mTorr 500 Watts). 24

Figure 11. Spectrum showing increase in OH after processing (100 mTorr 500 Watts). 25

Figure 12. Comparison of OH and OI intensities during processing at different applied power. 26

Figure 13. Spectrum at high pressure/low power (2.0 Torr 250 Watts). 27

Figure 14. Spectrum at high pressure/high power (2.0 Torr 500 Watts). 27

Figure 15. Intensity of lines at 309 (OH) and 778 (OI) at different power levels. 28

Figure 16. Untreated contact angle. 29

Figure 17. Treated contact angle (250 m Torr / 500 Watts). 29

Figure 18. Contact Angle values of tested samples before and after processing. Each data point shown represents the average of three measurements 30

Figure 19. Capacitively Coupled Discharge Processing Conditions 31

Figure 20. Unprocessed PET Sample 32

Figure 21. Processed PET Sample 32

Figure A1. Contact angle of untreated PET sample. 41

Figure A2. Contact Angle 1 of PET Sample (100 mTorr / 250 Watts) 42

Figure A3. Contact Angle 2 of PET Sample (100 mTorr / 250 Watts) 43

Figure A4. Contact Angle 3 of PET Sample (100 mTorr / 250 Watts) 44

Figure A5. Contact Angle 1 of PET Sample (2.0 Torr / 250 Watts). 45

Figure A6. Contact Angle 2 of PET Sample (2.0 Torr / 250 Watts). 46

Figure A7. Contact Angle 3 of PET Sample (2.0 Torr / 250 Watts). 47

Figure A8. Contact Angle 1 of PET Sample (100 mTorr / 500 Watts). 48

Figure A9. Contact Angle 2 of PET Sample (100 mTorr / 500 Watts). 49

Figure A10. Contact Angle 3 of PET Sample (100 mTorr / 500 Watts). 50

Figure A11. Contact Angle 1 of PET Sample (2.0 Torr / 500 Watts). 51

Figure A12. Contact Angle 2 of PET Sample (2.0 Torr / 500 Watts). 52

Figure A13. Contact Angle 3 of PET Sample (2.0 Torr / 500 Watts). 53

Figure B1. Process Spectrum at 100 mTorr/250Watts (t=3 minutes)..... 55

Figure B2. Process Spectrum at 100 mTorr/250Watts (t=6 minutes)..... 56

Figure B3. Process Spectrum at 100 mTorr/250Watts (t=9 minutes)..... 57

Figure B4. Process Spectrum at 100 mTorr/250Watts (t=12 minutes)..... 58

Figure B5. Process Spectrum at 100 mTorr/250Watts (t=15 minutes)..... 59

Figure B6. Process Spectrum at 100 mTorr/250Watts (t=18 minutes)..... 60

Figure B7. Process Spectrum at 2.0 Torr / 250Watts (t=3 minutes)..... 61

Figure B8. Process Spectrum at 2.0 Torr / 250Watts (t=6 minutes)..... 62

Figure B9. Process Spectrum at 2.0 Torr / 250Watts (t=9 minutes)..... 63

Figure B10. Process Spectrum at 2.0 Torr / 250Watts (t=12 minutes)..... 64

Figure B11. Process Spectrum at 2.0 Torr / 250Watts (t=15 minutes).....65

Figure B12. Process Spectrum at 2.0 Torr / 250Watts (t=18 minutes).....66

Figure B13. Process Spectrum at 100 mTorr / 500Watts (t=3 minutes).....67

Figure B14. Process Spectrum at 100 mTorr / 500Watts (t=6 minutes).....68

Figure B15. Process Spectrum at 100 mTorr / 500Watts (t=9 minutes).....69

Figure B16. Process Spectrum at 100 mTorr / 500Watts (t=12 minutes).....70

Figure B17. Process Spectrum at 100 mTorr / 500Watts (t=15 minutes).....71

Figure B18. Process Spectrum at 100 mTorr / 500Watts (t=18 minutes).....72

Figure B19. Process Spectrum at 2.0 Torr / 500Watts (t=3 minutes).....73

Figure B20. Process Spectrum at 2.0 Torr / 500Watts (t=6 minutes).....74

Figure B21. Process Spectrum at 2.0 Torr / 500Watts (t=9 minutes).....75

Figure B22. Process Spectrum at 2.0 Torr / 500Watts (t=12 minutes).....76

Figure B23. Process Spectrum at 2.0 Torr / 500Watts (t=15 minutes).....77

Figure B24. Process Spectrum at 2.0 Torr / 500Watts (t=18 minutes).....78

Chapter 1

Introduction

Overview

The secondary treatment of manufactured items is not new. Practically every technological artifact is created in several steps, each bringing the material further from the raw components and closer to the finished product. Metal parts receive coatings of different kinds to protect them from oxidation and damage and to improve their performance characteristics or to give them an attractive, finished appearance. Some materials, however, can be formulated, colored, and reinforced in the compounding stage and come from the molding press in nearly final form. These materials are, of course, plastics.

Many parts require additional treatment in order to develop qualities required by designers or users. Some of these processes are the same as those used on other materials but some are specific to plastic parts. One of the desirable qualities of a molded plastic item is its smooth “resistant” surface. Of course the texture of the surface can easily be manipulated in the molding process, but the quality of “resistance” of the surface in this case is less easily manipulated in a localized manner. A change to the compound-linked surface qualities of the plastic would require a change to the entire molecular makeup of the plastic compound. While these changes are possible earlier in the compounding stage, they do not come without the chance of modifying, in an unwanted manner, the base properties of the plastic.

Secondary processes can be used to modify the surface qualities of the material without requiring a change to the compound itself. These secondary processes become a

valuable tool to be used in the modification of surface properties. Some common secondary treatments used to modify plastic items are shown in Table 1.

Table 1. Secondary Surface Treatments used on Plastic Objects (Berins, 1991)

Process	Medium	Outcome	Surface Energy
Washing	Water	Decontaminate	Raise
Abrasion	Sand	Modify Surface	Raise
Flame	Fire	Cross-link/Activate	Raise
Corona	Arc	Cross-link/Activate	Raise

The molding process can leave foreign deposits on parts. Mold release can remain on the surface, leaving the finished part in a condition that cannot undergo further processing. For the simplest cases, washing with soap and water, solvent degreasing, or vapor cleaning may be used to prepare the part for the next operation. For more serious condition problems, an abrasive treatment may be used. Sand blasting can remove larger finish irregularities and can also increase the surface area because of the roughening effect of the process. Flame treatment causes surface modification by the addition of energy to the surface, creating cross-linkages of the polymer strands, and can additionally leave atomic fragments bound to the surface, a condition called activation. Corona treatment exposes the surface to an electrical discharge, or arc, and also causes cross-linking and activation of the surface. As can be seen in Table 1, the outcome of each of these treatments is that the surface energy is increased. An increase in surface energy is directly related to an increase in the wettability (or decrease in resistance to wetting) of the part surface.

Further research into the mechanics of these processes, especially corona and plasma treatments, have produced refinements that allow current applications to modify an even wider number of qualities including wear properties, hydrophilic and hydrophobic selectivity, and the use of oxygen rich plasmas for material cleaning and sterilization. All of these improved applications have been developed through research undertaken at both the industry and academic levels. These procedures will be discussed further in Chapter 2.

In the 1991 reference, Berins outlines a rather short list of plasma treatments used on plastics. Most of these were used, at the time, simply to allow the printing of ink labels and graphics on plastic sheet goods. This proposed study will serve to examine a plasma treatment process related to current material processing methods used by the semiconductor industry.

Purpose and Objectives of the Study

The purpose of this study is to investigate the chemical and physical changes in a poly (ethylene terepthalate) polymer (PET) sample brought about by exposure to an energetic oxygen discharge.

The objectives of the study are: (a) assemble a processing apparatus capable of generating and containing an oxygen discharge dense enough to modify the polymer sample, (b) use standard methods of monitoring the chemical changes in the sample during controlled exposure to the discharge, and (c) use generally accepted methods to characterize the changes, if any, in the sample as a result of processing in an oxygen process atmosphere.

The use of plasma processing to prepare polymer parts for further processing avoids some of the problems inherent in other methods of processing. Exposure of parts to open flame (flame treatment) can damage parts by melting or scorching; abrasive treatment (sand blast) can abrade parts, damaging their function; and washing of the parts merely yields clean parts with minor surface changes.

None of these processes, though all are capable of surface modification at some level, comes with a real-time (other than visual inspection) method of quantifying the changes they create. Plasma processing not only allows modification of the sample surface at an atomic level but the capability of using non-invasive process monitoring (OES) and contact angle measurement allows real-time characterization of the plasma/sample interaction.

Research Questions

The primary research question of this experimental work is: can a capacitive discharge, energetic plasma-based processing system, operating at fixed set-points, modify the surface of a representative plastic sample? Second, can the researcher control the rate of the reactions through manipulation of process pressure and time of exposure and arrive at a satisfactory characterization of process rate? Third, can the researcher reliably characterize both the interaction of the sample with the plasma, using optical emission spectroscopy, and the degree of modification of the surface by the plasma, using contact angle measurement, in a laboratory setting?

Summary

Manufacturers use plastics to produce many objects we use every day. Although polymers have intrinsic properties that make them the best choice for many products, these properties can also cause difficulties if these objects require secondary processing such as printing or painting. Many different methods have been used to modify the surface qualities of plastics in order to make secondary processing easier. Although plasmas have been studied since the 19th Century, first described by Crookes in 1879, plasma processing for the local modification of plastic surfaces is a relatively new application.

This study proposes to use a relatively new process to modify the surface of the plastic samples. Exposure of plastic samples to an oxygen plasma is a variation on the methods used to manufacture semiconductors. The results of the study can confirm the usefulness of this process for the modification of plastics.

Chapter 2

Review of Literature

Overview

The progression from the use of natural polymers (horn, hide, and shellac) in the manufacture of technological artifacts to the discovery in the early 20th century of chemical-based replacements (Bakelite and Nylon) is well documented in the literature of technology history (Berins, 1991; Kalpakjian & Schmid, 2006). At the present time polymers--more specifically, engineered plastics--make up a large portion of materials used in the manufacturing of many classes of products. Plastics can be found in many items from containers to children's fittings and toys to automotive, scientific, and aerospace applications.

Secondary processing of plastic parts with the goal of enhancing the adhesion of inks and other decorations has existed since the "discovery" of modern plastics. The list of secondary processes used to accomplish this goal as outlined in standard textbooks (Berins, 1991; Kalpakjian & Schmid, 2006) includes solvent cleaning, mechanical abrasion, chemical etching, flame treatment, and priming, as well as the more technologically advanced (at the time) processes of corona, plasma, and ultraviolet treatments. All of these treatments had as their goal the increase of the surface energy of the plastic in order to enhance the effectiveness of upcoming processes. The current state of plastic processing still includes all of the methods mentioned in Berins (1991), but in the intervening years, those that were considered advanced processes, as a result of continued research, are now

commonplace. Corona processing, exposing the plastic sheet to an electrical discharge (ozone) and the related dielectric barrier plasma processing produced great research interest due to the ability to process large areas of sheet goods in an atmospheric discharge while moving the material through the processor (Schultz-von der Gathen, 2005). Chemical vapor deposition (CVD), a process of vaporizing metals or other compounds that are then deposited onto a substrate in order to fabricate mirrors, antireflective coatings, and optical filters has been improved by the addition of energetic plasmas, plasma enhanced CVD, which allows the deposition of diamond and other advanced coatings onto the substrate (Zhou, McCauley, Qin, Krauss & Gruen, 1997). Plasma-aided deposition of metals and refractory materials is also used to deposit wear surfaces onto manufactured parts (Fauchais, Montavon, Vardelle & Cedelle, 2006). Recent investigations of plastic processing using low-pressure plasmas include the inductive plasma treatment of plastic sheet (Krstulovic, Labazan, Milosevic, Cvelbar, Vesel & Mozetic, 2006) as well as the treatment of cotton thread (Selli et al., 2005) and paper sheets (Vesel et al., 2007) in order to characterize the change in surface qualities.

Processing of polymer materials has progressed from the initial methods using chemical etching (Chapman, 1988) to plasma processing (Graves, 1989) using a capacitive discharge used for sputtering of aluminum to make mirrors, to inductive generation methods that increased the plasma density, enabling the application of more power to the process.

The inductive method of plasma generation allows for the production of a more dense plasma (electron density) compared to the capacitive technique, which means that more electrons are available for modification of the substrate. This approach is widely used in the semiconductor industry where quick processing is more directly related to product

manufacture. Initially plasma processing of materials using capacitive plasma processing was exclusively used by the semiconductor industry; the majority of processing is done with an inductive plasma process chamber. Capacitive discharge processing of materials has begun to be reexamined by the manufacturers of semiconductor fabrication equipment as a method that offers ease of plasma generation and better control of plasma conditions, using newer control methods than the inductive systems currently in use (Shannon, 2008).

Polymers

Polymers are long chainlike molecules formed by joining short chain molecules, monomers, in a polymerization reaction. If all of the molecules are the same, the polymer is called a homopolymer (polyethylene). The addition of different monomers is called a copolymer. The two main types of plastics are thermoplastics and thermoset plastics. Thermoplastics are formed of long chains of molecules that lay alongside each other but are not attached to the other chains of molecules. Since there is no connection to other strands of molecules, the thermoplastic chains can be melted and solidified repeatedly by heating and cooling. Thermoset plastics undergo a reaction during processing forming connections between the long chains. These crosslinks form a plastic that cannot be remelted or reprocessed. Although thermoset plastic waste cannot be reprocessed using the same methods as thermoplastic waste, it can be treated by pyrolysis to recover the inorganic fillers for reuse but is generally ground and used as filler in other products.

The thermoplastic of interest in this work is Mylar™, poly (ethylene terepthalate) polyester, or PET. This polymer is made up of a backbone of carbon atoms accompanied by associated atoms of hydrogen, oxygen, and other carbon atoms, shown in Figures 1 and 2.

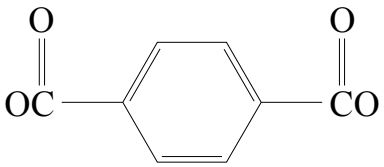

Figure1. Poly(ethylene-terepthalate) monomer

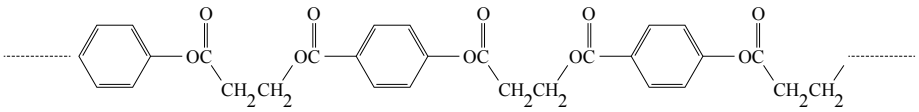

Figure 2. PET Polymer chain.

PET polyester is used as the starting material for beverage bottles, electrical insulation, reflective films, and dimensionally stable films for archival document printing. When used as sheet stock, PET can be supplied as biaxially oriented, that is, having undergone a manufacturing process that stretches the material in both the long and narrow direction. This process, coupled with forced cooling below the crystallization temperature, yields a material that has no "grain" i.e., anisotropic tendencies built into the material. An additional benefit of the forced cooling is that crystal growth in the finished sheet is small, yielding excellent clarity. It is this process, shown in Figure 3, which accounts for the additional stability of this material (Rao, Greener, Avila-Orta, Hsiao, & Blanton, 2008).

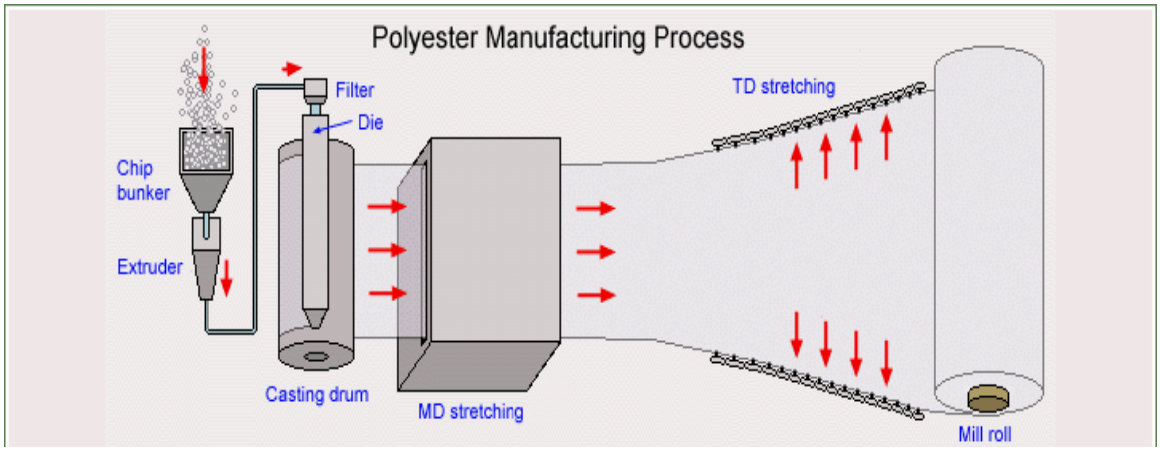

Figure 3. Polyester Sheet Manufacturing Process (HIFI Industrial Films, UK)

Plasma Processing

Plasma is a state of matter where electrons are removed from atoms within the plasma medium (usually air or an inert gas) by the addition of energy. This energy may come in the form of light, heat, electricity, or electromagnetic wave energy. The addition of energy by any of these methods can increase the movement or activity of the processing method used.

A 3 kilowatt, 13.56 MHz RF-plasma reactor system, consisting of an anodized aluminum chamber, RF-matching network, RF-generator, gas flow controller and vacuum system, a generous gift from Applied Materials, Inc. and Advanced Energy Inc., was used to modify the plastic surfaces (see Figure 4). The chamber and methods of process plasma generation and control will be outlined and discussed in Chapter 3.

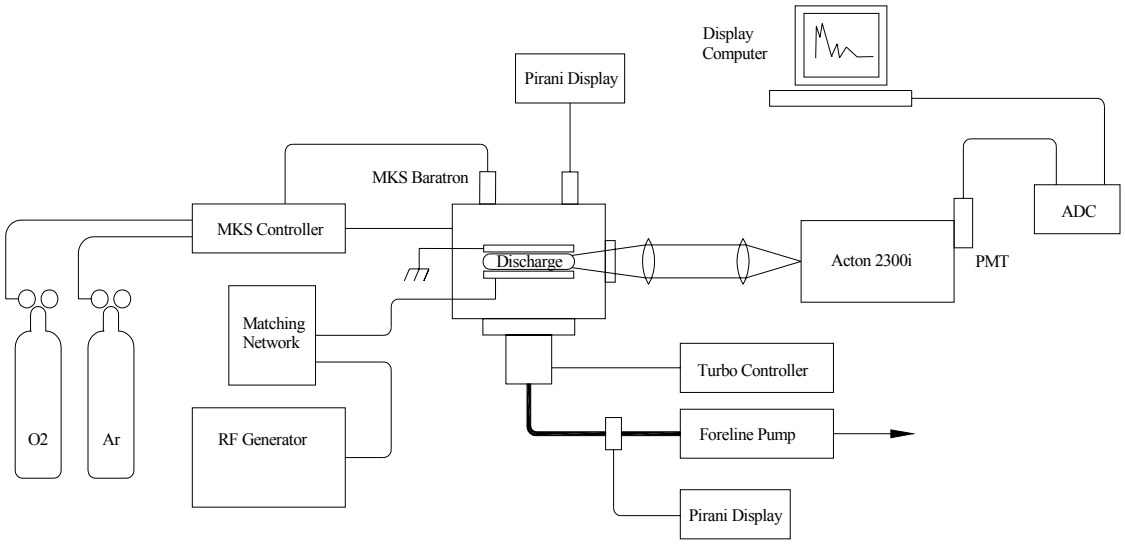

Figure 4. Experimental Plasma Discharge System.

The sample rested on the powered electrode and was exposed to the discharge. The interaction between the electric fields and the process gas generated excited, neutral and ionized, atomic and molecular species. The ionization occurred very rapidly, generating a plasma consisting of atoms, ions, and free electrons. Some of the free electrons accelerate across the outer layer of the plasma cloud and are propelled onto and into the surface of the sample. The change in state of the surface atoms and molecules as a result of this bombardment modifies the surface of the sample.

Plasmas are often described as the fourth state of matter (Chen, 1984). Plasmas, or as low fractional ionized plasmas are called, gas discharges, are generated by the addition of energy, usually electrical e.g., direct current (DC) or radio frequency (RF), into a gaseous system usually at or below atmospheric pressure. A plasma is distinguished from an ordinary gas by the fact that its characteristics are dominated by electrostatic forces rather

than by classical fluid mechanics (Lieberman & Lichtenberg, 2005). These energetic plasmas also generate electromagnetic radiation of many different wavelengths depending upon the type of discharge, but almost always give off visible light (Selwyn, 1989).

When energy carried by the RF fields is added to a gaseous system, kinetic energy is given primarily to the electron due to its small mass but large, relatively speaking, charge. Some of the electrons gain enough energy such that they break free of the atom or molecules leaving behind an ion (Chen & Chang, 2003). These highly energetic free electrons bump into the molecular and atomic gas constituents and ionize enough of them in what is known as breakdown (Brown, 1994), that the gas glows and the electrical resistivity is greatly reduced. The gas is then said to be ionized and in a plasma state. The degree of ionization depends upon the gas pressure and form of energy added to the gas. Anywhere from 10^{-4} to 10^{-5} of the atoms and/or molecules are ionized in an RF discharge. It doesn't sound like much but Coulomb (electromagnetic) forces are so strong that they dominate hydrodynamic forces (Chen, 1984). The atoms/molecules and free electrons gain energy through elastic and inelastic collisions with the free electrons. These ionized systems can maintain an ionized state as long as the energy source continues to supply energy to the electrons of the system such that over time the ionization process eventually occurs at the same rate as the recombination processes; the electron density equals the ion density and remains constant as long as energy continues to be absorbed by the plasma (Chen & Chang, 2003).

An RF plasma, particularly one in the megahertz range, will generate a "plasma sheath" (Lieberman & Lichtenberg, 2005). A plasma sheath is a thin layer of ions that surround both the powered (lower, in this case) and upper (grounded) electrode. The sheaths are comprised of ions, and because there are very few electrons to collide with, the

molecules of the gas do not “glow”, i.e., they are not visible to the eye (Chen, 1984; Lieberman & Lichtenberg, 2005). The bulk plasma contains ions, electrons, and neutral atoms/molecules and is contained between the two electrodes. This is the glowing region of the discharge.

Ionized species from the bulk of the plasma are accelerated across the sheath due to the potential that builds up during the RF cycle. Ions bombard the target, resulting in sputtering and/or chemical etching of the substrate due to free radicals such as oxygen (Lieberman & Lichtenberg, 2005; Chen & Chang, 2003). Transfer of momentum drives the sputtering process where the energy imparted to the ions during the RF cycle is transferred to the atoms of the substrate surface via collisions.

Etching is a related process, in that ions strike the surface, but depends more on repeated transfer of energy until the energy level of a surface atom grows large enough, through repeated collisions, that the atom can overcome the bonding forces holding it to the sample surface and breaks free (Lieberman & Lichtenberg, 2005;Chen & Chang, 2003).

Diagnostics

Optical Emission Spectroscopy (OES) is the most widely used diagnostic method in the plasma sciences (Selwyn, 1989; Griem, 1997; Hutchinson, 1987) and is the primary method that was used in this experiment. OES has an advantage over other diagnostics in that it is non-invasive, i.e., no instrumentation touches the plasma or sample. The identity of the emitting species is determined by examination of the light emitted by the plasma as a function of wavelength and compared to the known wavelengths of expected species

(Herzberg, 1950). OES allowed verification of the interaction between the plasma and the sample since it showed the existence of free atomic and molecular species that could only come from interactions with the surface of the sample. For example, lines from OH are observed. There is no hydrogen within the system except in the bonds of the plastic so OH must originate from the oxygen gas interacting with the plastic.

Light produced by the discharge is collected and imaged onto the entrance slit of an Acton 2300i monochromator using appropriate optics, as shown in Figure 2.3. Standard quartz glass lenses and mirrors can be used since the emitted spectra of the atomic and molecular species of interest are expected to lie within the visible light region between 300 nm and 800 nm. The gaseous products of the plasma-plastic interactions are characterized by identifying the visible peaks of light given off by each of the species of interest (Selwyn, 1989). The spectra are collected for analysis using software, shown in Figure 5, supplied with the Acton monochromator.

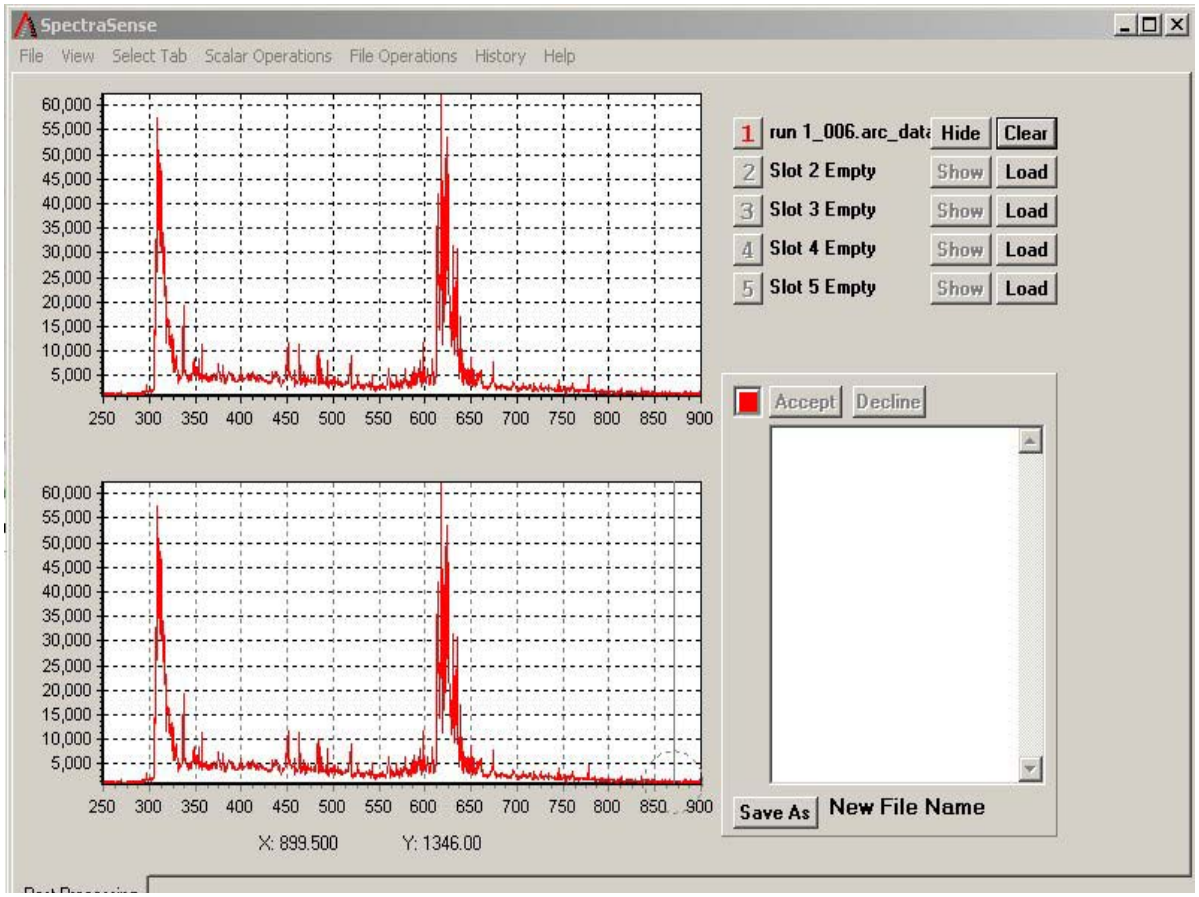

Figure 5. SpectraSense post processing screen.

Contact Angle

One of the desirable qualities of plastics is the ability to form a smooth, 'resistant' surface. While this is one of the expected qualities of plastics, it creates problems during secondary processing of products. The quality "resistance" is defined as the surface tension or surface energy of the material. A high solid surface tension indicates that the surface atoms of the polymer are "not interested" in combining with other materials.

Measurement of contact angle is a common method of quantifying the change in a processed plastic part. The relationship between contact angle and surface energy is a widely accepted method of characterizing local surface changes in response to treatment of the parts (Papakonstantinou, Amanatides, Mataras, Ioannidis, & Nikolopoulous, 2007; Deshmukh, & Bhat, 2003; Chirila, 2005).

Summary

Engineered plastics make up a large portion of materials used in the manufacture of products today. Processing of these plastic parts in order to "improve" the surface qualities is an ongoing goal of process and manufacturing engineers. The search for better processing methods began with the development of synthetic polymers in the early part of the last century; flame treatment, washing, abrasives and electric arc processing have been used.

Plasma processing is often used for processing of these materials. The interaction between the plastic and the plasma locally modifies the surface of the plastic to facilitate later operations while only minimally changing the bulk qualities of the material.

The use of OES as a diagnostic allows real-time monitoring of the changes taking place in the material at the atomic and molecular level. The use of diagnostics to monitor changes as they happen allows finer control of the treatment process over time as well as the recognition of recurring states of the processed materials.

Chapter 3

Experimental Methodology

Overview

The experimental plan is divided into four main portions: (a) initial preparation and cleaning of the samples, (b) initial characterization of the samples before treatment, (c) plasma treatment**,** and (d) characterization of the samples after treatment.

Materials and Methods

Sample coupons (13.0 mm x 13.0 mm x 0.5 mm) of PET material were cut from biaxially oriented sheets as supplied by the vendor. The coupons were cleaned in isopropyl alcohol, rinsed in deionized water, and blown dry with clean air. After the initial preparation and cleaning, the samples were attached to standard microscope slides using 3M double sided tape. Cleaned samples were subjected to an initial characterization by sessile drop contact angle measurement, thus setting the baseline contact angle of the unprocessed samples.

Processing System Design

The processing system consists of a hard-anodized aluminum chamber 40 cm by 20 cm by 18 cm with a volume of 14,000 cm^3. The chamber is modeled after the GEC standard

experimental chamber, i.e., the system consists of a chamber containing upper and lower insulated electrodes with RF power connected to the lower electrode where the samples are placed (Olthoff, & Greenburg, 1995). The chamber is equipped with a transparent front door that can be opened to insert or retrieve samples. The chamber is designed to operate at vacuum pressures. Capacitive discharges are not designed to run at atmospheric pressure. See Figure 6 for a diagram of the chamber.

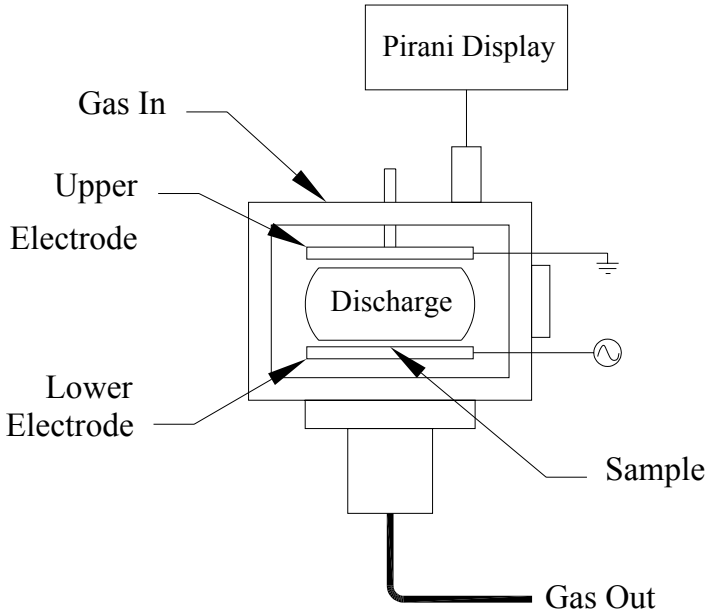

Figure 6. Experimental Chamber Setup.

RF energy is supplied by a 3kW, water cooled ENI Genesis RF Generator model GHW-50 and operates at a frequency of 13.56 MHz. The matching network, an Advanced Energy Navigator™ 7013-L90 (engineering sample) is an L-type matching circuit consisting of a pair of variable vacuum capacitors and a fixed high power inductor. The Navigator™ was operated in automatic matching mode but can also monitor process conditions and make

on-line adjustments in real time using Applied Materials Virtual Front Panel (VFP) proprietary software.

Oxygen gas (99.8%) flows into the reactor through a manifold system consisting of the process gas supply (gas bottle), MKS mass flow controller modules controlled by an MKS Model 305 gas controller feeding into the top of the process chamber through an in-line shut-off valve.

A pirani gauge and an MKS capacitive baratron pressure monitoring gauge in the chamber are monitored by the MKS controller. Closed-loop feedback from the baratron gauge allows the MKS mass controller to adjust the gas flow in order to maintain the set point pressure in the process chamber. An additional pirani gauge monitors the foreline pressure.

The chamber vacuum is generated by a Varian Model D70V Turbo pump backed up by a Varian roughing pump in the foreline. Pneumatically controlled valves direct the vacuum from and to the foreline pump. A VAT Model 64 gate valve allows the process chamber to operate in either a closed (static pressure/stirred tank) regime or in a throttled flow mode.

Process Diagnostics

Optical Emission Spectroscopy (OES) analyses are performed to identify species and in some cases measure the temperatures, plasma density, and the concentration of the observed emitting species. Since the spectra of interest lie in the visible part of the electromagnetic spectrum, spectral data are acquired through a quartz window in the

chamber and are imaged onto the slit of the monochromator using a 50 mm diameter quartz f/9 collimated optics chain. The monochromator is an Acton 2300i Czerny-Turner style instrument with a 300 mm focal length. The spectral light travels through the instrument to the exit slit. At the exit slit is a photomultiplier tube detector (Hamamatsu R955). The resulting signal is passed through an A/D converter and sent to the processing workstation. Real-time display of spectral acquisition is carried out by the supplied (Acton) SpectraSense software. Additional spectral line identification is carried out using Spectrum Analyzer; see Figure 7, an additional software application available from Zdenek Navratil of Masaryk University, Brno.

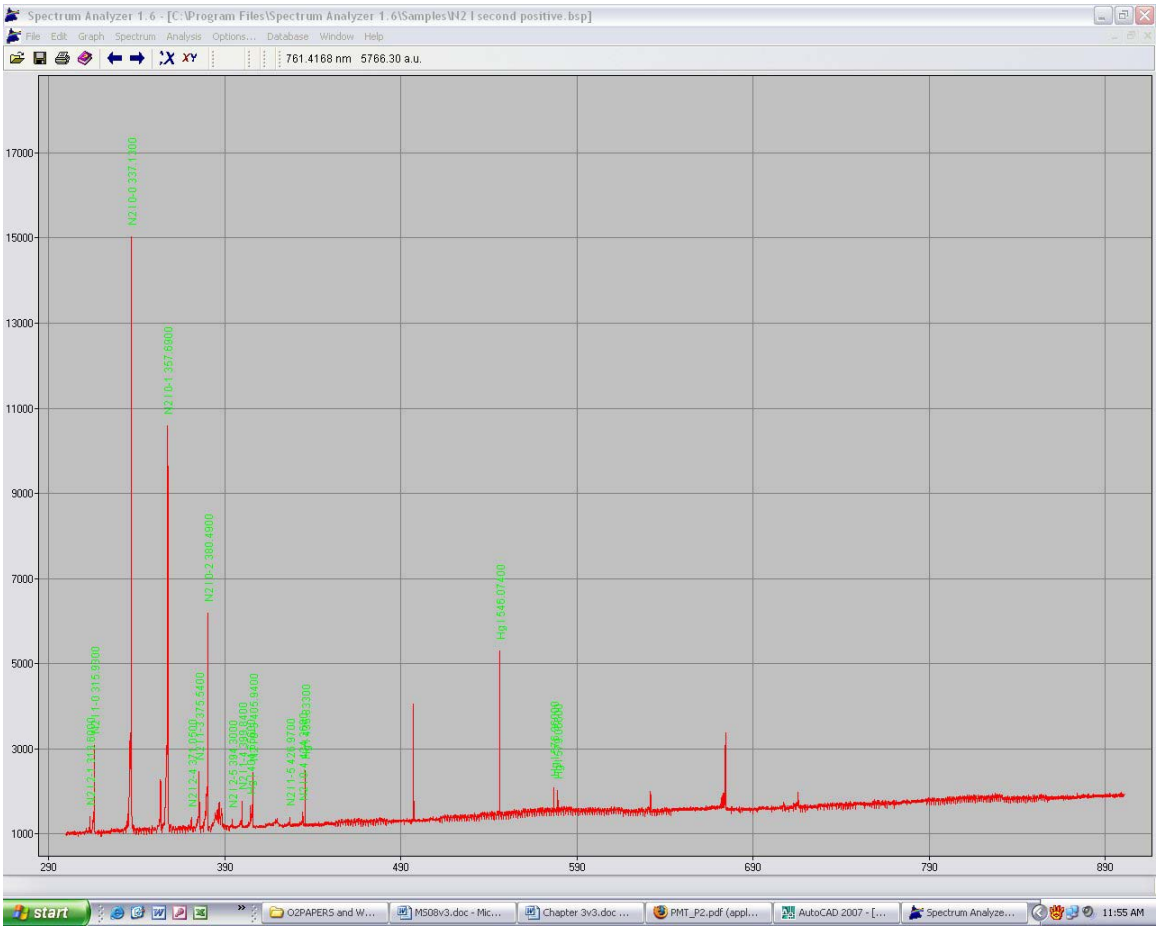

Figure 7. Spectrum Analyzer 1.6 software.

Contact Angle

Characterization of the sample contact angle is carried out using an FTA200 Dynamic Contact Angle Tester. The FTA200 consists of a computer controlled fluid metering system, a moving stage, and a video capture subsystem. The test liquid is dispensed under computer control, and the resultant drop is analyzed using proprietary software. The included software application calculates the contact angle formed tangent to the dispensed drop and the sample on the measurement stage; see Figure 8.

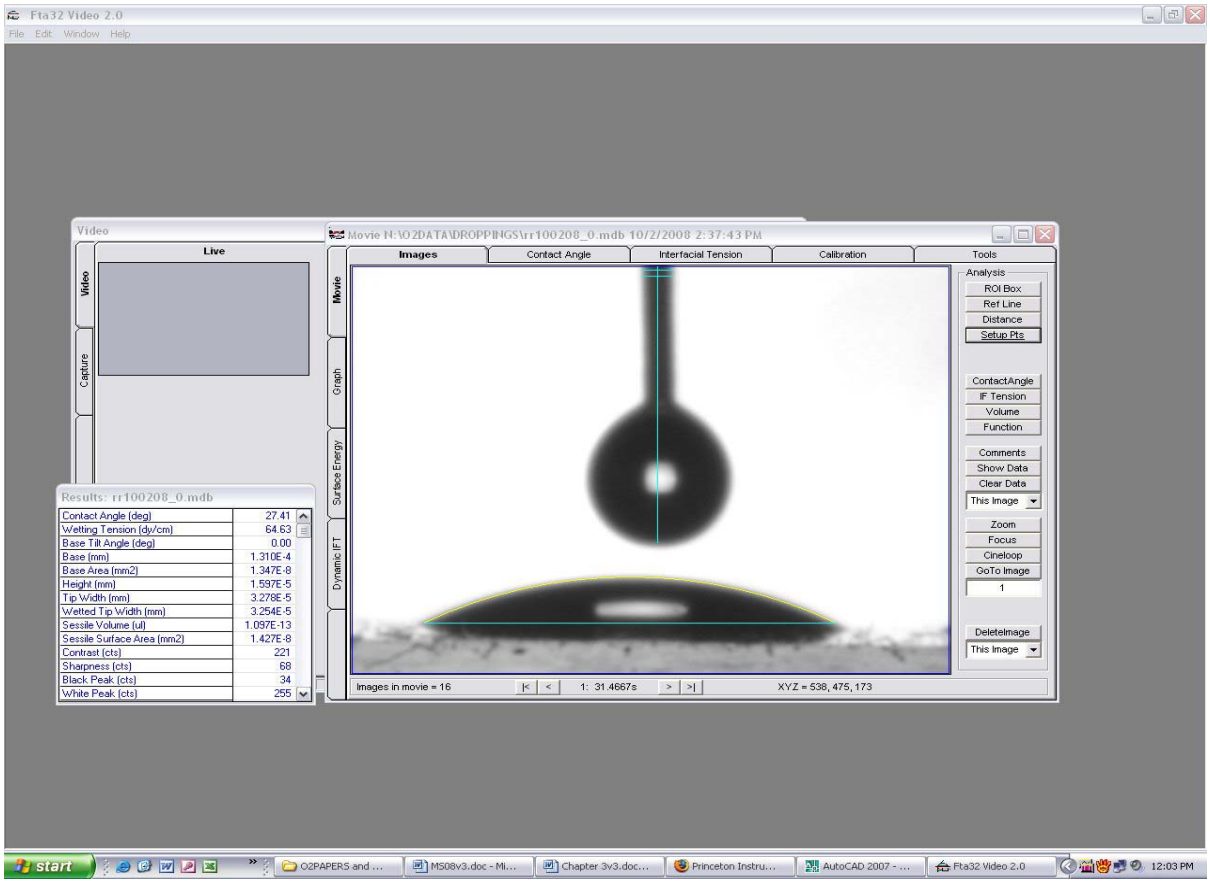

Figure 8. FTA Analysis software showing contact angle calculation screen.

Chapter 4

Experimental Results

Overview

The process chamber was monitored, using Optical Emission Spectroscopy, before, during, and after processing to not only ensure there was no contamination but to allow plasma characterization during all phases of the process. After treatment the samples were examined using a comparison of the measured contact angle of both treated and untreated samples to quantify the degree of modification undergone by the samples during processing. Finally, samples were visually compared (treated vs. untreated) as another metric of the effect of processing.

Optical Emission Spectroscopy

Optical Emission Spectroscopy (OES) was used to monitor spectral changes in each sample during processing in the discharge. The acquired spectra showed significant changes over the treatment period. The OES spectrum taken during the initial characterization of the empty chamber, seen in Figure 9, shows the initial state of the process system after cracking of the process gas (O_2). Initially the discharge emits a large peak at 778 nm, indicating the presence of neutral oxygen (OI). An occasional secondary peak is also seen at 845 nm (OI), but since oxygen discharges are generally dim and the 778 nm line is the most prominent of the series (NIST, 2008), the line at 845 nm can only be used as a secondary indicator of

plasma activity. The spectrum shows no indications of any other atomic species other than a low intensity OH bandhead at 309 nm (generally attributed to the existence of residual water vapor in the system).

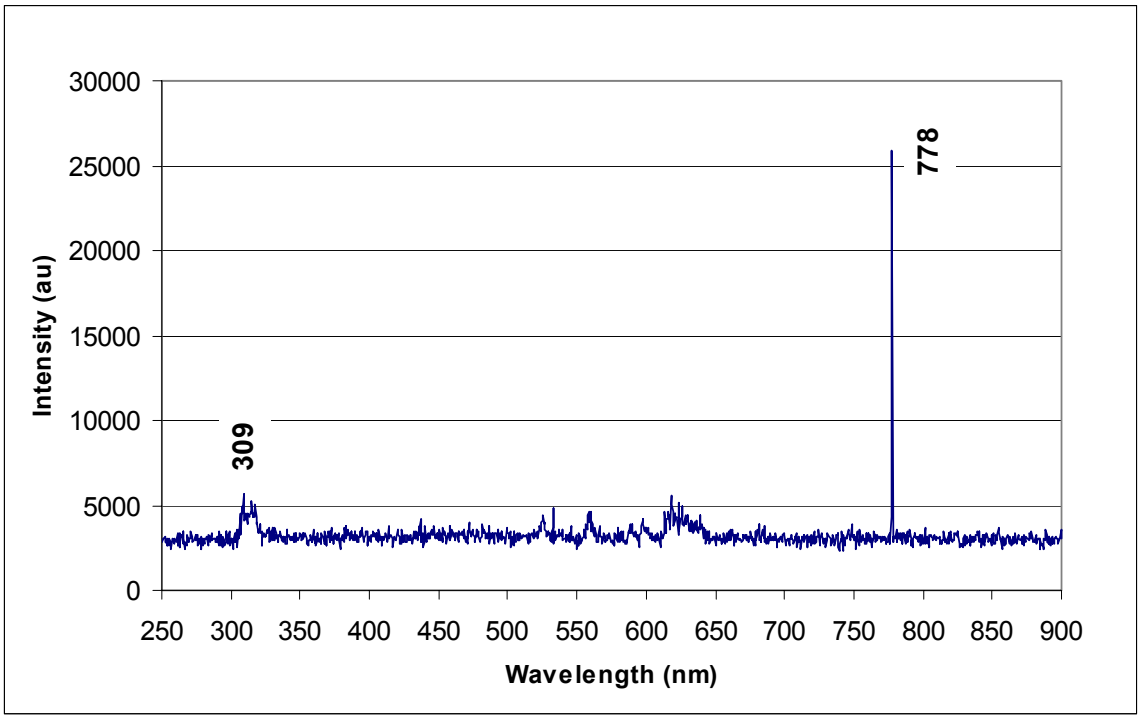

Figure 9. Spectrum of process reactor prior to introduction of sample.

The introduction of the first sample into the process reactor results in a change in the observed spectrum, shown in Figure 10. An increase in the intensity of the molecular bandhead of OH (hydroxyl), at 309 nm, was seen almost immediately upon exposure of the sample to the discharge. An increase in the intensity of the bandhead of CO at 312 nm (partially overlapping the OH band) and in the intensity of OI at 778 nm and 845 nm was also seen.

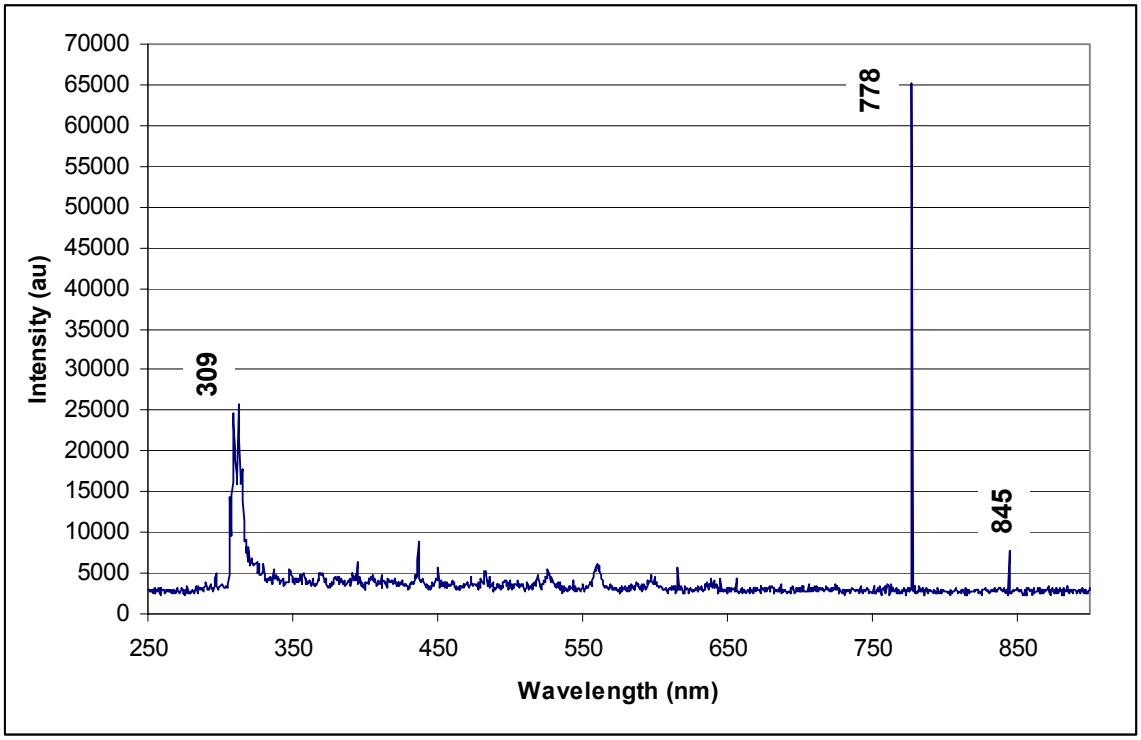

Figure 10. Spectrum showing increase in OH after processing (100 mTorr 500 Watts).

After an increase in applied power, a decrease in intensity of the oxygen (OI) lines at 778 nm and 845 nm was seen, as shown in Figure 11. This corresponded to an increase in the lines at 309 nm (OH) as well as an increase in intensity of CO seen at 326 nm.

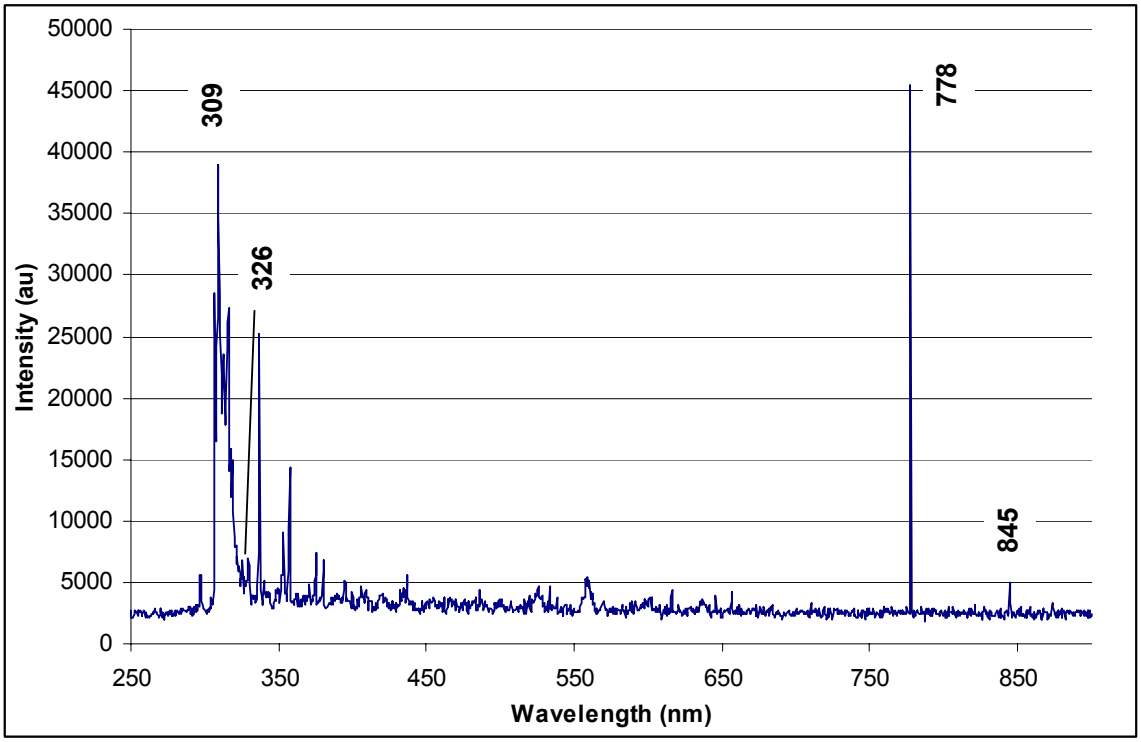

Figure 11. Spectrum showing increase in OH after processing (100 mTorr 500 Watts).

A comparison of the intensity of OH and OI is shown in Figure 12 for the two applied powers of 250 Watts and 500 Watts. Understandably, more power absorbed by the plasma resulted in higher line intensities for OH and OI. The intensities stay approximately at the same level as a function of time with the exception of OI for the high power case. The intensity of OI (778 nm) more than doubles during the 18 minute run. The rate that hydrogen is removed from the plastic stays fairly constant, but the degree of O_2 dissociation appears to increase with time at the higher power. It is difficult to further explain this effect without a comprehensive chemical kinetics model. The construction of a kinetics model of this process is beyond the scope of this study.

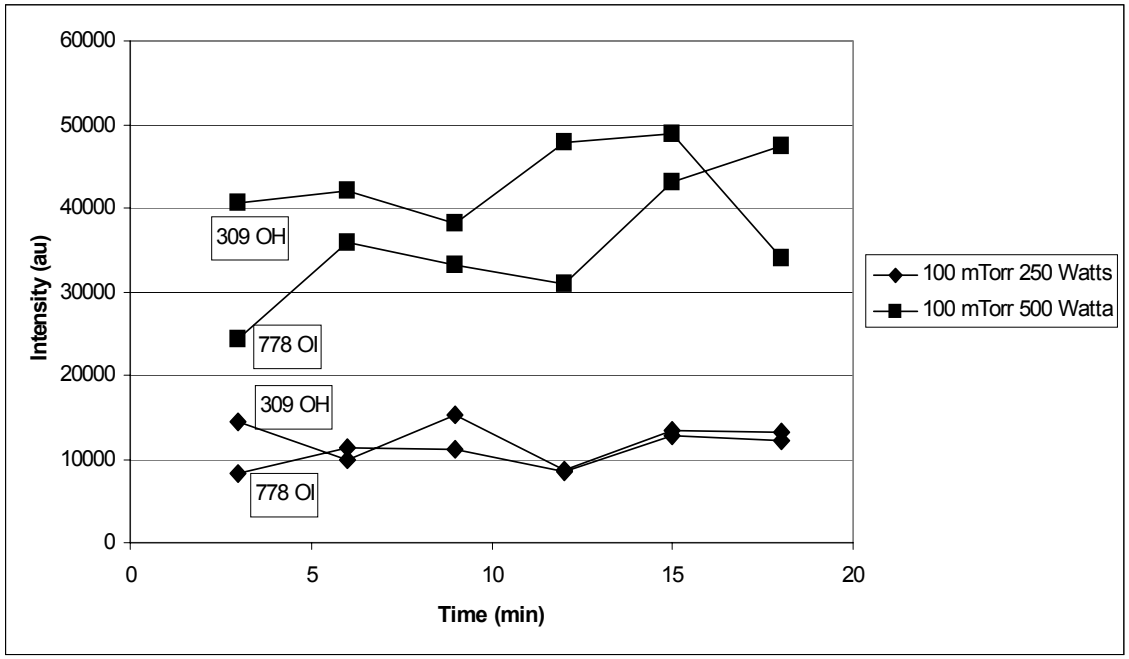

Figure 12. Comparison of OH and OI intensities during processing at different applied power.

Spectra taken at the highest pressure are shown in Figure 13 and 14. The spectra acquired at 2.0 Torr--250Watts shows a greatly increased intensity at the 309 nm and 778 nm lines when compared to the lowest pressure (100 mTorr--250 Watts). An increase in power (500 Watts) slightly reduces the intensity at 309 nm but greatly reduces the intensity of the oxygen line at 778 nm.

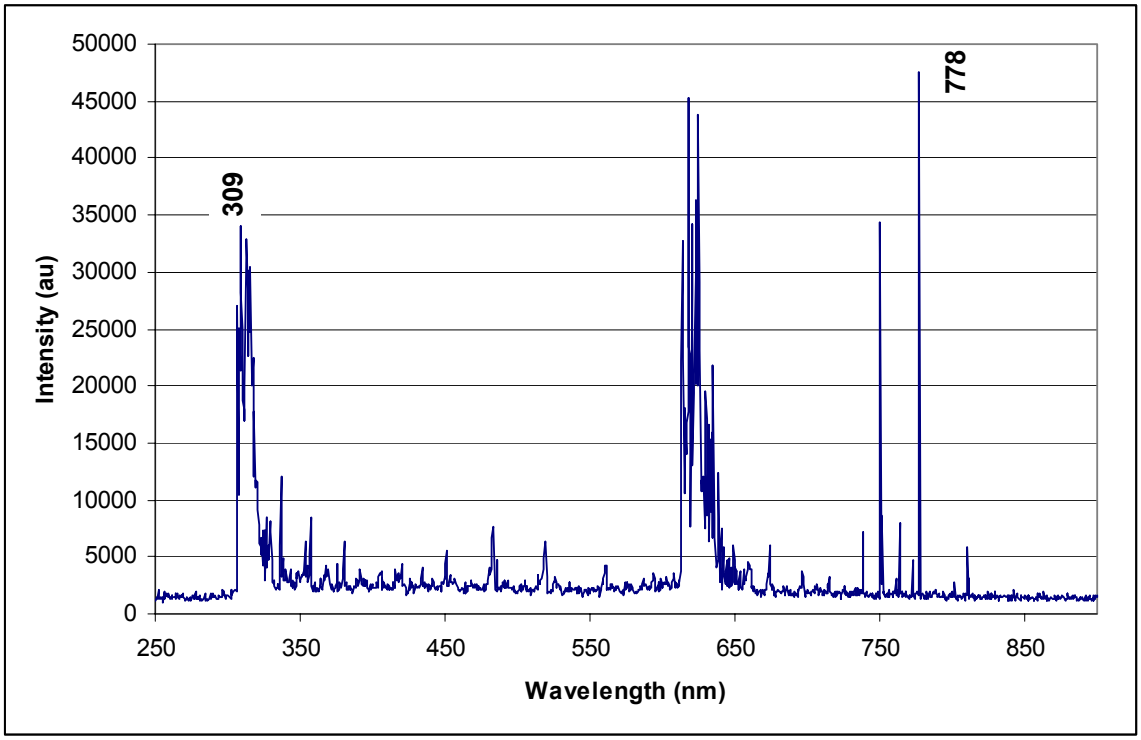

Figure 13. Spectrum at high pressure/low power (2.0 Torr 250 Watts).

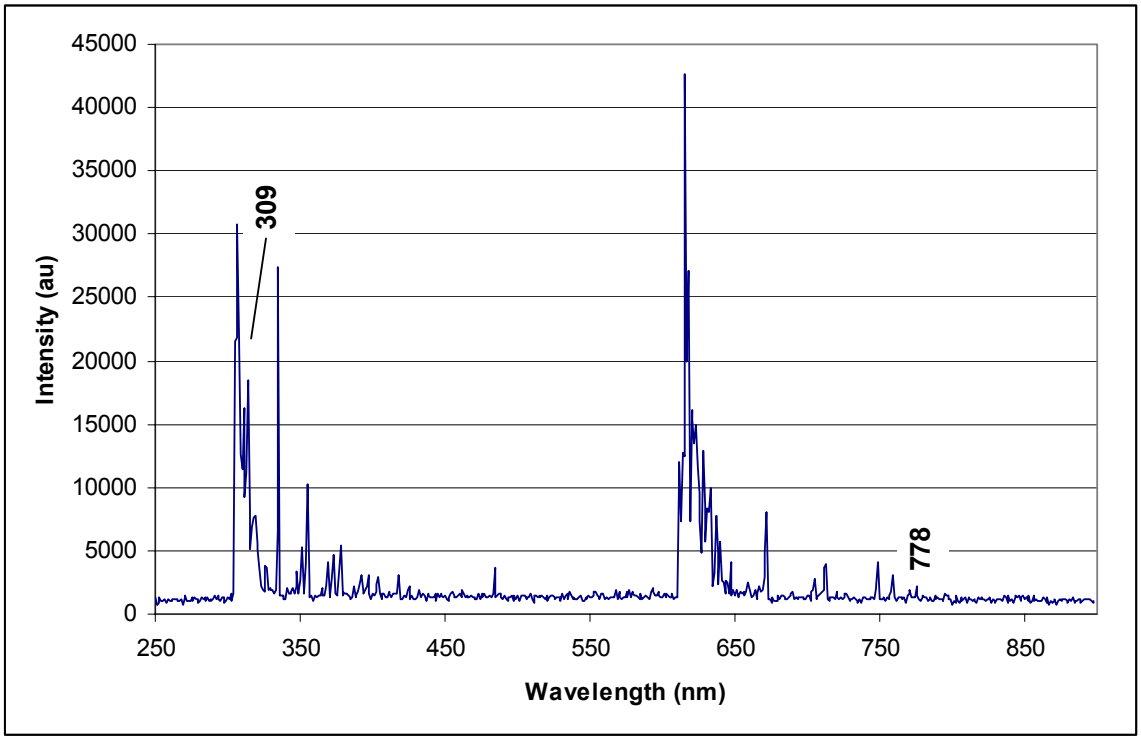

Figure 14. Spectrum at high pressure/high power (2.0 Torr 500 Watts).

A comparison of spectra at two powers but at the same high pressure is shown in Figure 15. Interestingly, the lower power resulted in higher intensities for both OH and OI. The intensities are approximately constant with the exception of the low power case where OI doubles during the runtime. In the high power case, OH decreased with increased runtime.

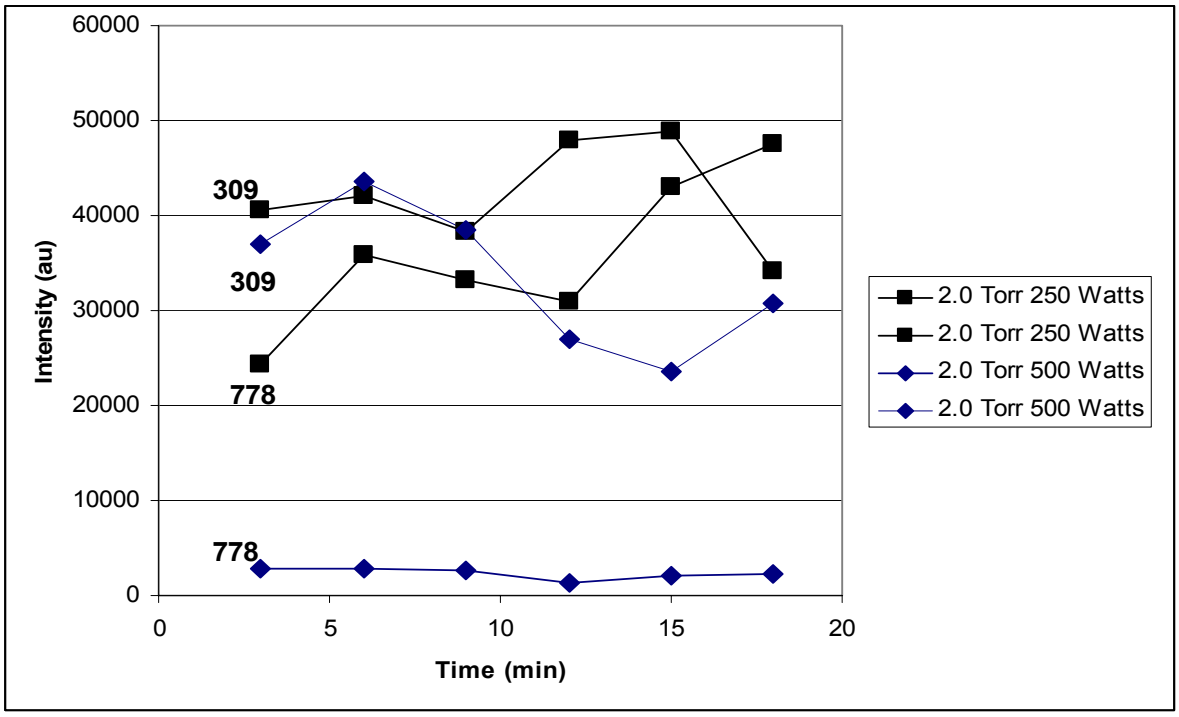

Figure 15. Intensity of lines at 309 (OH) and 778 (OI) at different power levels.

Processing of the samples showed a change in OES components during the processing sequence. Initial OES spectra of the process tank (empty) showed a large emission at the oxygen line at 778 nm and minimal emissions at the 309 nm bandhead of OH. During processing, however, there seemed to be an increase in free hydrogen in the system as the OH line at 309 nm was much more prominent. The eight sets of data shown here are but a small representative sample of the many runs made for this thesis. Additional spectral data can be found in Appendix B.

Contact Angle

Video capture images of the sample/water interface were used with the FTA200 proprietary software to calculate the contact angle of the sessile drop. The images also serve to illustrate the change in surface wettability between the samples. The initial condition of the cleaned but untreated sample, Figure 16, shows a large contact angle indicating low surface energy and a hydrophobic initial condition. The final image in the series, taken at the highest pressure and power, reveals a large change in the contact angle when compared to the starting condition; see Figure 17. Subsequent images taken at each of the pressure and power combinations (Appendix A) confirm a varying but consistent decrease in the contact angle after processing at each combination.

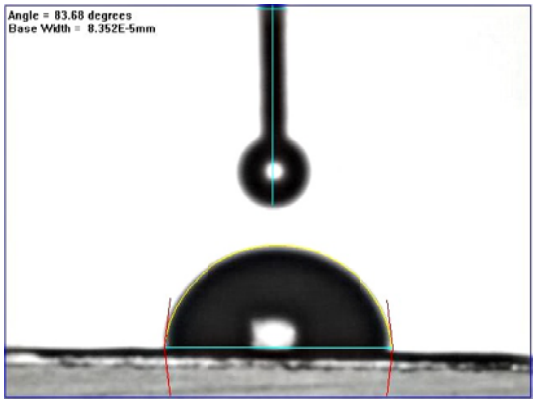

Figure 16. Untreated contact angle.

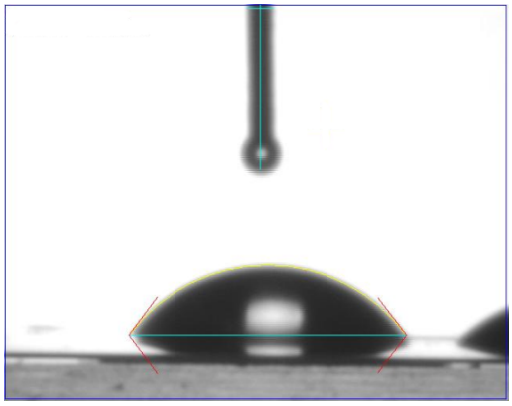

Figure 17. Treated contact angle (250 m Torr / 500 Watts).

A plotted comparison of the change in contact angle values for selected pressure and power combinations is given in Figure 18. The initial deionized (DI) water contact angle averaged 84° and decreased to a low of 45° over the period of treatment, around 18 minutes.

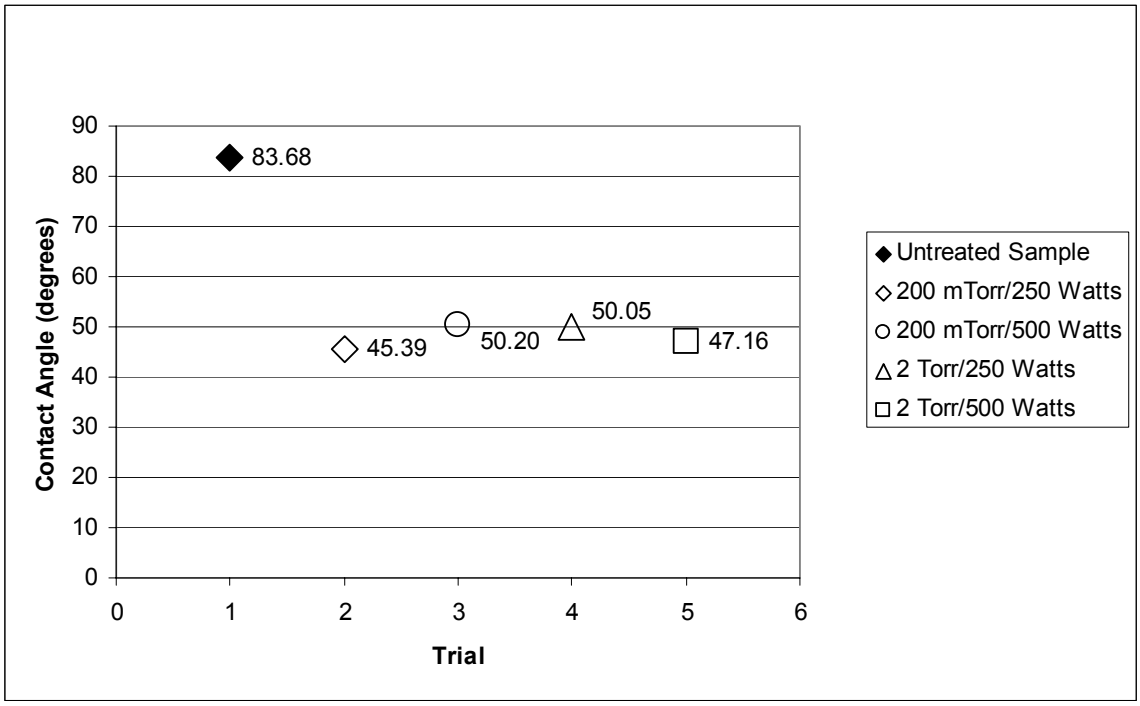

Figure 18. Contact Angle values of tested samples before and after processing. Each data point shown represents the average of three measurements

Each data point in Figure 18 represents the average of three measurements taken across the surface of each trial. The contact angles exhibited a decrease from the untreated state for each set of three readings and a reduction in angle of over half overall. Discharge processing conditions are shown in Figure 19.

- **Capacitively coupled discharge**
  - Frequency: 13.56 MHz
  - Electrode diameter: 11 cm
  - Electrode spacing: 2.5 cm
  - Process pressure: 100 – 2000 mTorr
  - Process Power: 250 – 500 Watts
  - Process gas: O_2 and O_2/Ar

Figure 19. Capacitively Coupled Discharge Processing Conditions

Visual Comparison of Samples

The visual comparison of the sample coupons, shown in Figure 20 and Figure 21, shows a smooth, slightly shiny surface of the sample when viewed under normal conditions. Visual inspection of the succeeding samples shows an increasingly matte surface condition. Distinctions between samples processed at the various running conditions are too minute to be further visually differentiated.

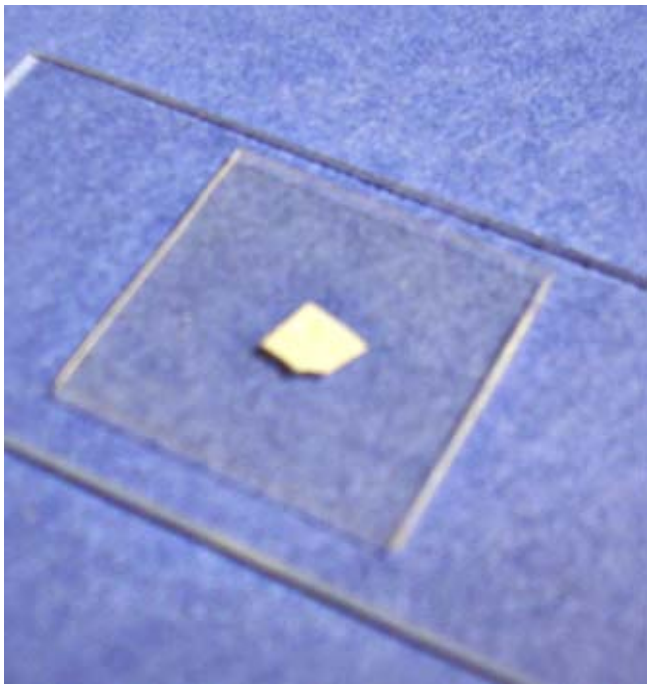

Figure 20. Unprocessed PET Sample

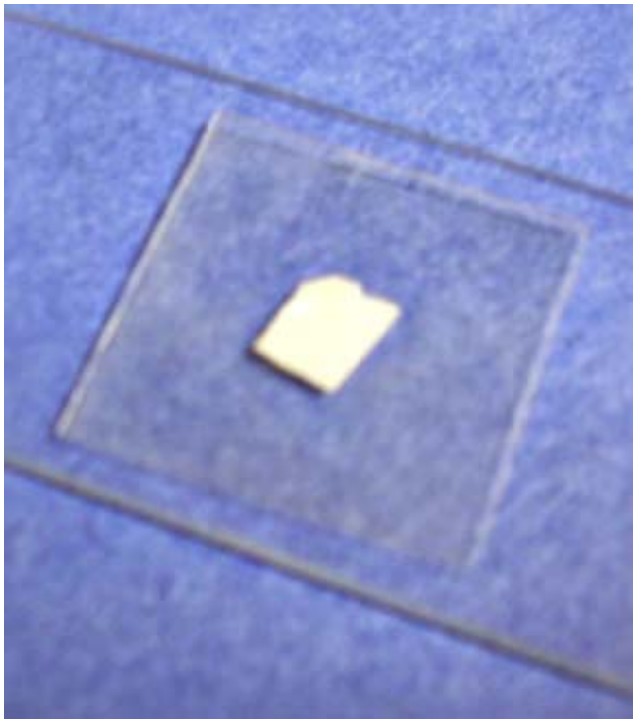

Figure 21. Processed PET Sample

Chapter 5

Conclusions (Summary) and Suggestions for Further Work

Overview

Samples of PET were exposed to an energetic oxygen plasma for a fixed time at varying pressures and power levels. Exposure to the discharge modified the surface characteristics, specifically the contact angle and surface condition of the samples. Surface modification was inferred by the fact that carbon and hydrogen-based molecules were observed with Optical Emission Spectroscopy although the feed gas was pure oxygen.

The samples were characterized initially by measuring the contact angle formed by a metered quantity of deionized water applied to the material surface. The averaged sample readings were tabulated (Figure 18) and taken as the base condition of the material before processing. The initial measured value of the contact angle (85°) indicated a material having a low surface energy, equating to a surface resistant to wetting by the test liquid.

The samples were monitored during processing by measurement of the intensity of the visible (300-900 nm) light given off by the excited atoms and molecules during the interaction between the sample and the discharge. The resultant spectra showed the presence of oxygen, which was supplied as feed gas, and the molecular signatures of both OH and CO molecules beginning shortly after the beginning of processing. All of the monitored spectral lines showed variation depending on the combination of process power and process pressure in the chamber.

The samples were characterized again after exposure to the discharge using the Sessile Drop Method used in the initial characterization step. The measured angles were compared to the initial readings (Figure 18) and showed a decrease of 40-50% in contact angle after treatment. The decrease in contact angle indicated an increase in the surface energy of the samples. The increase in surface energy indicates a surface that is less resistant to wetting by the test liquid.

Visual examination of the samples before processing showed a smooth, shiny surface. The surface of the processed samples showed varying degrees of surface degradation, or roughening, correlating roughly with each set of processing conditions.

Oxygen plasma processing was shown to be a useful method for surface modification of PET plastic samples, generating changes in contact angle and surface condition. Collected data showed an overall decrease in contact angle as well as a visible change in the appearance of the sample. These results indicate that neither change in process pressure nor in process power had any significant effect on the degree of modification of the sample surface.

Further Work

Experimental data gathered from this research indicate that oxygen discharge processing is a viable method for surface modification of plastics. Additional investigations that could extend and expand on the current information include an additional characterization of the treated surfaces using a Scanning Electron Microscope (SEM). Investigation of the treated sample using a SEM would allow the compilation of a highly-magnified visual record of the changes in the surface morphology as a result of the process treatment. This method of characterization is widely used in the literature and in industry (Vesel et al, 2007; Yip, Chan, Sin, & Lau, 2004).

An increase in the power absorbed by the discharge could yield greater information about the relationship between the intensity of observed (Berins, 1991) spectral lines of OH and CO relative to the modification of the surface. Increased power and pressure may even result in partial or complete disintegration of the sample. Equipment modifications are being made to increase the amount of delivered power.

Additionally, X-ray Photoelectron Spectroscopy (XPS) of the surfaces would allow the characterization of the initial chemical state of the sample and allow the verification and quantification of the plasma induced surface reactions that generate the OH and CO molecules seen in the process spectra data (Trigwell, Boucher, & Calle, 2006; Vesel et al, 2007).

References

Berins, M.L., (1991) (Ed.) *Plastics Engineering Handbook of the Society of the Plastics Industry*. New York:Chapman & Hall

Brown, S. (1994). *Basic Data of Plasma Physics.* New York: American Institute of Physics.

Chapman, B. (1980). *Glow Discharge Processes*. New York: John Wiley & Sons.

Chen, F. F. (1984). *Plasma Physics and Controlled Fusion, Volume 1: Plasma Physics.* New York: Plenum Press.

Chen, F. F., & Chang, J. P. (2003). *Lecture Notes on Principles of Plasma Processing.* New York: Plenum Publishers.

Chirila, V., Marginean, G. & Brandl, W. (2005). Effect of the oxygen treatment parameters on the carbon nanotubes surface properties. *Surface & Coatings Technology 200*,548-551.

Deshmukh, R., Bhat, N. (2003). The mechanism of adhesion and printability of plasma processed PET films. *Mat. Res. Innovat., 7*, 283-290.

Fauchais, P., Montavon, G., Vardelle, M., & Cedelle, J. (2006). Developments in direct current plasma spraying. *Surface & Coatings Technology, 201*, 1908-1921.

Graves, D. (1989). Plasma Processing in Electronic Materials Processing, *AIChE J. (Journal Review), 35*, 1-29.

Griem, H., (1997). Hutchinson, I. H., Hopcroft, K. I., Schindler, K., & Haines, M. G. (Eds.). *Principles of Plasma Spectroscopy.* Cambridge: Cambridge Press.

Herzberg, G. (1950). *Molecular Spectra and Molecular Structure: 1. Spectra of Diatomic Molecules.* New York: Von Nostrand Reinhold Co.

Hutchinson, I. (1987). *Principles of Plasma Diagnostics.* New York, NY: Cambridge University Press.

Kalpakjian, S., & Schmid, S. (2006). *Manufacturing Engineering and Technology* (5th ed.) Upper Saddle River N.J.:Pearson Prentice-Hall.

Krstulovic, N., Labazan, I., Milosevic, s., Cvelbar, U., Vesel, A., & Mozetic, M. (2006). Optical emission spectroscopy characterization of oxygen plasma during treatment of a PET foil. (2006). *J. Phys. D: Appl. Phys. 39*, 3799-3804.

Lieberman, M. A., & Lichtenberg, A. J. (2005). *Principles of Plasma Discharges and Materials Processing.* (2nd ed.) Wiley:Hoboken.

Olthoff, J.K., & Greenberg, K.E. (1995). The Gaseous Electronics Conference RF Reference Cell—An Introduction, *J. Res. Natl. Inst. Stand. Technol.* 100, 327

Rao, Y., Greener, J., Avila-Orta, C., Hsiao, B., & Blanton, T. (2008) The Relationship between microstructure and toughness of biaxially oriented semicrystalline polyester films. *Polymer. 49*, 2507-2514.

Raichenko, Y., Kramada, A.E., Reader, J., & NIST ASD Team (2008). NIST Atomic Spectra Database (version 3.1.5), [online]. Available: http://physics.nist.gov/asd3 [2009, January 31]. National Institute of Standards and Technology, Gaithersburg, MD

Papakonstantinou, D., Amanatides, E., Mataras, D., Ioannidis, V., & Nikolopolous, P. (2007). Improved Surface Energy Analysis for Plasma Treated PET Films. *Plasma Process. Polym., 4*, 51057-51062.

Roth, R., Li, Q., Tsai, P., Chen, Z. (2007, June). *Polymer Surface Modification with a one atmosphere uniform Glow Discharge Plasma (OAUDGP®)*. Presented at the at the 6th International Symposium on Polymer Surface Modification at University of Cincinnati, Cincinnati, Ohio.

Schultz-von der Gathen, V. (2005) *Atmospheric Pressure Glow Discharges for Surface Treatment: Selected Examples*. In *Proceedings of the XXVII International Conference on Phenomena in Ionized Gases, Eindhoven, the Netherlands, 18-22 July, 2005* (pp. 1-2). Eindhoven, the Netherlands:ICPIG.

Selli, E., Mazzone, G., Oliva, C., Martini, F., Riccardi, C., Barni, R., Marcandalli, B., & Massafra, M. (2001). Characterization of poly (ethylene terepthalate) and cotton fibres after cold SF_6 plasma treatment. *J. Mater. Chem., 11*, 1985-1991.

Selwyn, G. (1989). *Optical diagnostic techniques for plasma processing.* Bellingham, WA: International Society for Optical Engineering.

Shannon, S. (2008, January). *Multi-frequency CCP Discharges for State of the Art Micro- and Nano- Scale Manufacturing*. Presentation made at the Colloquium of the Department of Nuclear Engineering at North Carolina State University.

Trigwell, S., Boucher, D., & Calle, C. (2007). *Journal of Electrostatics. 65*(7), 401-407.

Vesel, A., Mozetic, M., Hladnik, A., Dolenc, J., Zule, J., Milosevic, S., Krstulovic, N., Klanjsek-Gunde, M., & Hauptmann, N. (2007). Modification of ink-jet paper by oxygen-plasma treatment. *J. Phys. D: Appl. Phys., 40*, 3689-3696.

Yip, J., Chan, K., Sin, K., & Lau, K., (2004). Comprehensive Study of polymer fiber surface modifications Part 2: low-temperature oxygen-plasma treatment. *Polymer International. 53,* 634-639.

Zhou D., McCauley, T., Qin, L., Krauss, A., & Gruen, D. (1997) Synthesis of nanocrystalline diamond thin films from Ar-CH4 microwave plasma. *J. Appl. Phys. 83*. 1.

Appendix A

Contact angle video captures

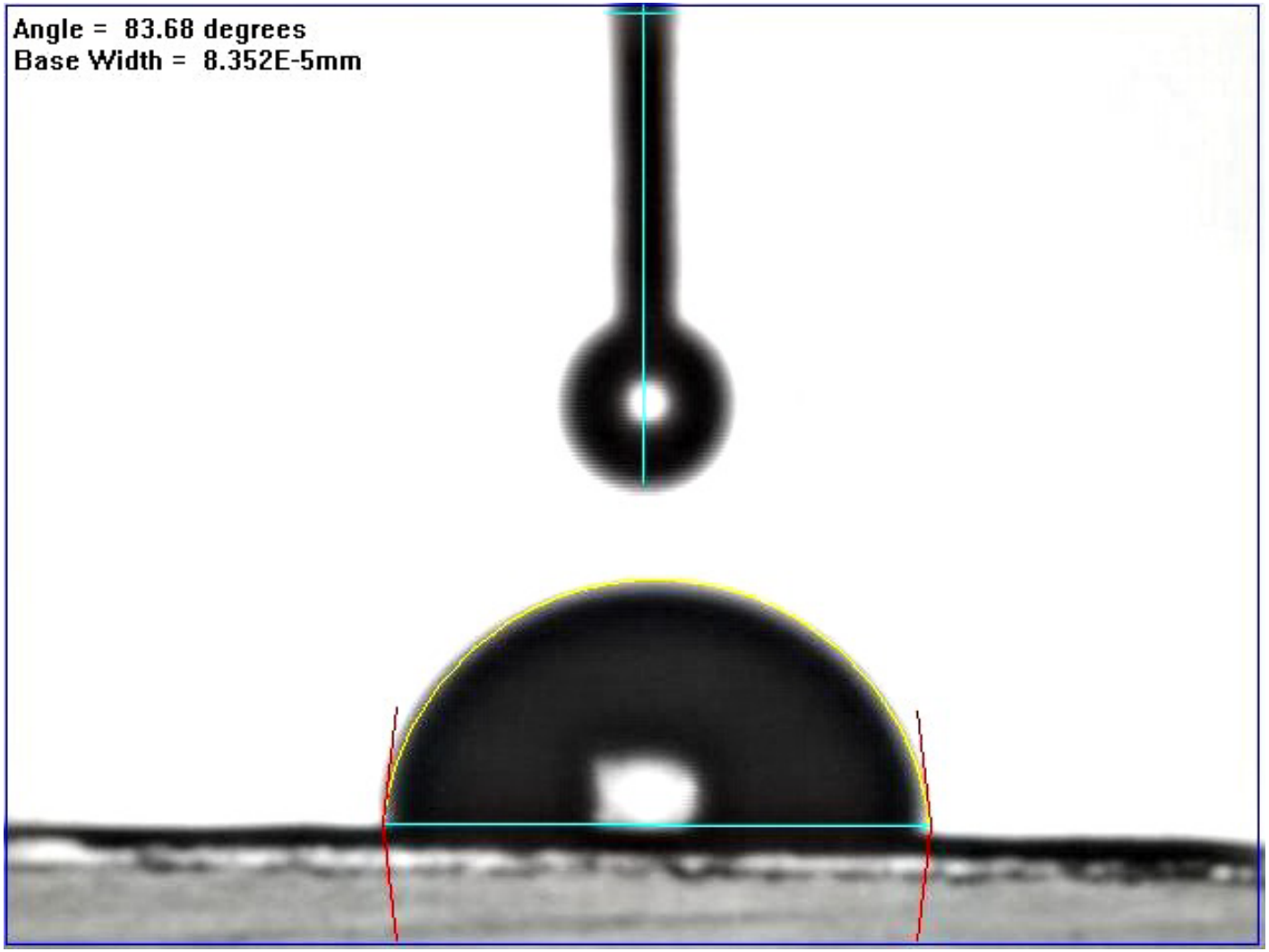

Figure A1. Contact angle of untreated PET sample.

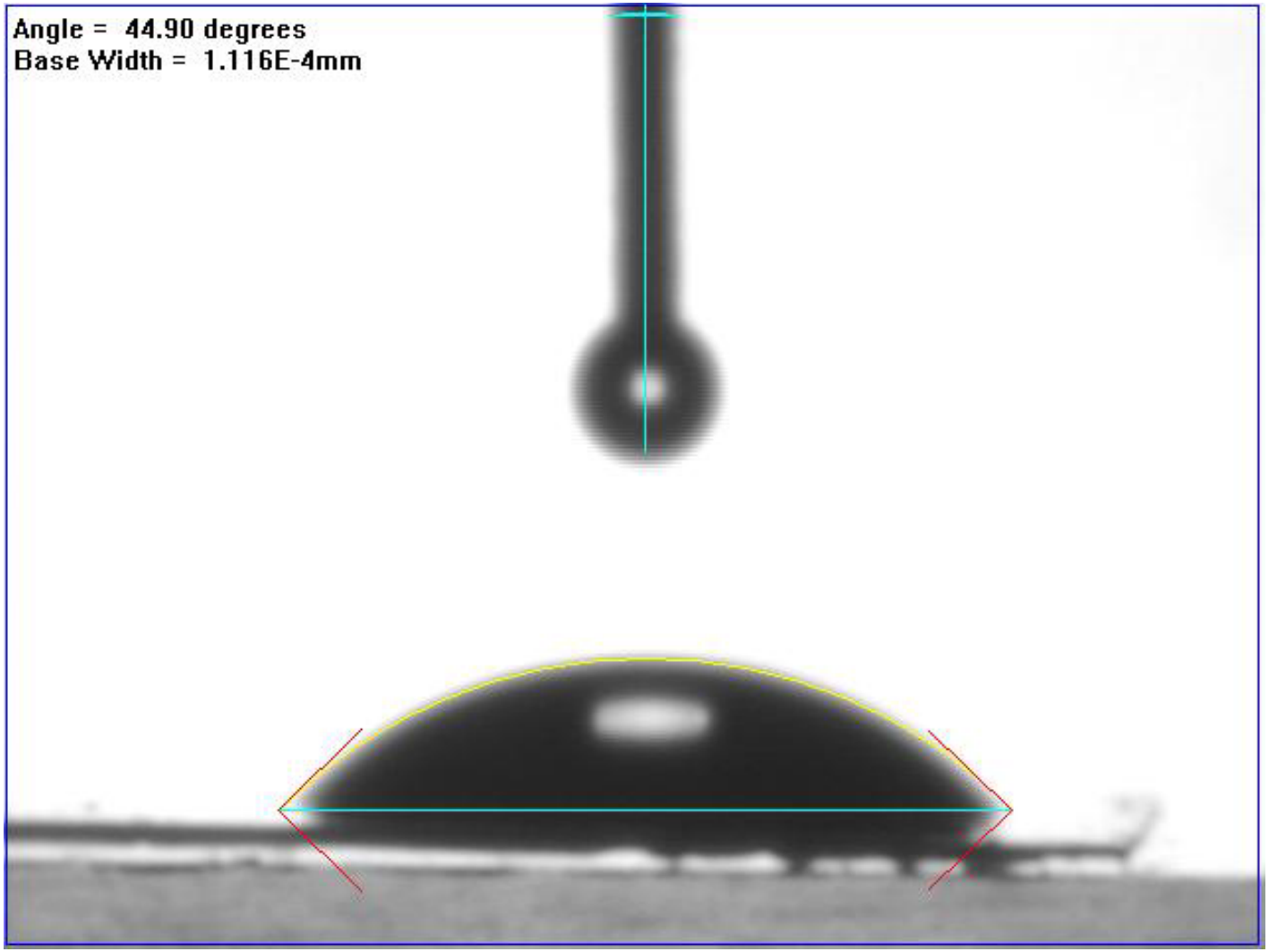

Figure A2. Contact Angle 1 of PET Sample (100 mTorr / 250 Watts)

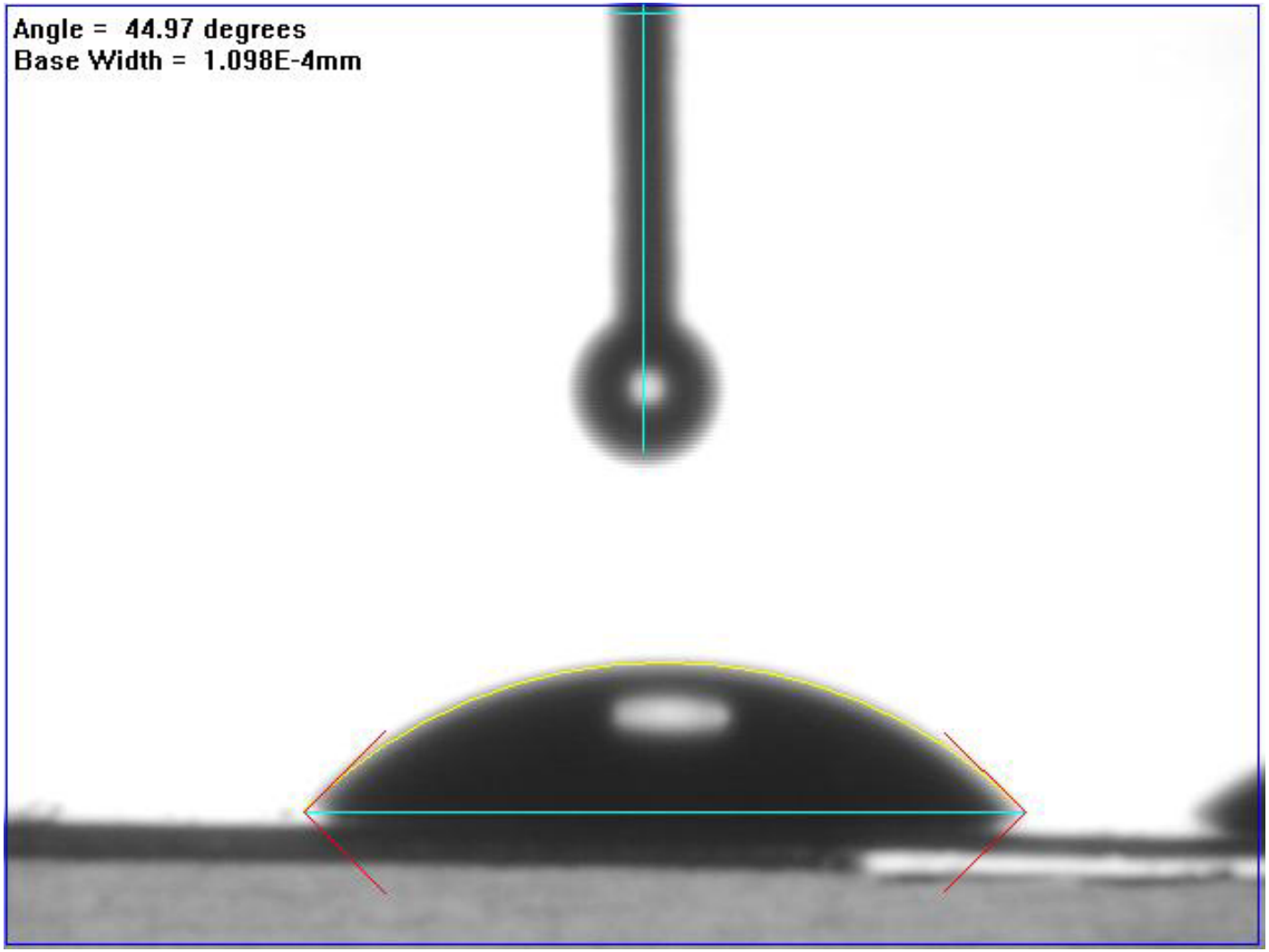

Figure A3. Contact Angle 2 of PET Sample (100 mTorr / 250 Watts)

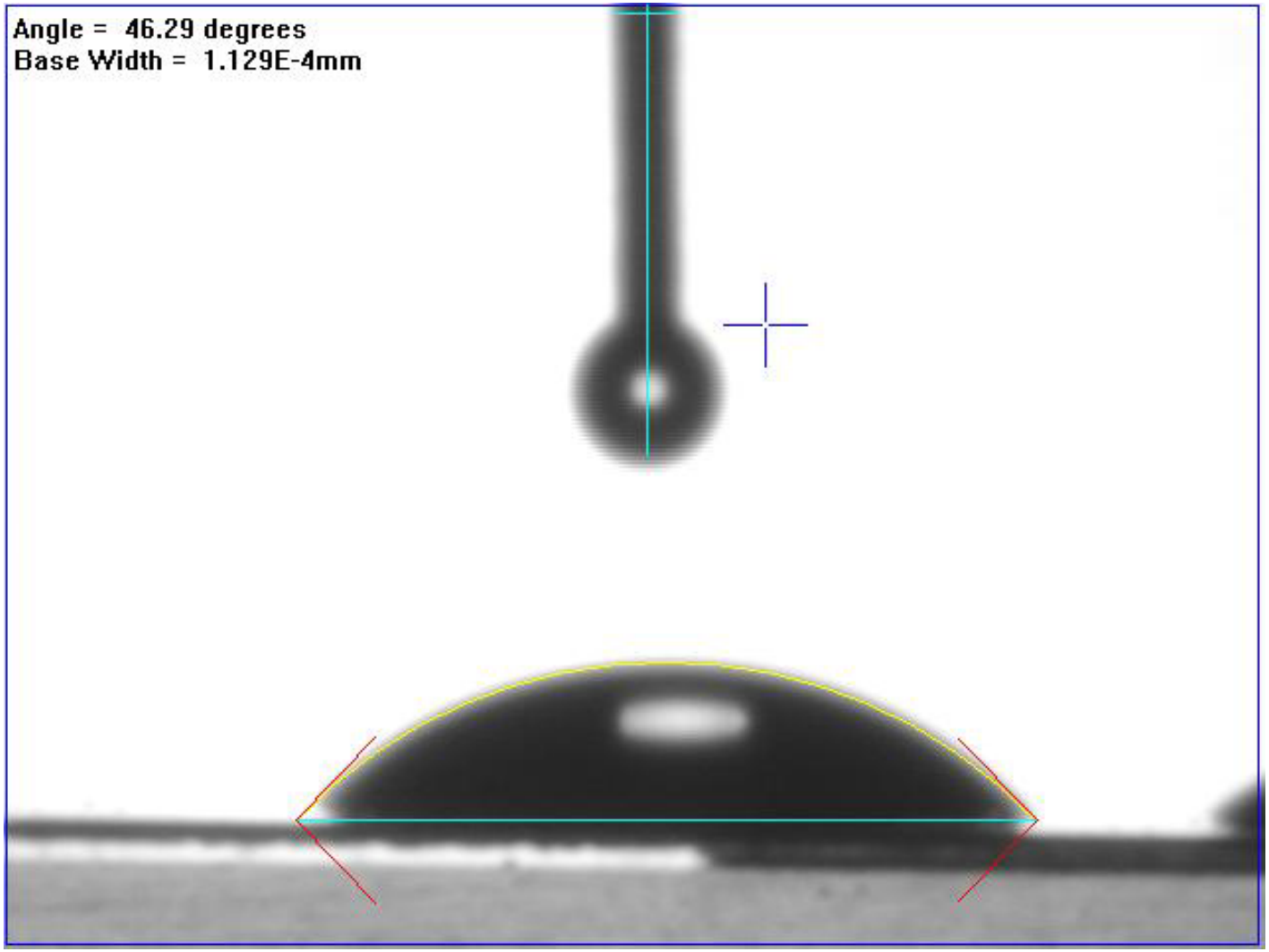

Figure A4. Contact Angle 3 of PET Sample (100 mTorr / 250 Watts)

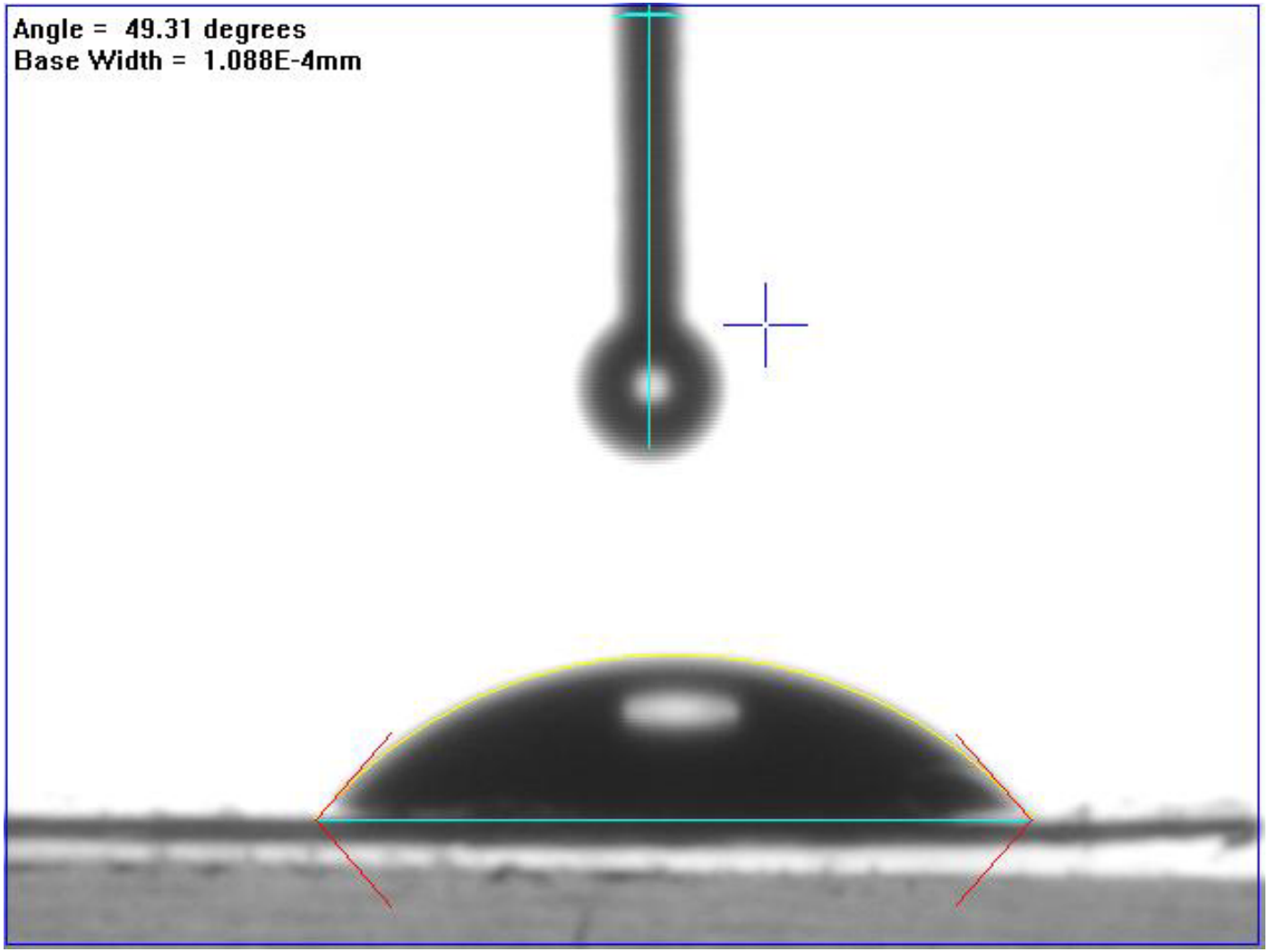

Figure A5. Contact Angle 1 of PET Sample (2.0 Torr / 250 Watts).

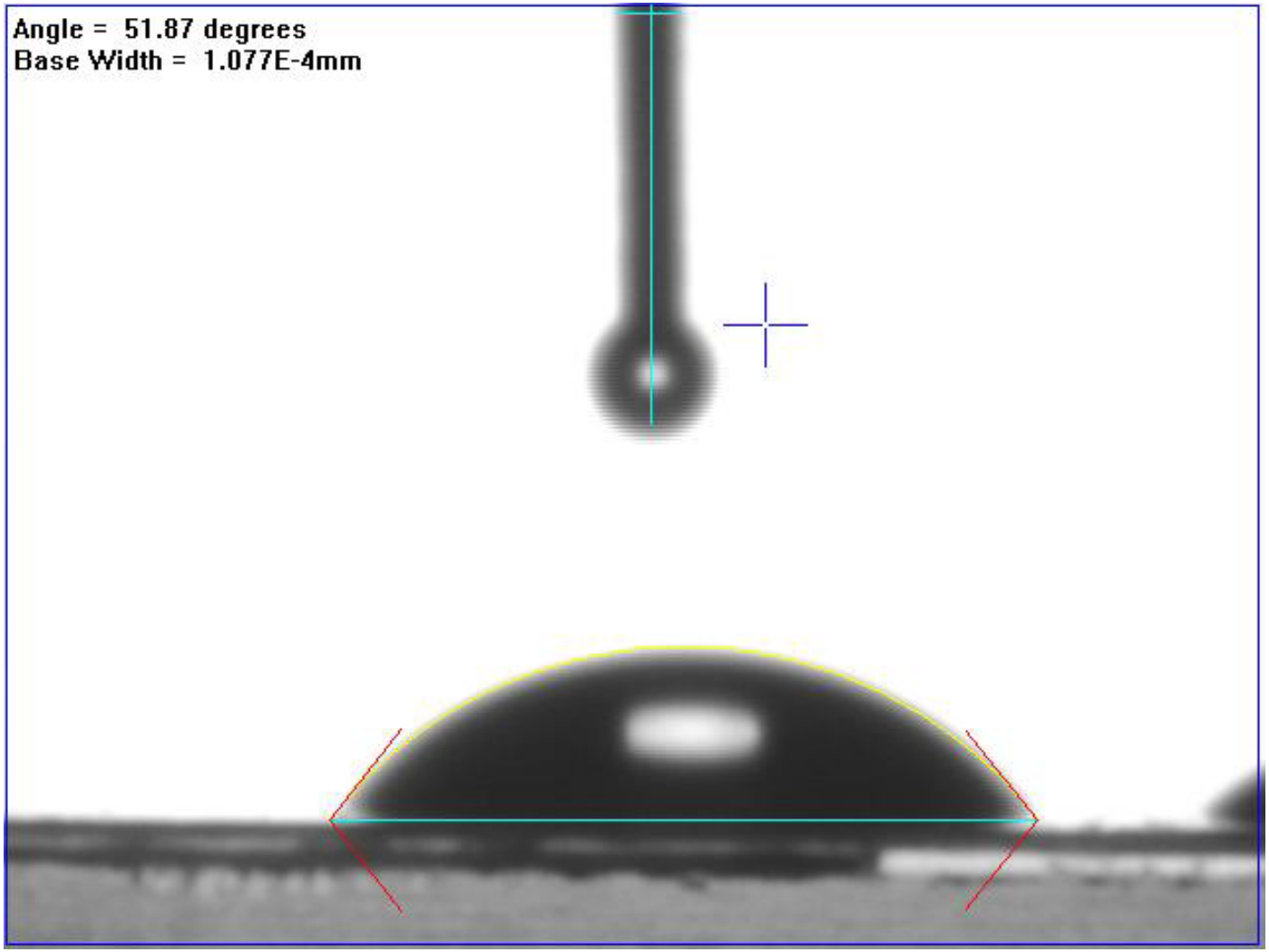

Figure A6. Contact Angle 2 of PET Sample (2.0 Torr / 250 Watts).

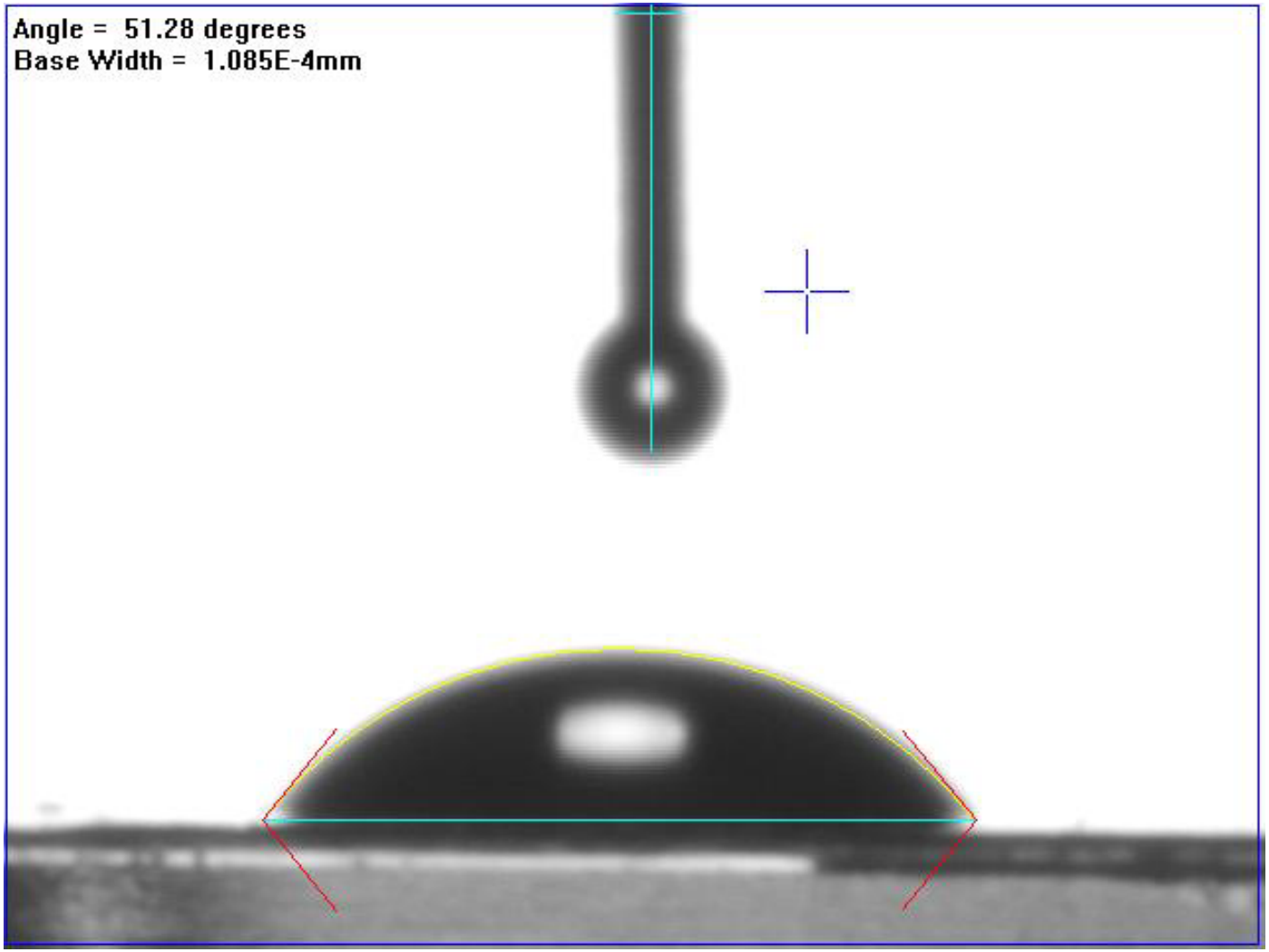

Figure A7. Contact Angle 3 of PET Sample (2.0 Torr / 250 Watts).

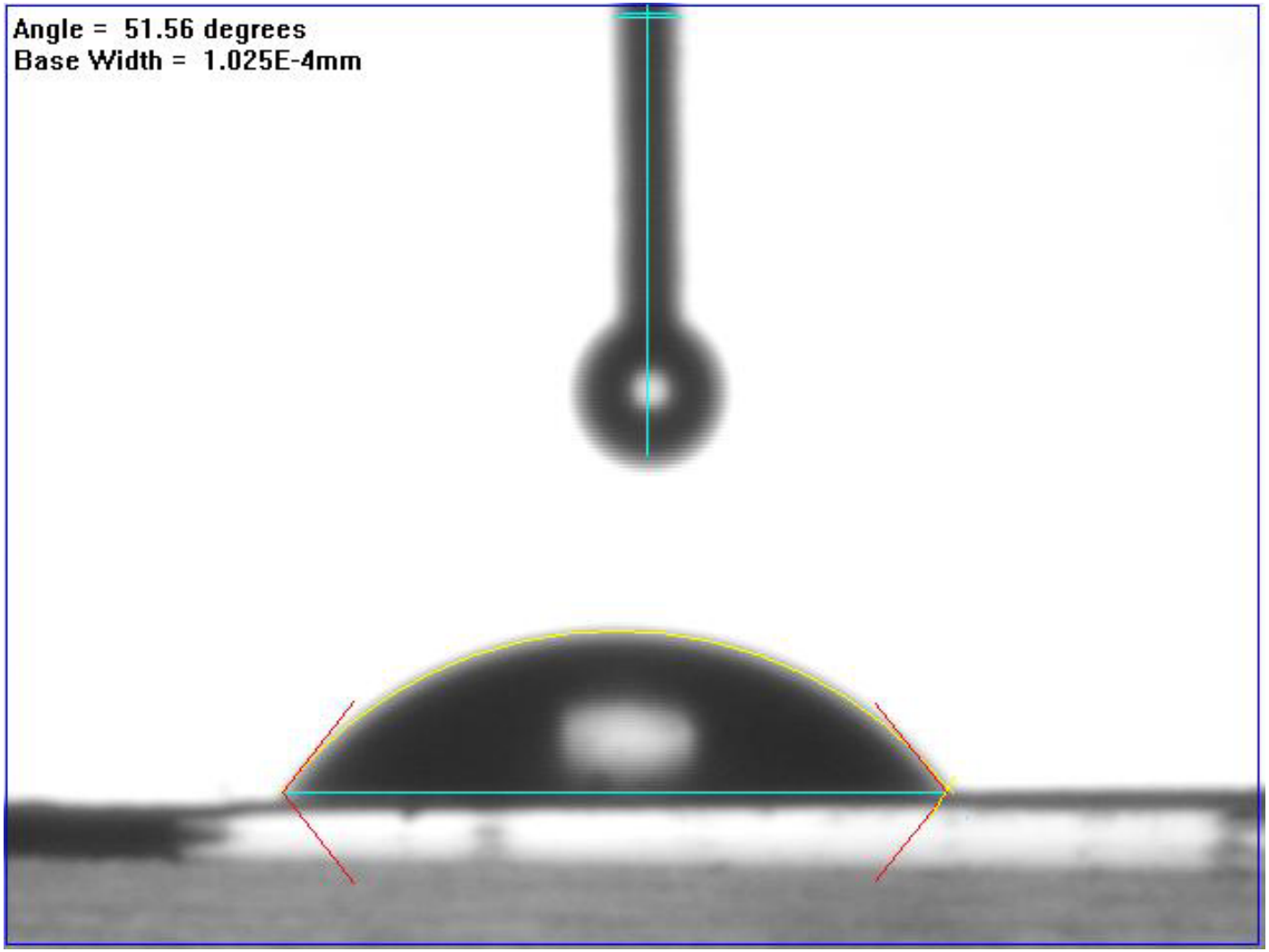

Figure A8. Contact Angle 1 of PET Sample (100 mTorr / 500 Watts).

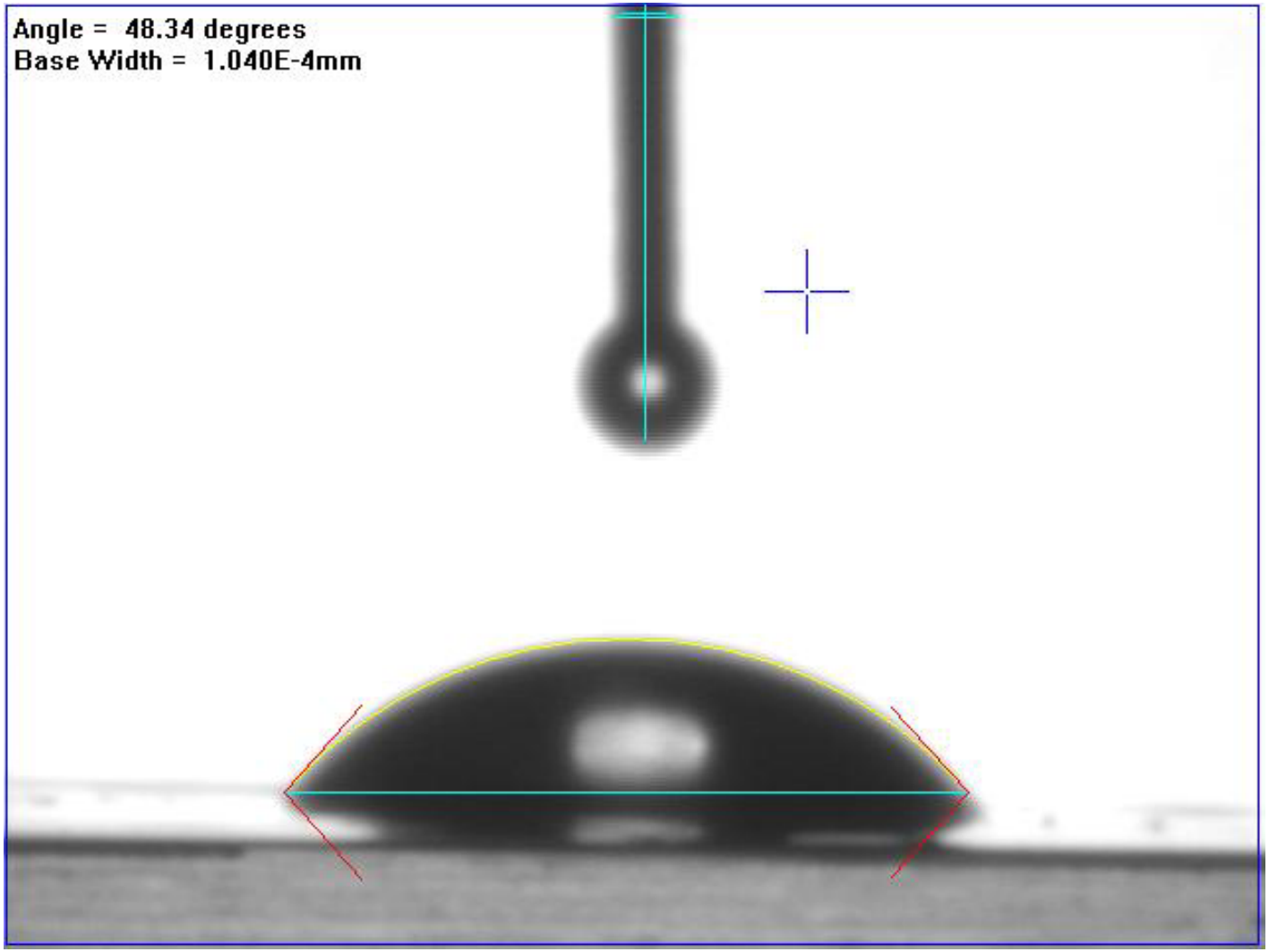

Figure A9. Contact Angle 2 of PET Sample (100 mTorr / 500 Watts).

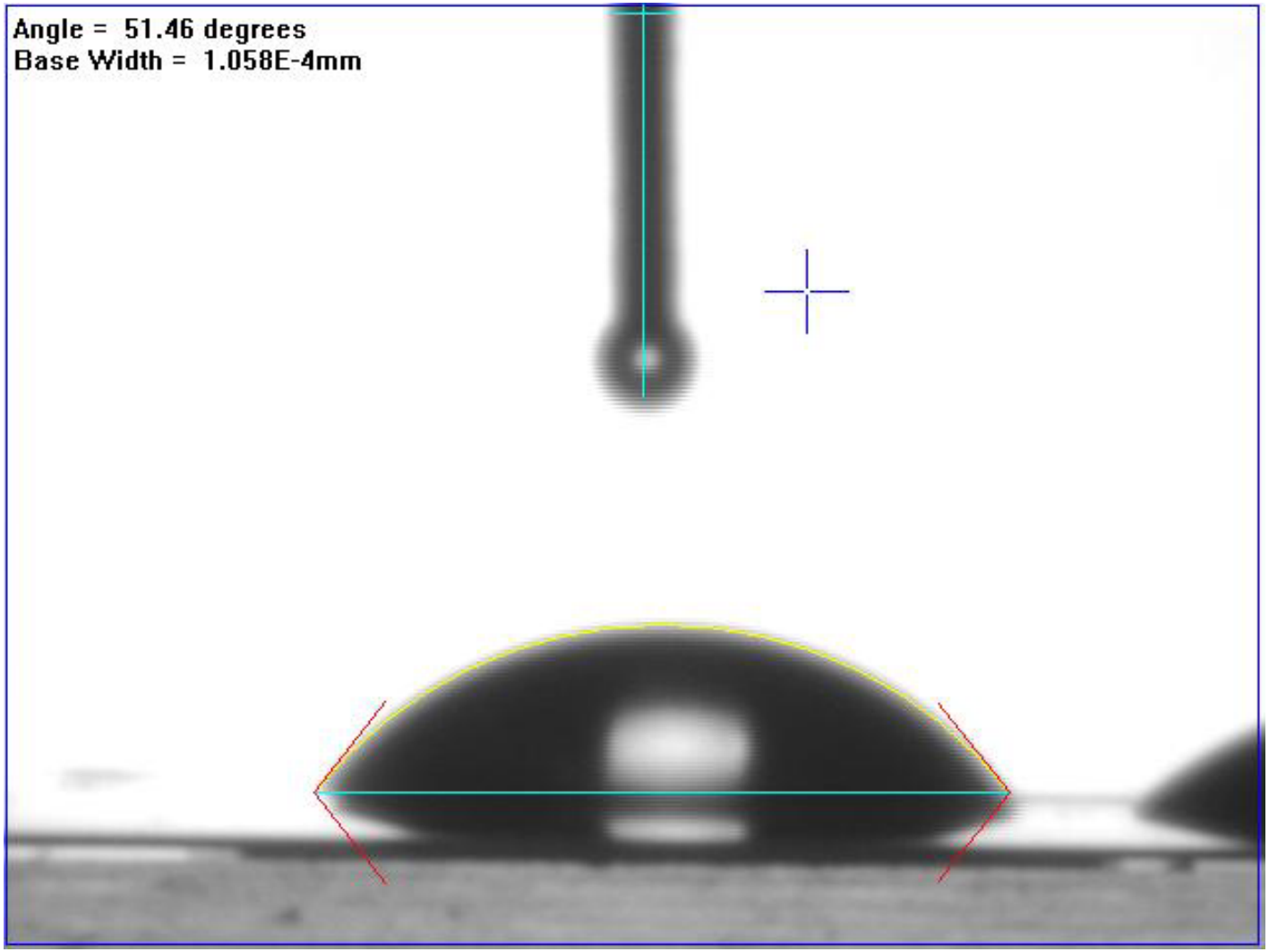

Figure A10. Contact Angle 3 of PET Sample (100 mTorr / 500 Watts).

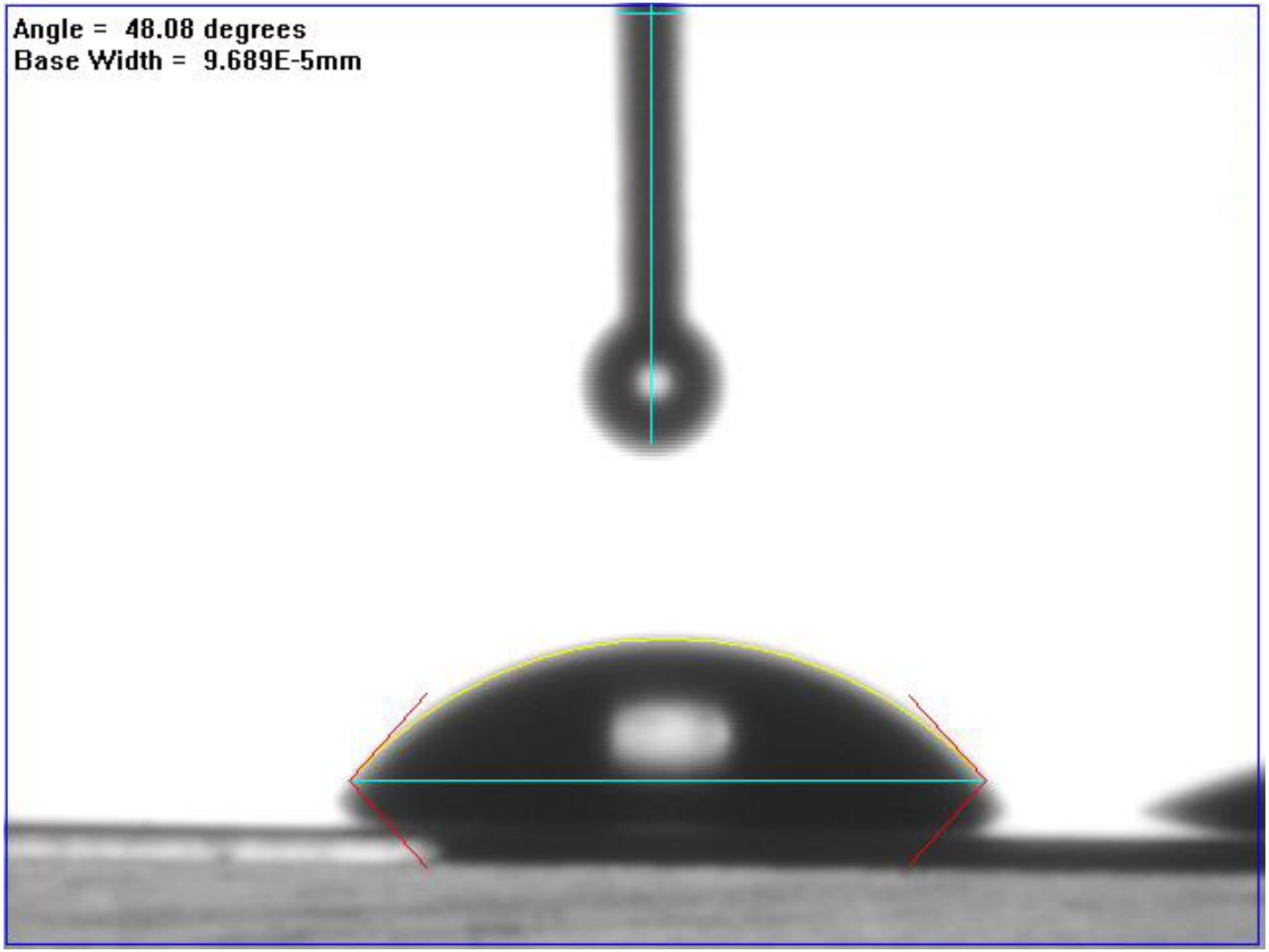

Figure A11. Contact Angle 1 of PET Sample (2.0 Torr / 500 Watts).

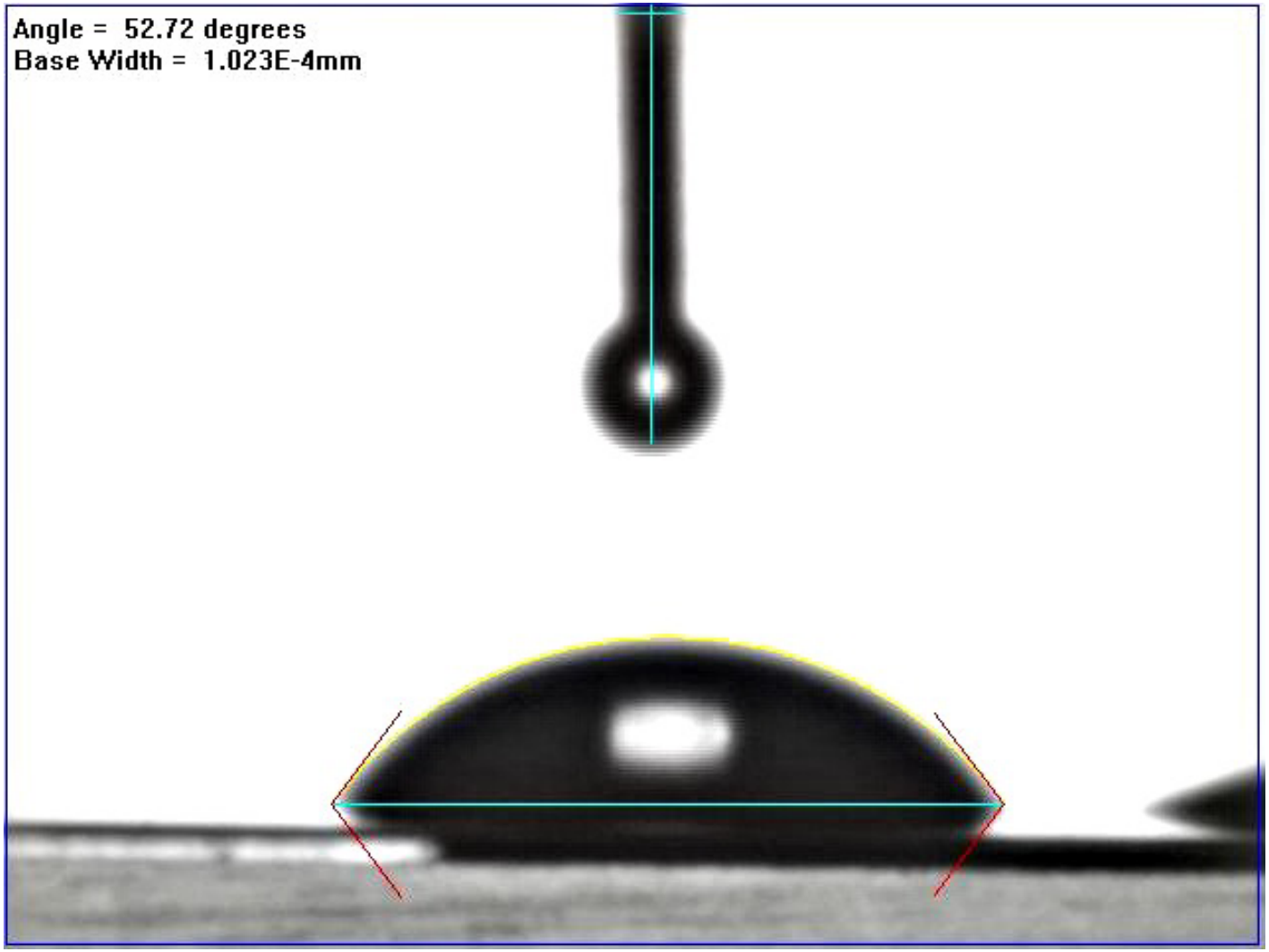

Figure A12. Contact Angle 2 of PET Sample (2.0 Torr / 500 Watts).

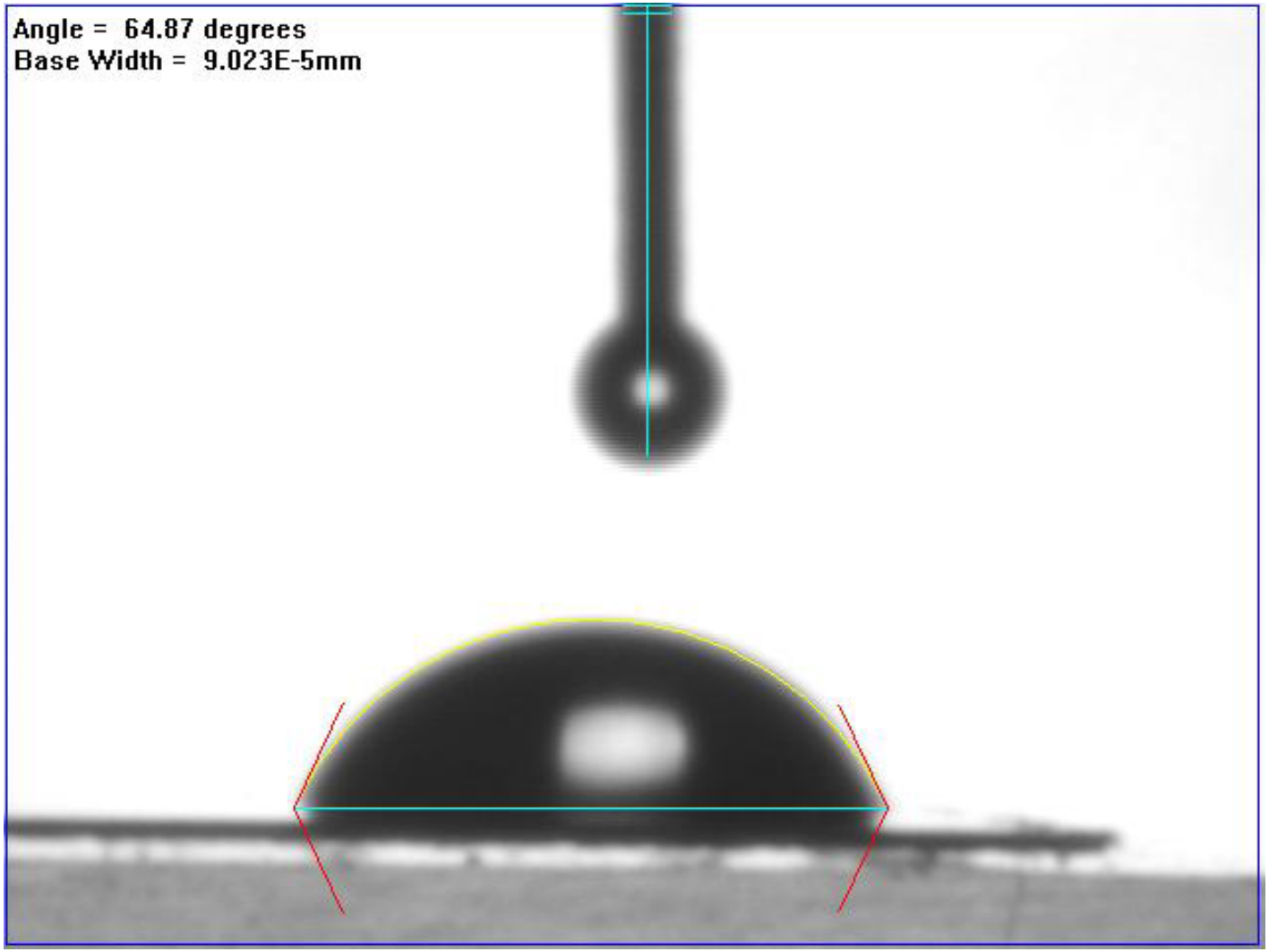

Figure A13. Contact Angle 3 of PET Sample (2.0 Torr / 500 Watts).

Appendix B

Process Spectra

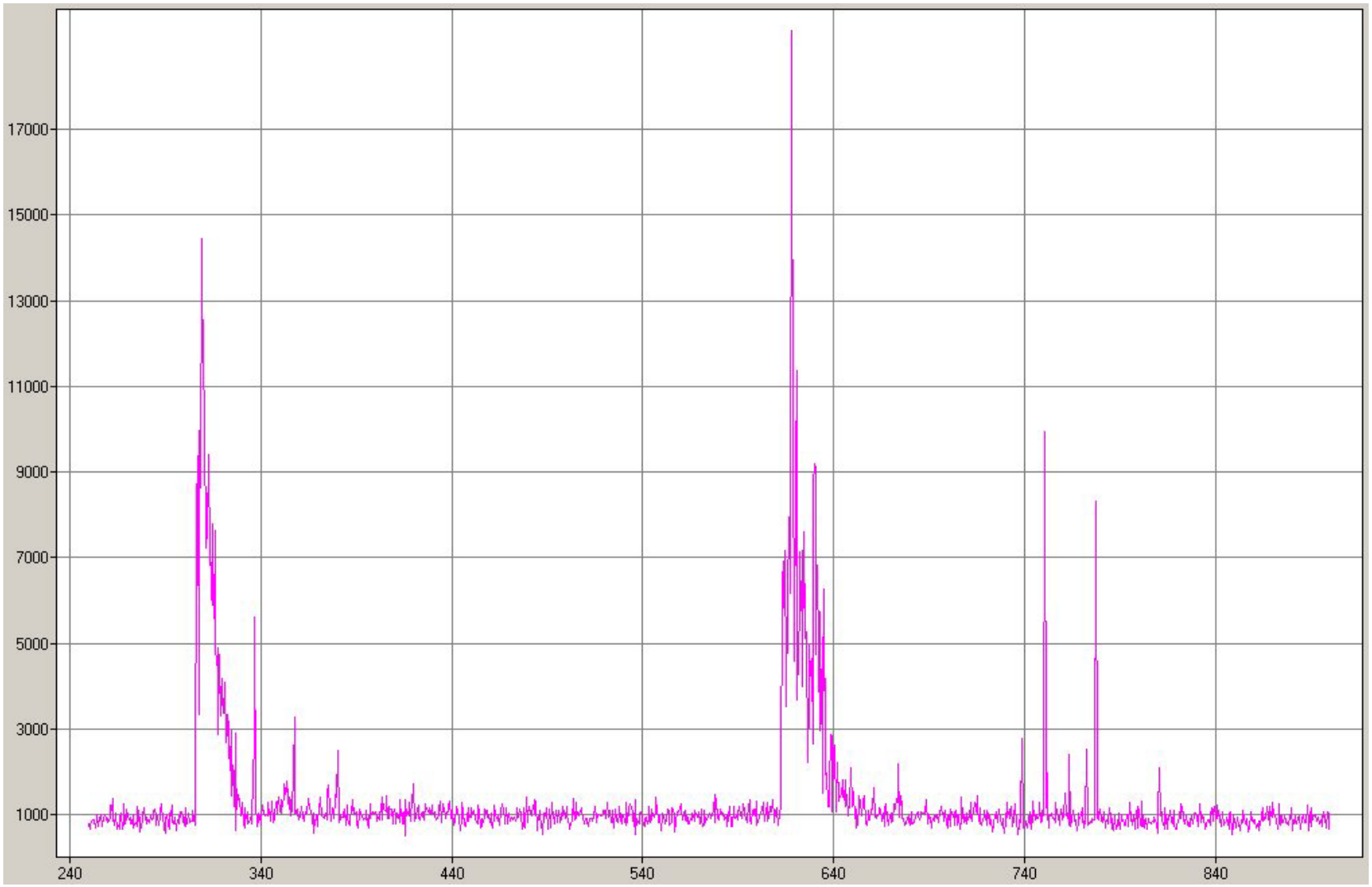

Figure B1. Process Spectrum at 100 mTorr/250Watts (t=3 minutes).

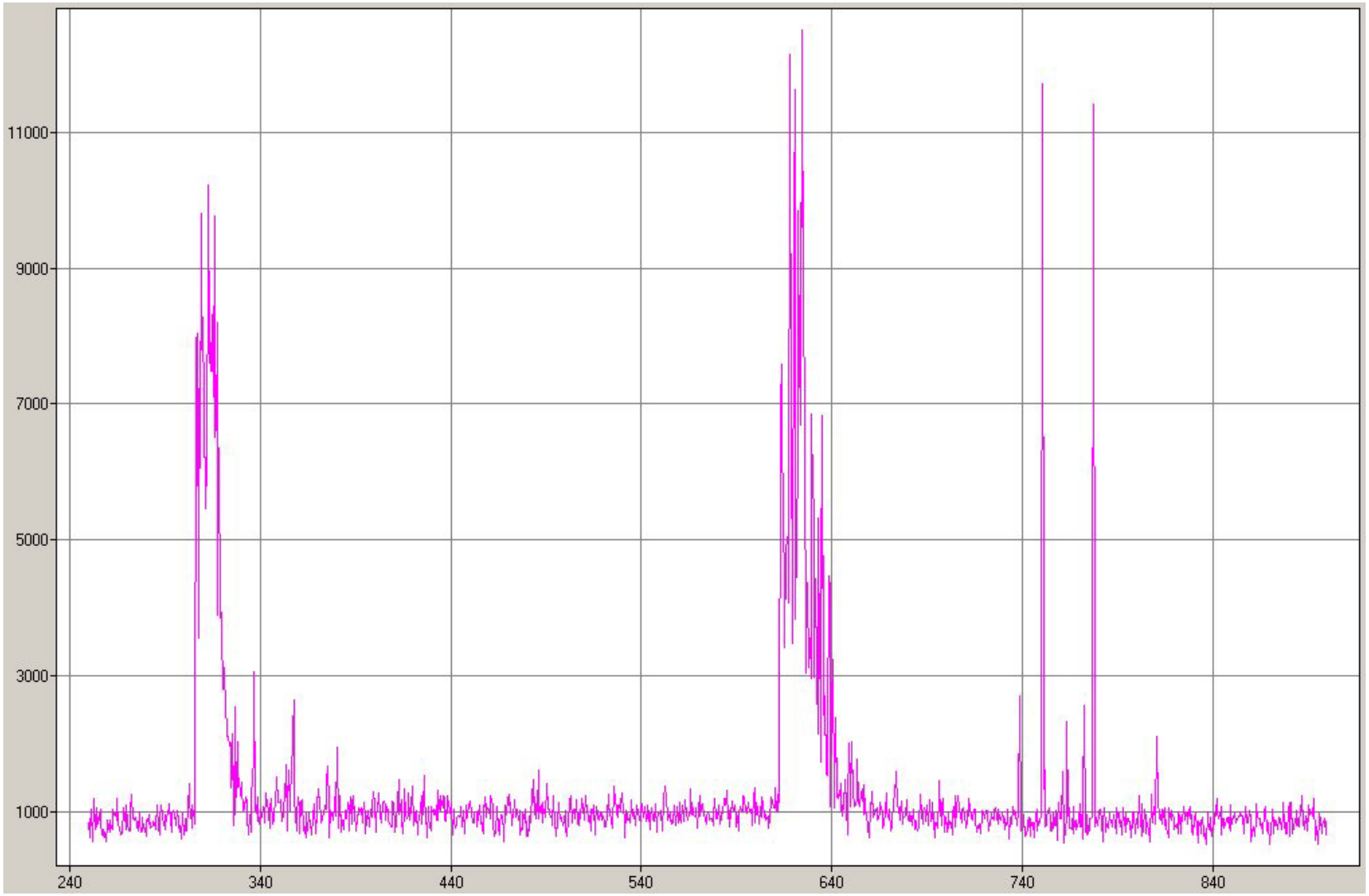

Figure B2. Process Spectrum at 100 mTorr/250Watts (t=6 minutes).

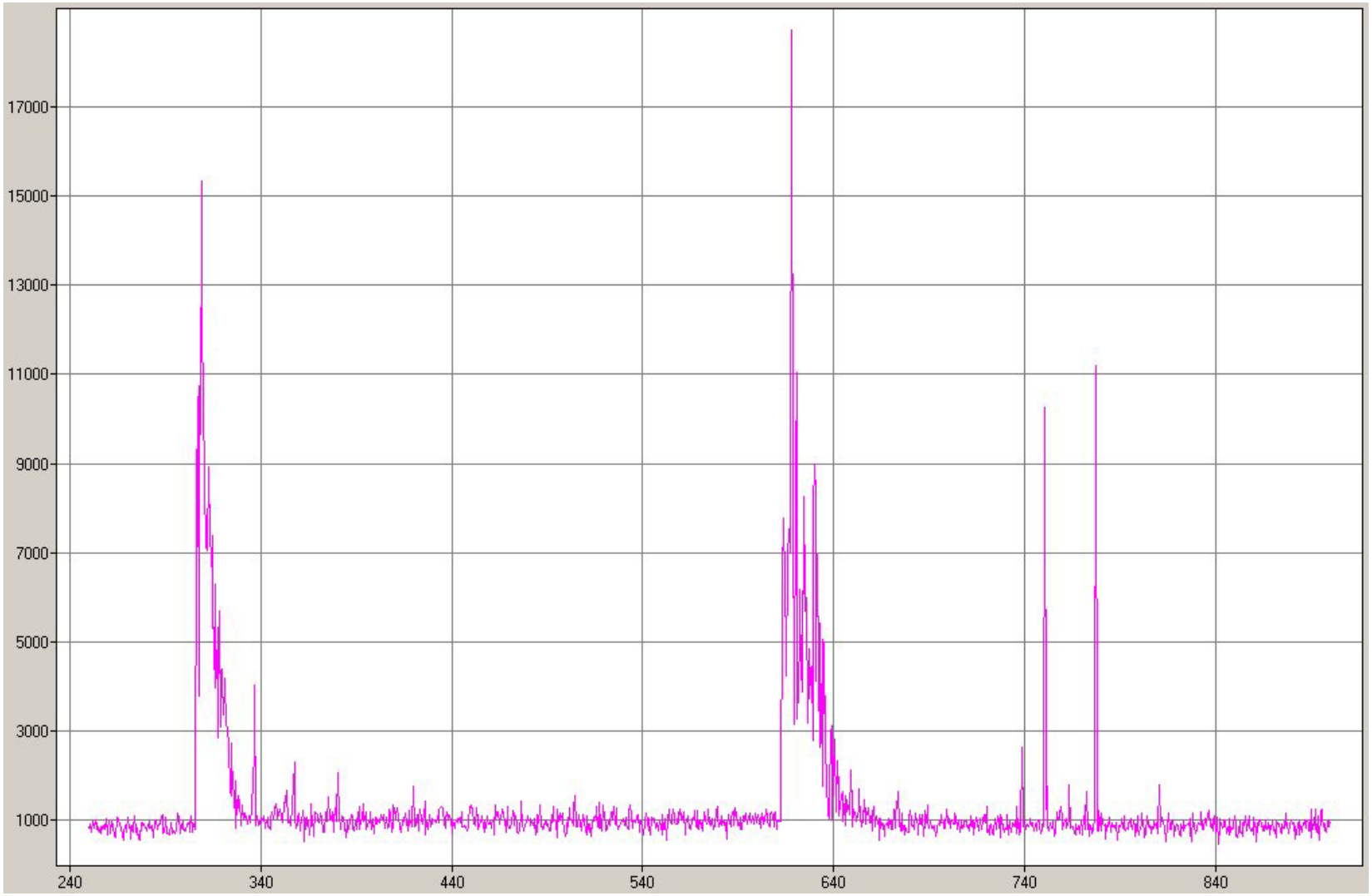

Figure B3. Process Spectrum at 100 mTorr/250Watts (t=9 minutes).

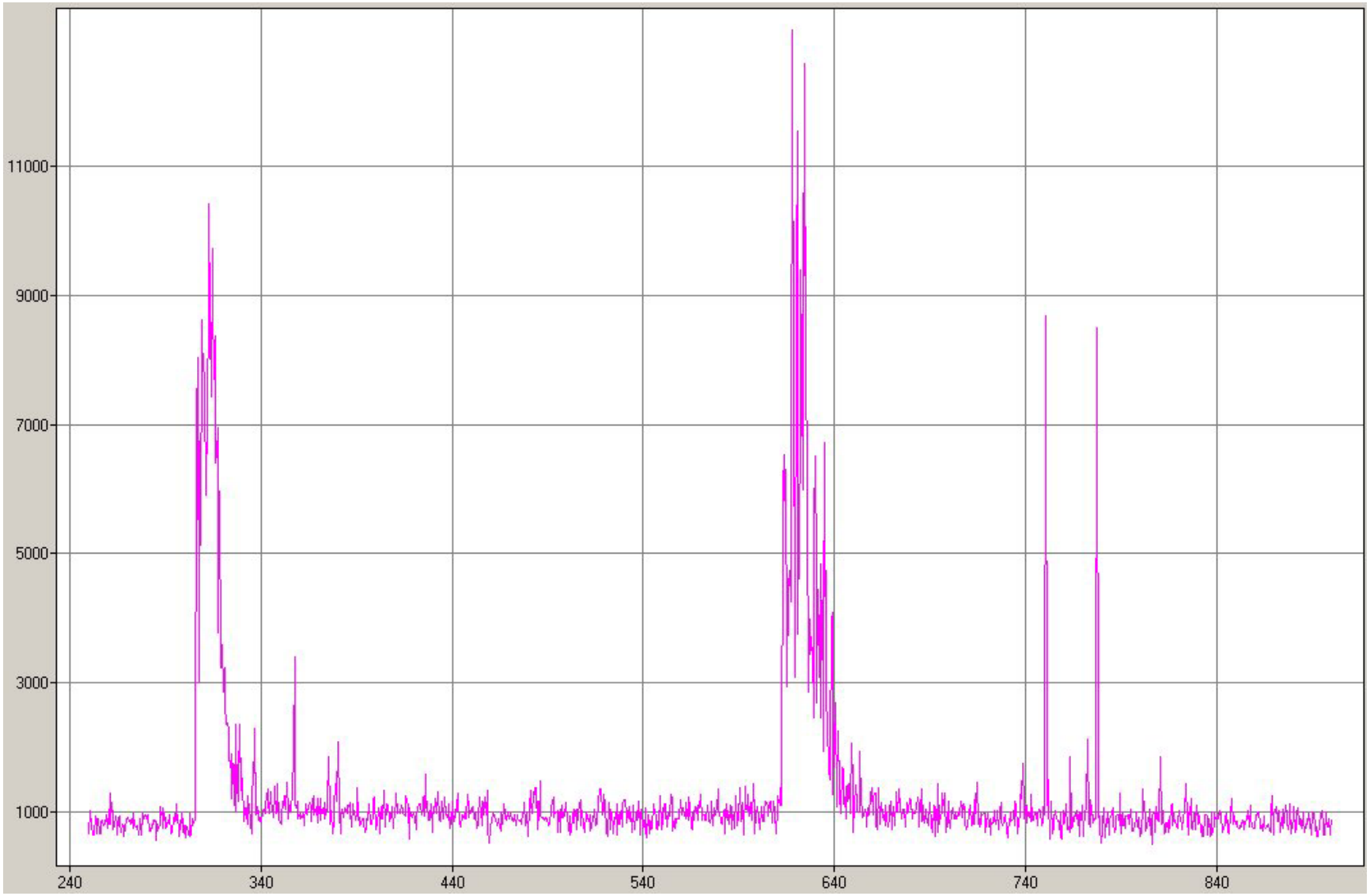

Figure B4. Process Spectrum at 100 mTorr/250Watts (t=12 minutes).

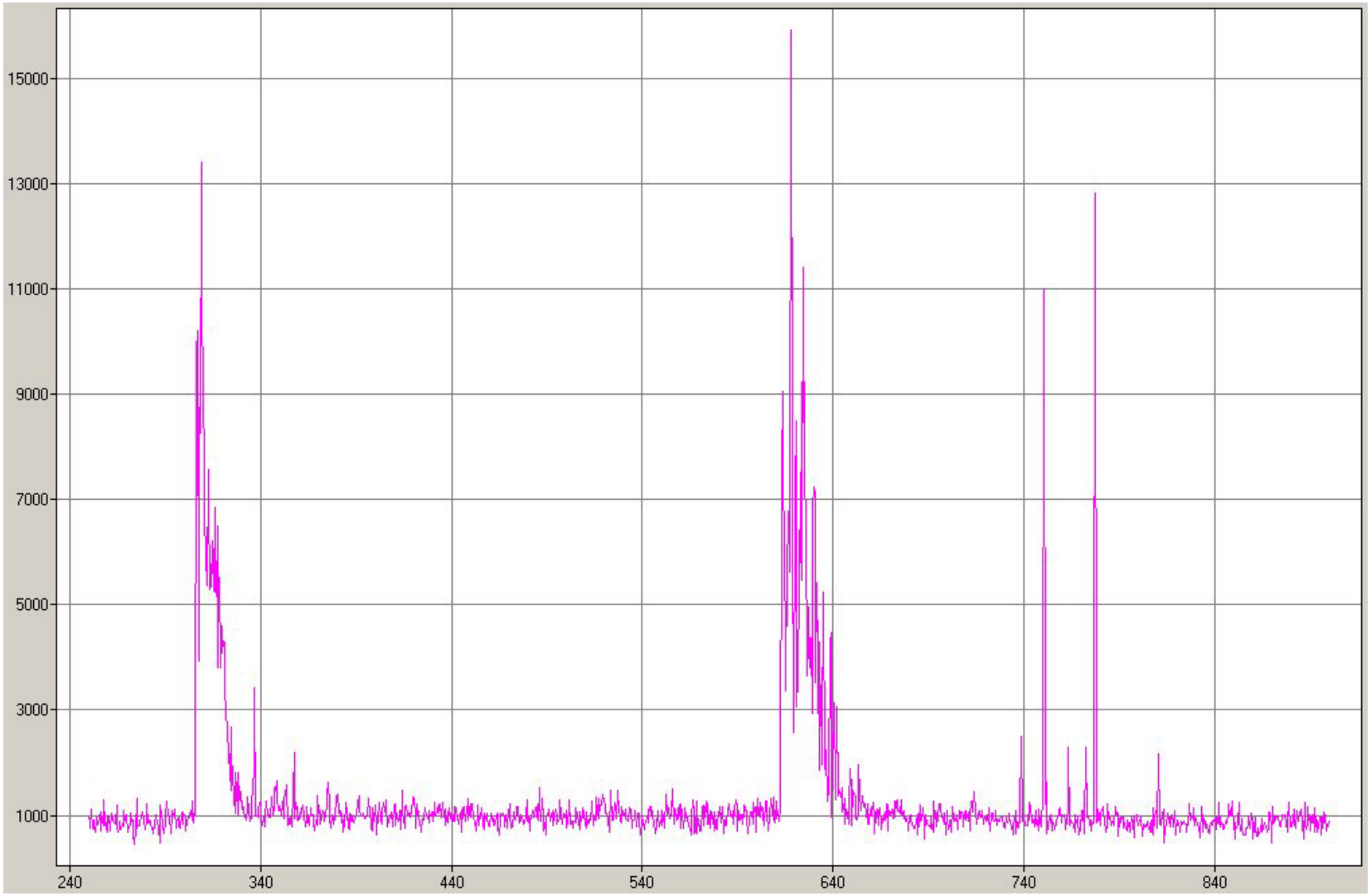

Figure B5. Process Spectrum at 100 mTorr/250Watts (t=15 minutes).

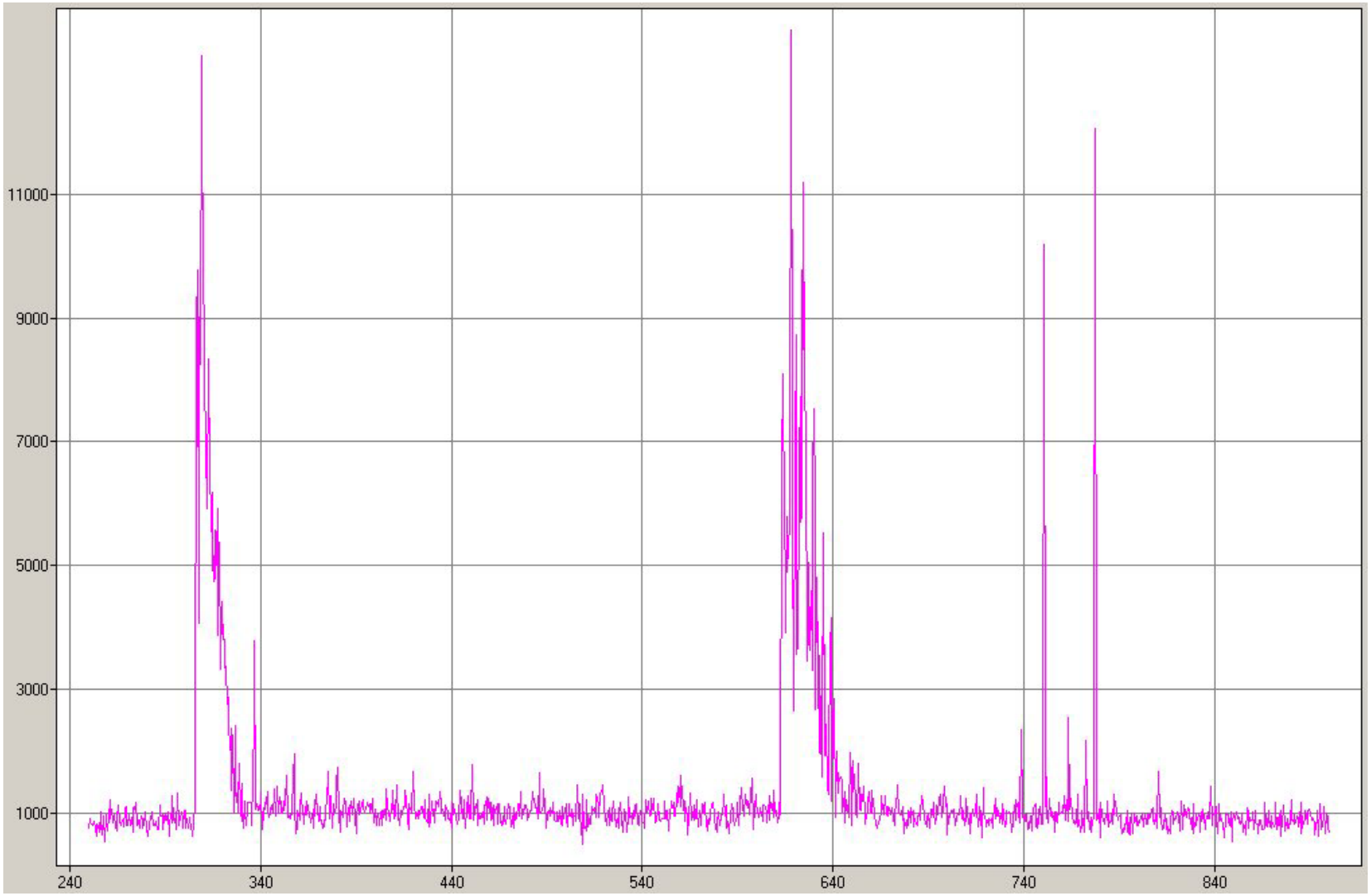

Figure B6. Process Spectrum at 100 mTorr/250Watts (t=18 minutes).

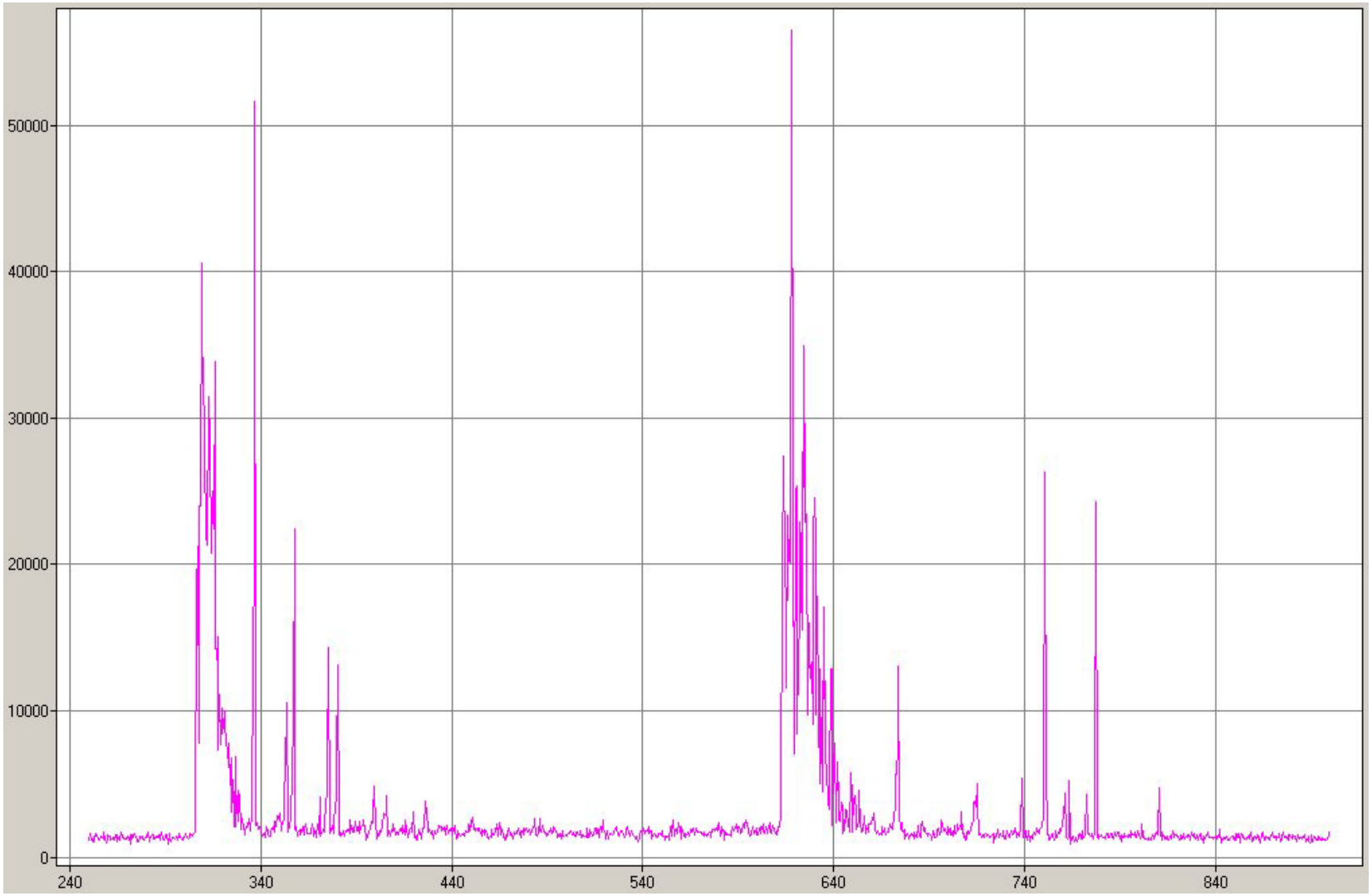

Figure B7. Process Spectrum at 2.0 Torr / 250Watts (t=3 minutes).

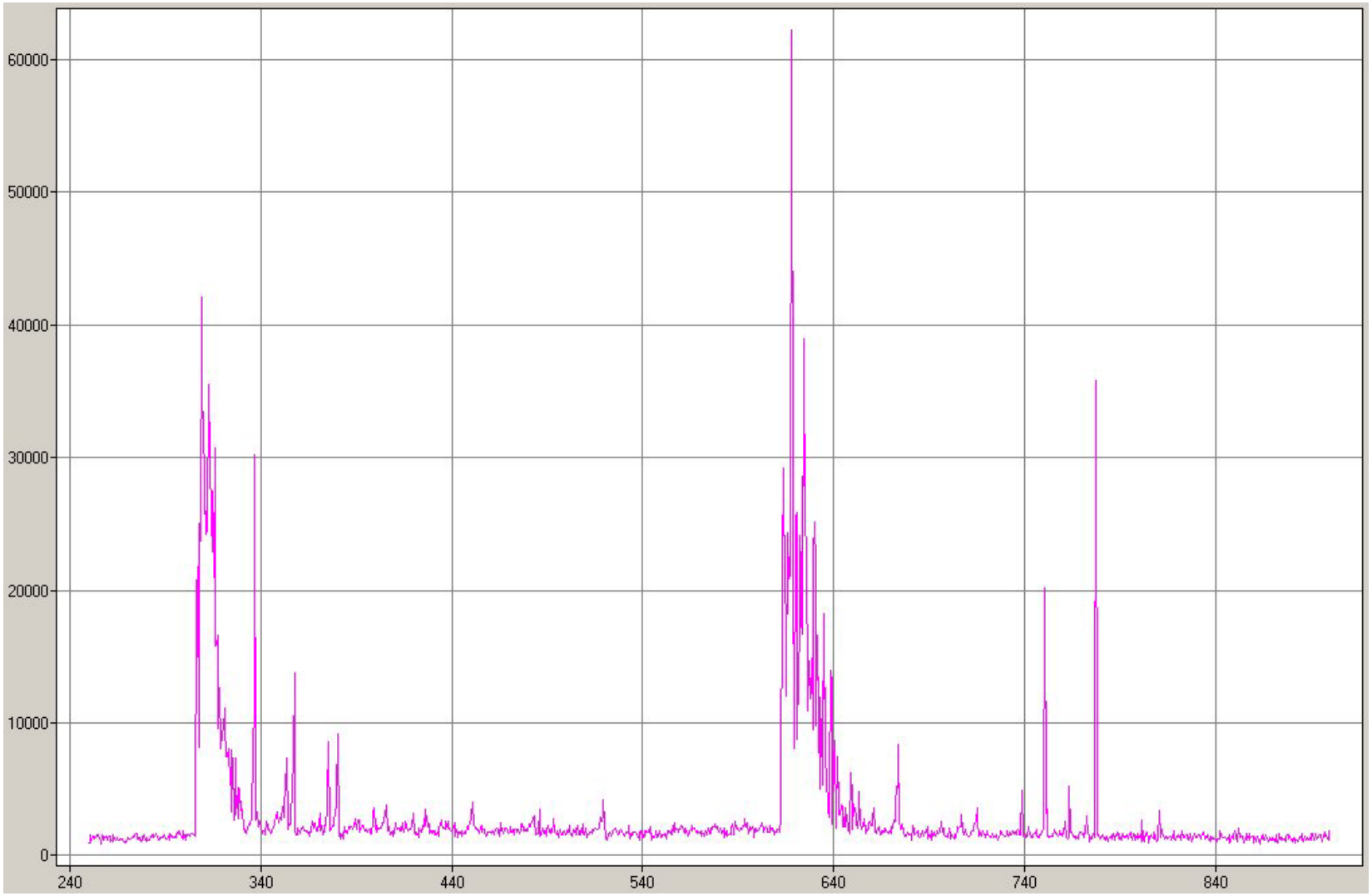

Figure B8. Process Spectrum at 2.0 Torr / 250Watts (t=6 minutes).

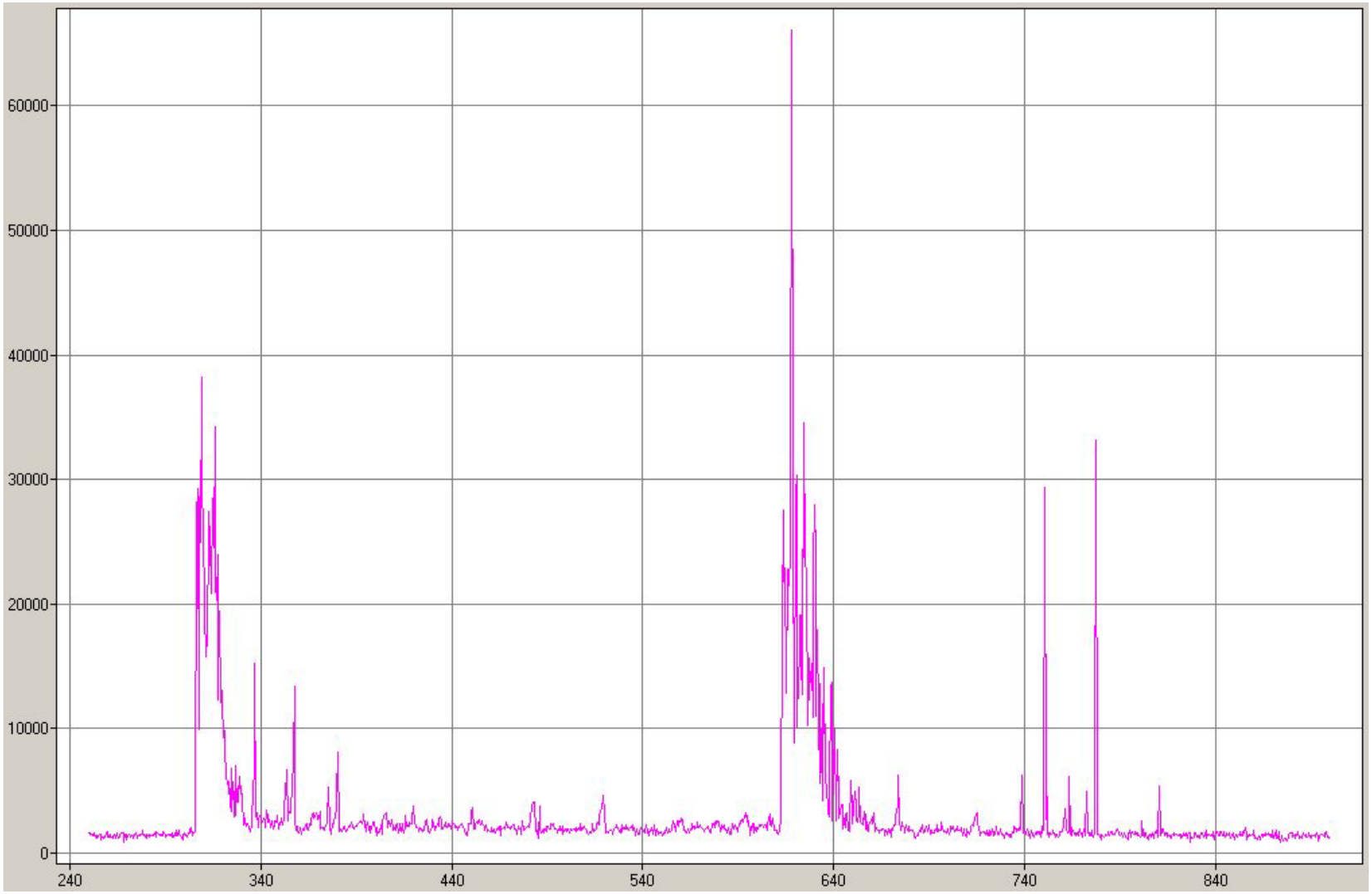

Figure B9. Process Spectrum at 2.0 Torr / 250Watts (t=9 minutes).

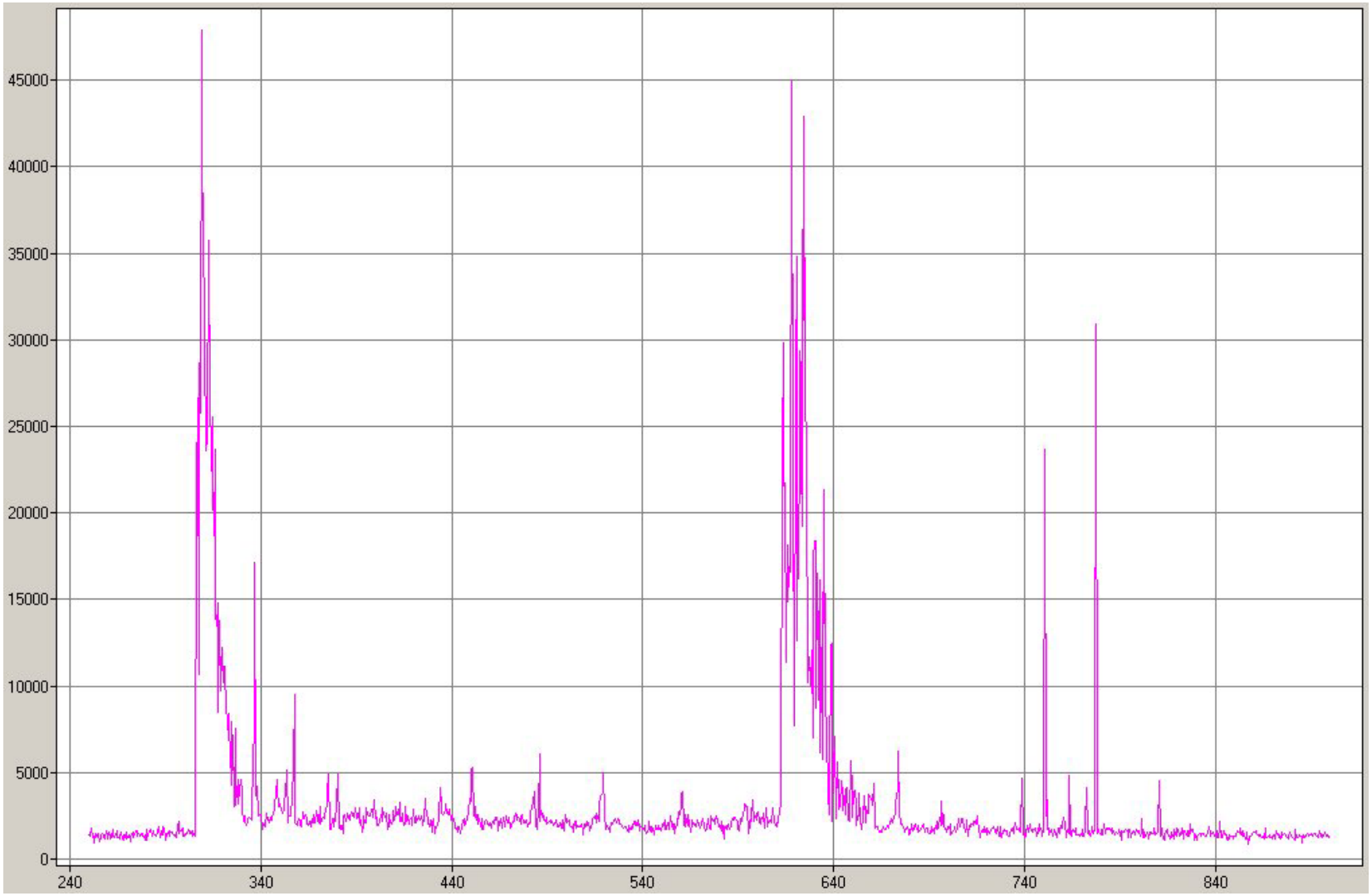

Figure B10. Process Spectrum at 2.0 Torr / 250Watts (t=12 minutes).

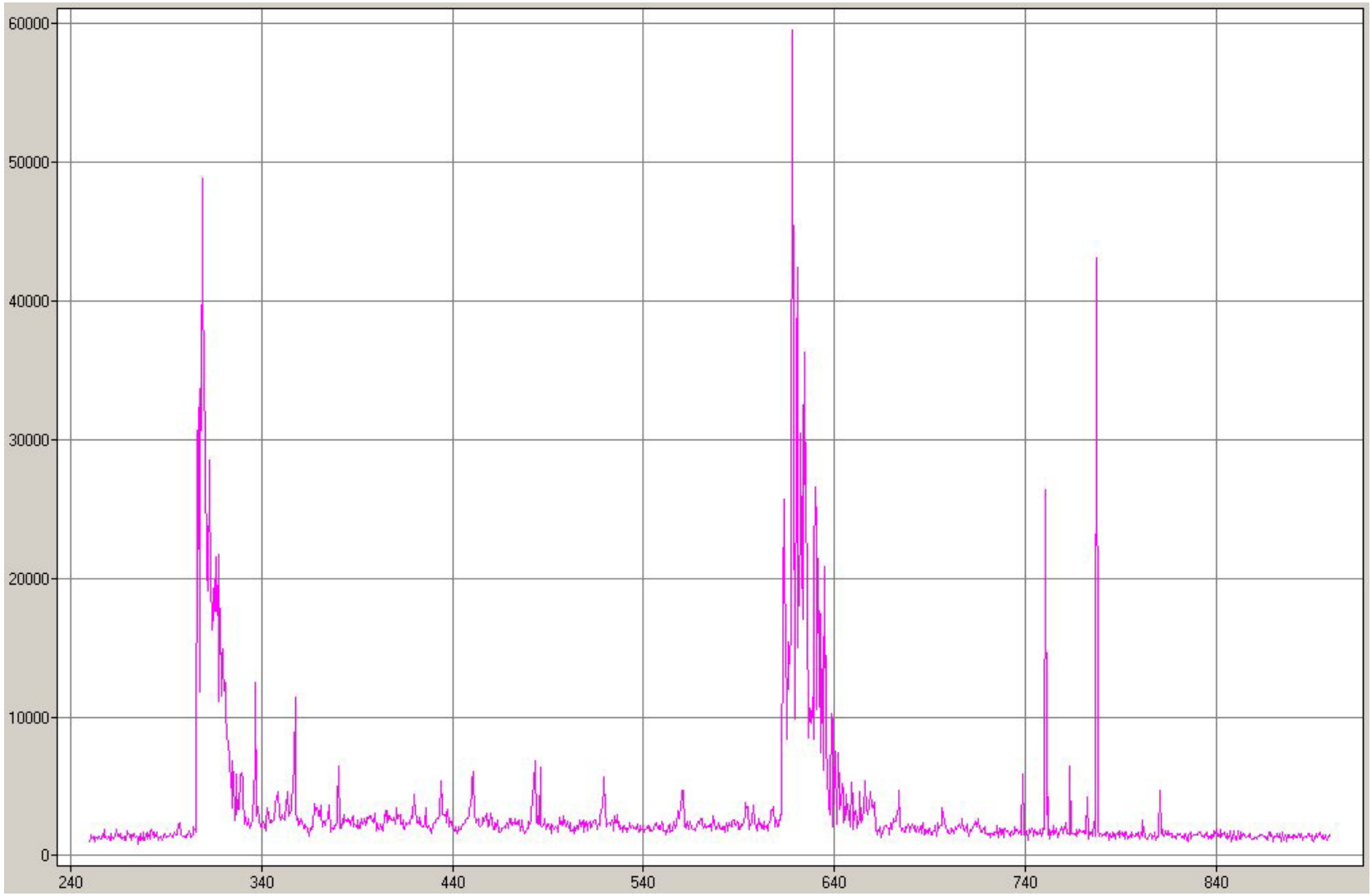

Figure B11. Process Spectrum at 2.0 Torr / 250Watts (t=15 minutes).

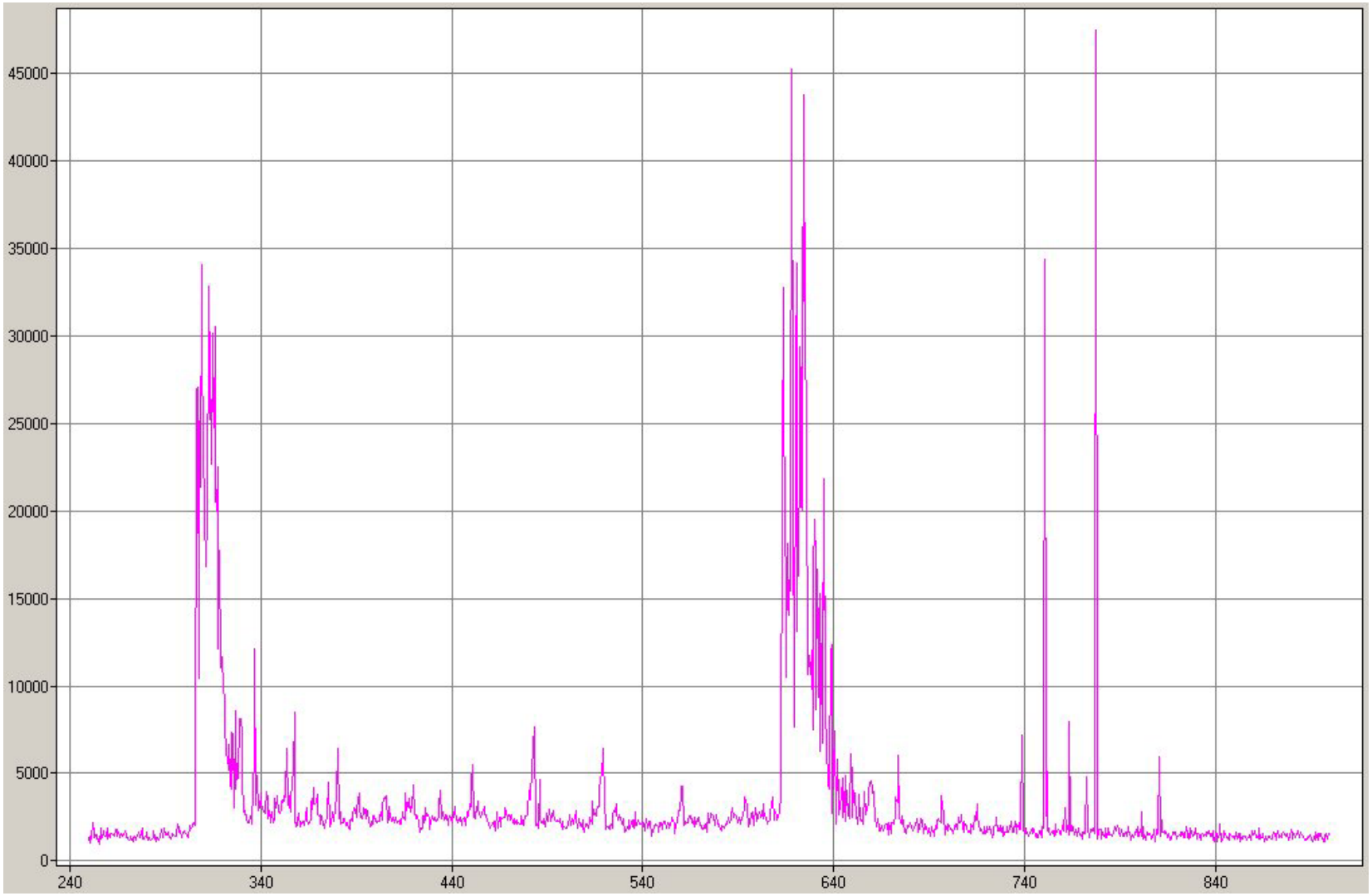

Figure B12. Process Spectrum at 2.0 Torr / 250Watts (t=18 minutes).

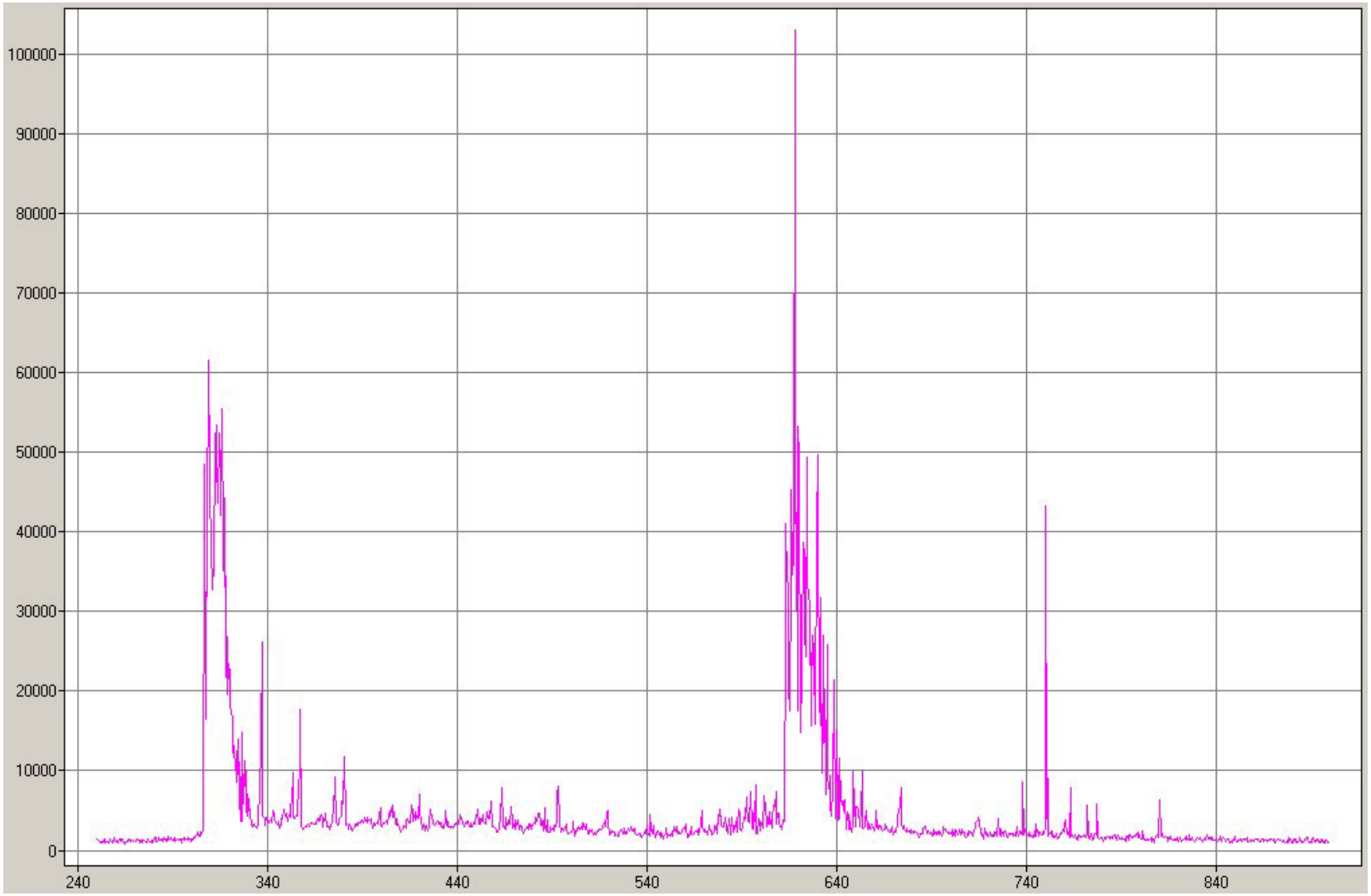

Figure B13. Process Spectrum at 100 mTorr / 500Watts (t=3 minutes).

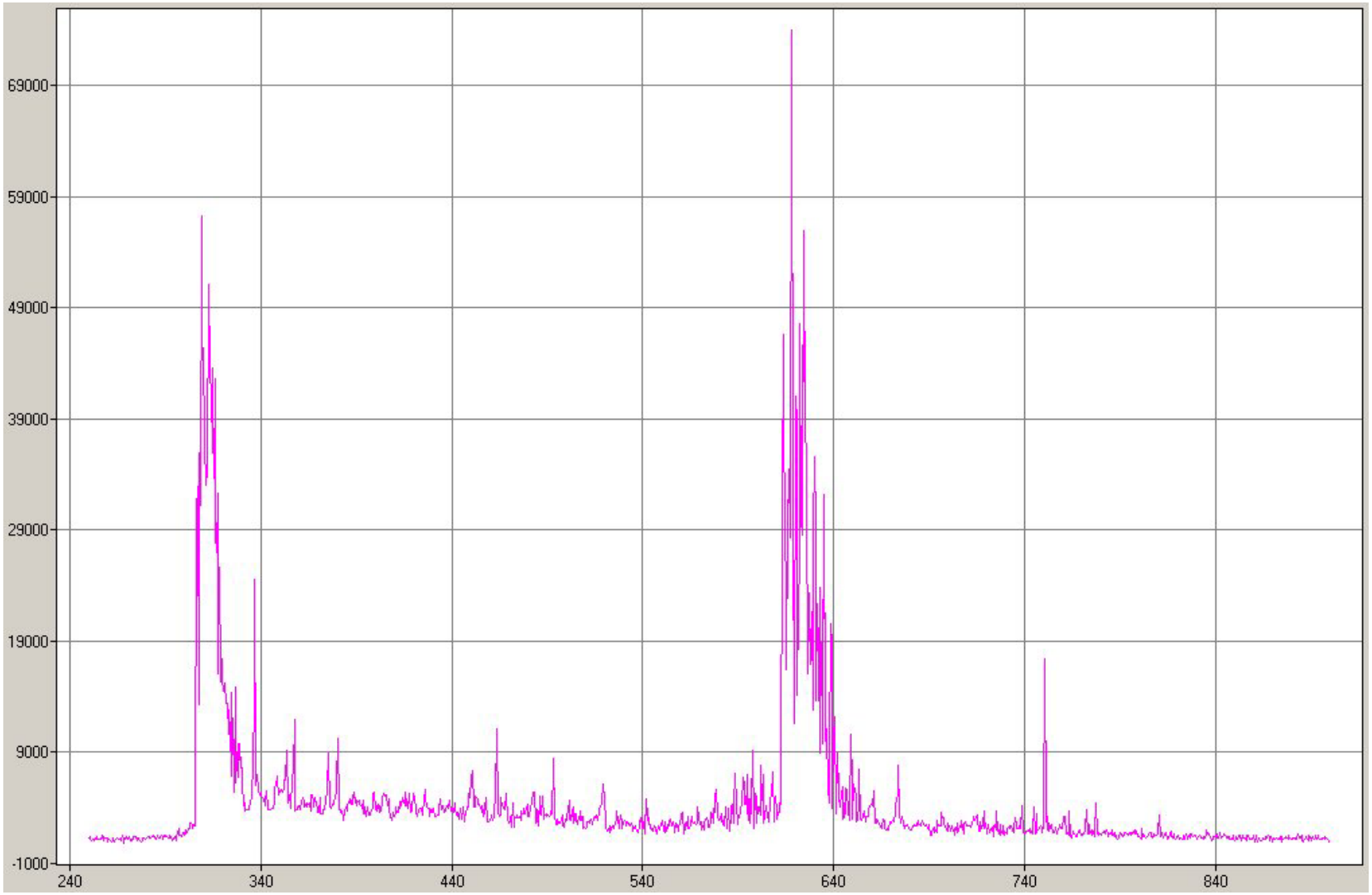

Figure B14. Process Spectrum at 100 mTorr / 500Watts (t=6 minutes).

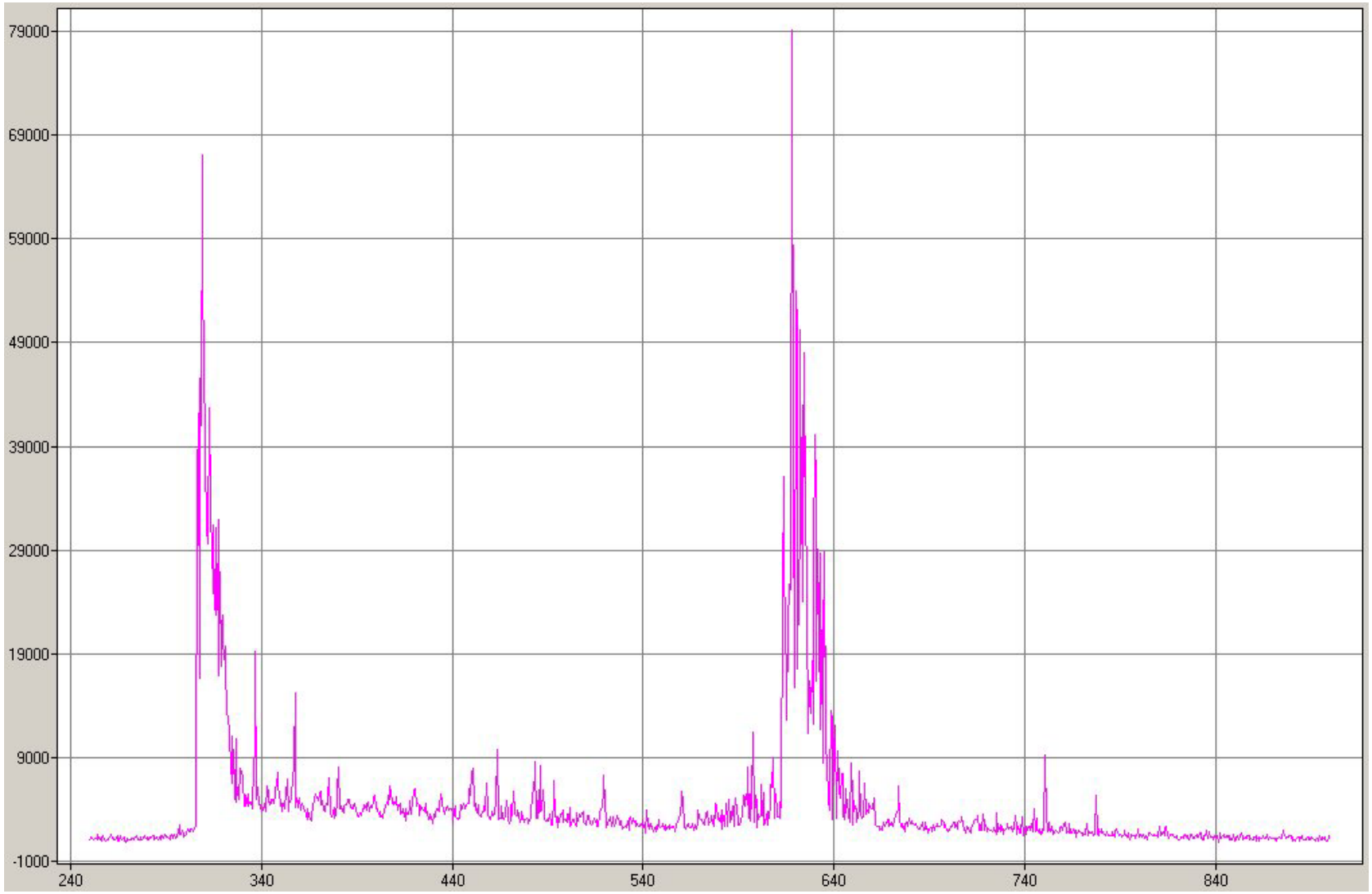

Figure B15. Process Spectrum at 100 mTorr / 500Watts (t=9 minutes).

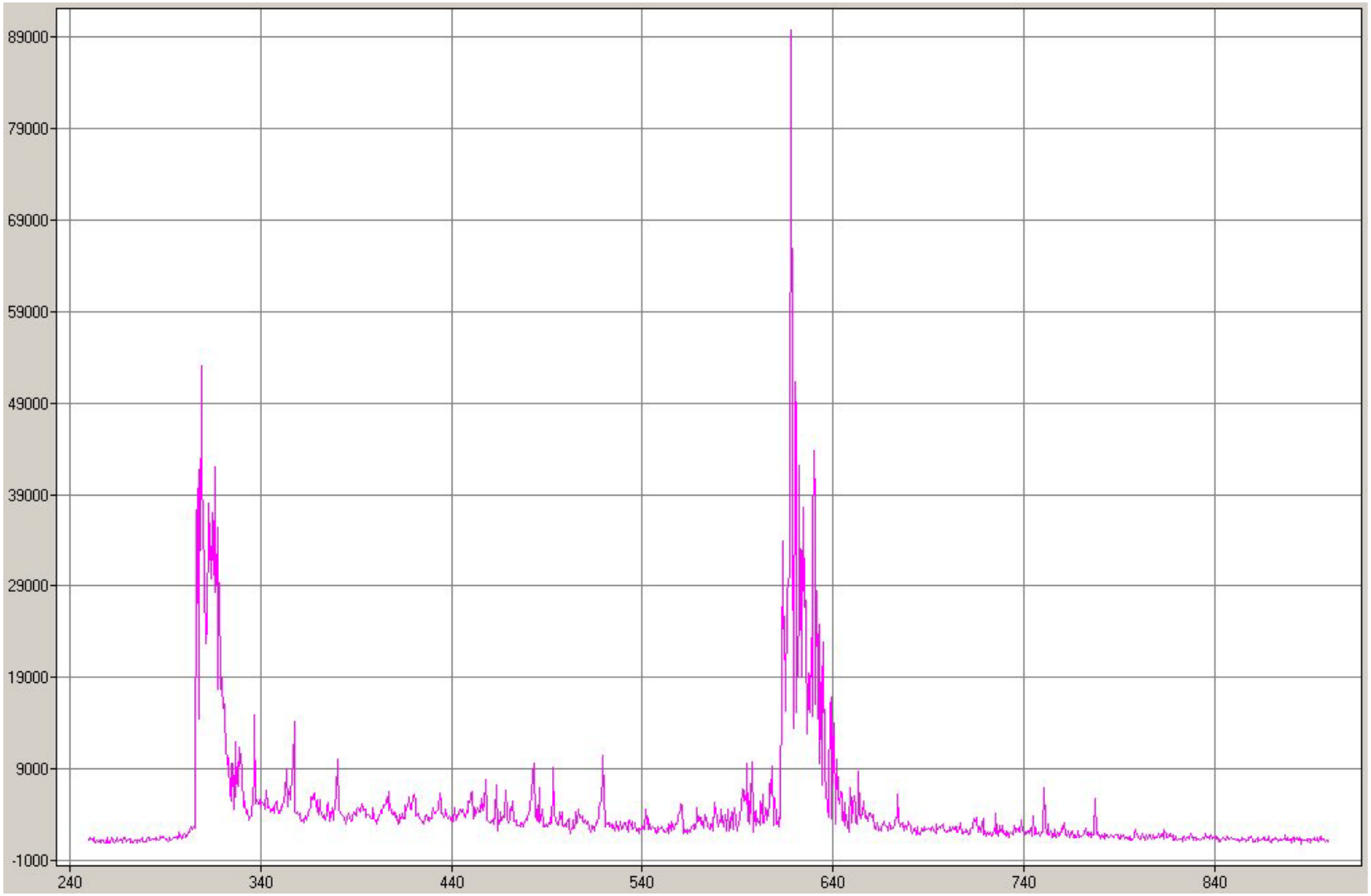

Figure B16. Process Spectrum at 100 mTorr / 500Watts (t=12 minutes).

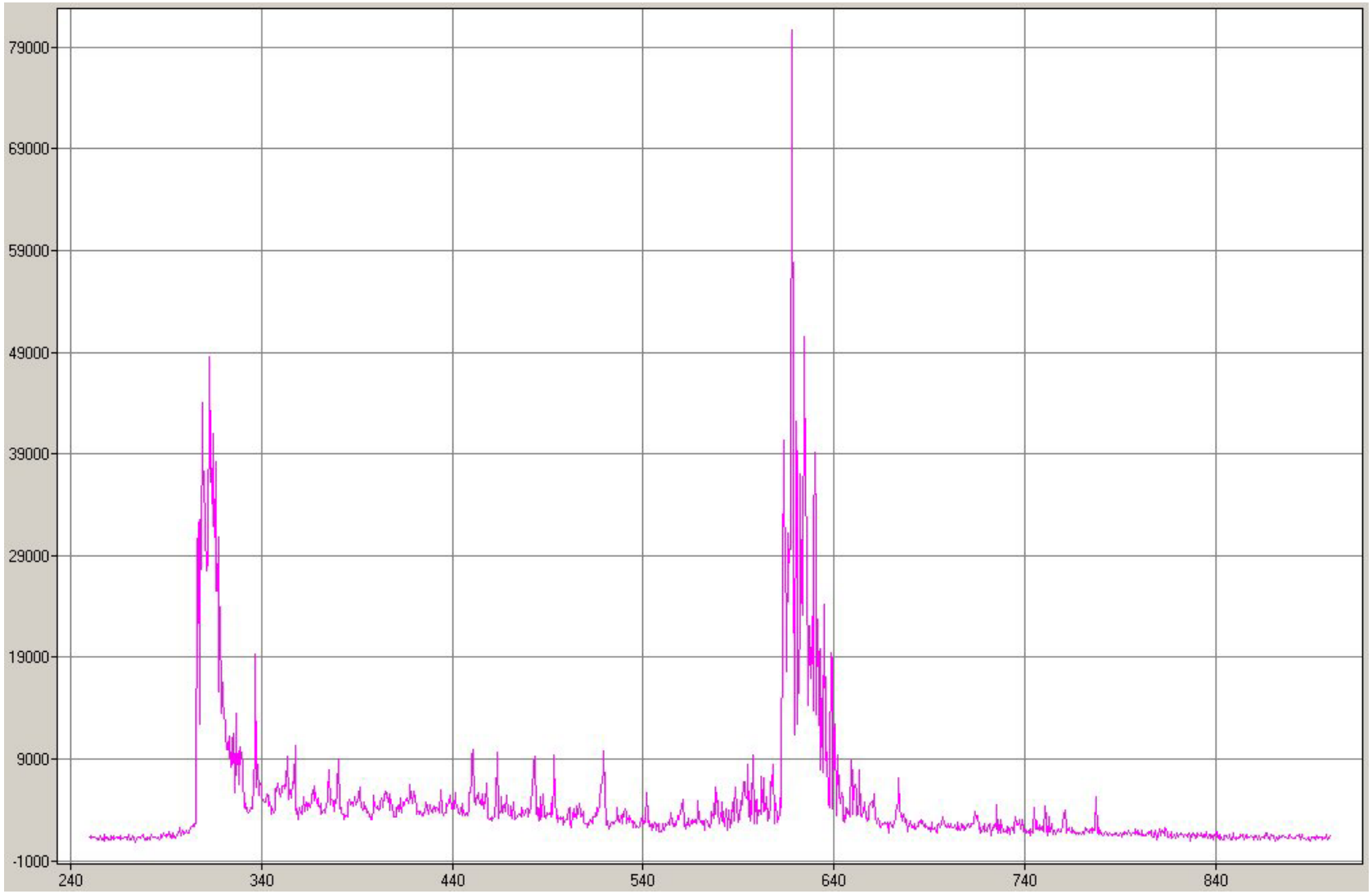

Figure B17. Process Spectrum at 100 mTorr / 500Watts (t=15 minutes).

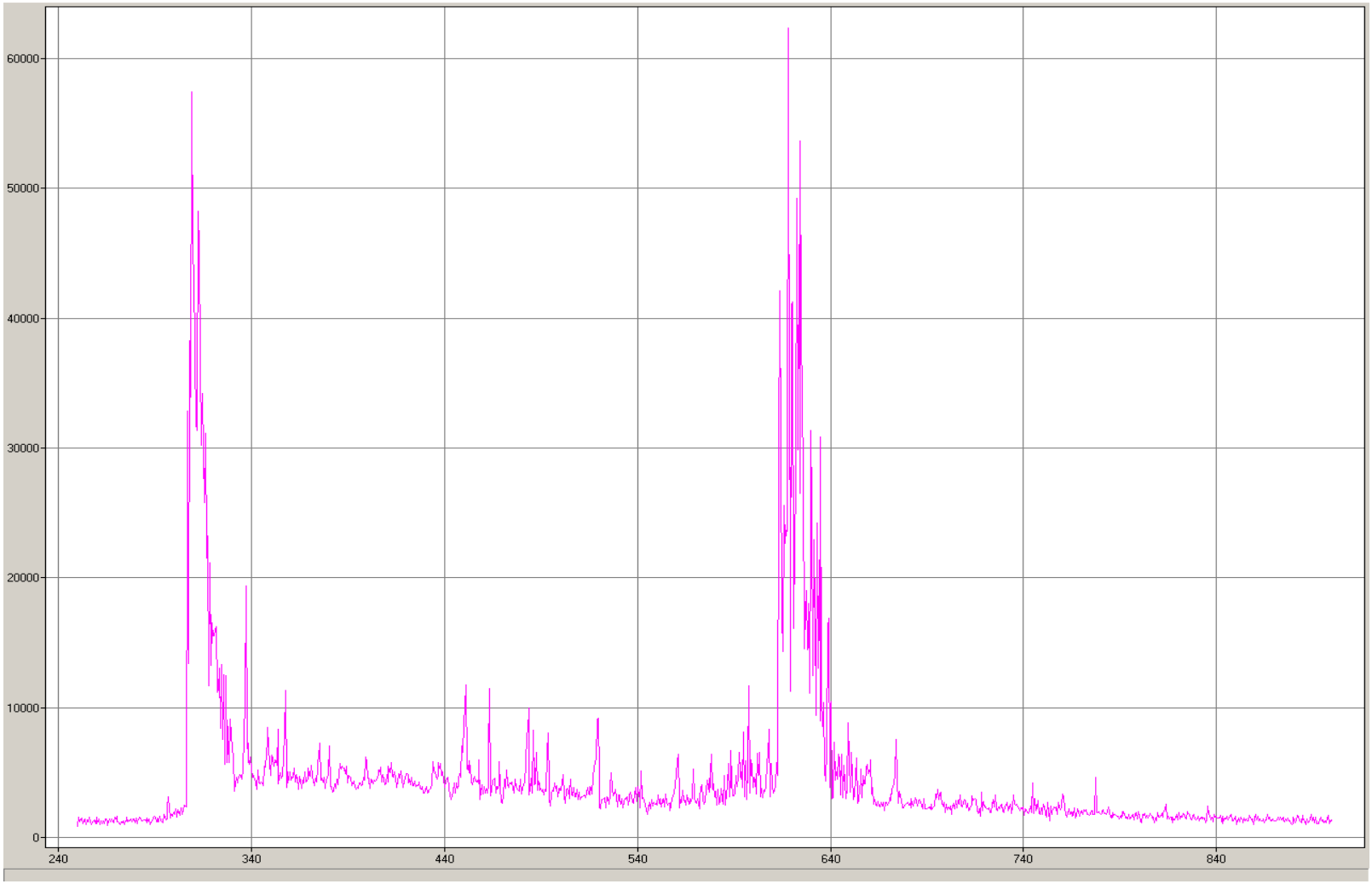

Figure B18. Process Spectrum at 100 mTorr / 500Watts (t=18 minutes).

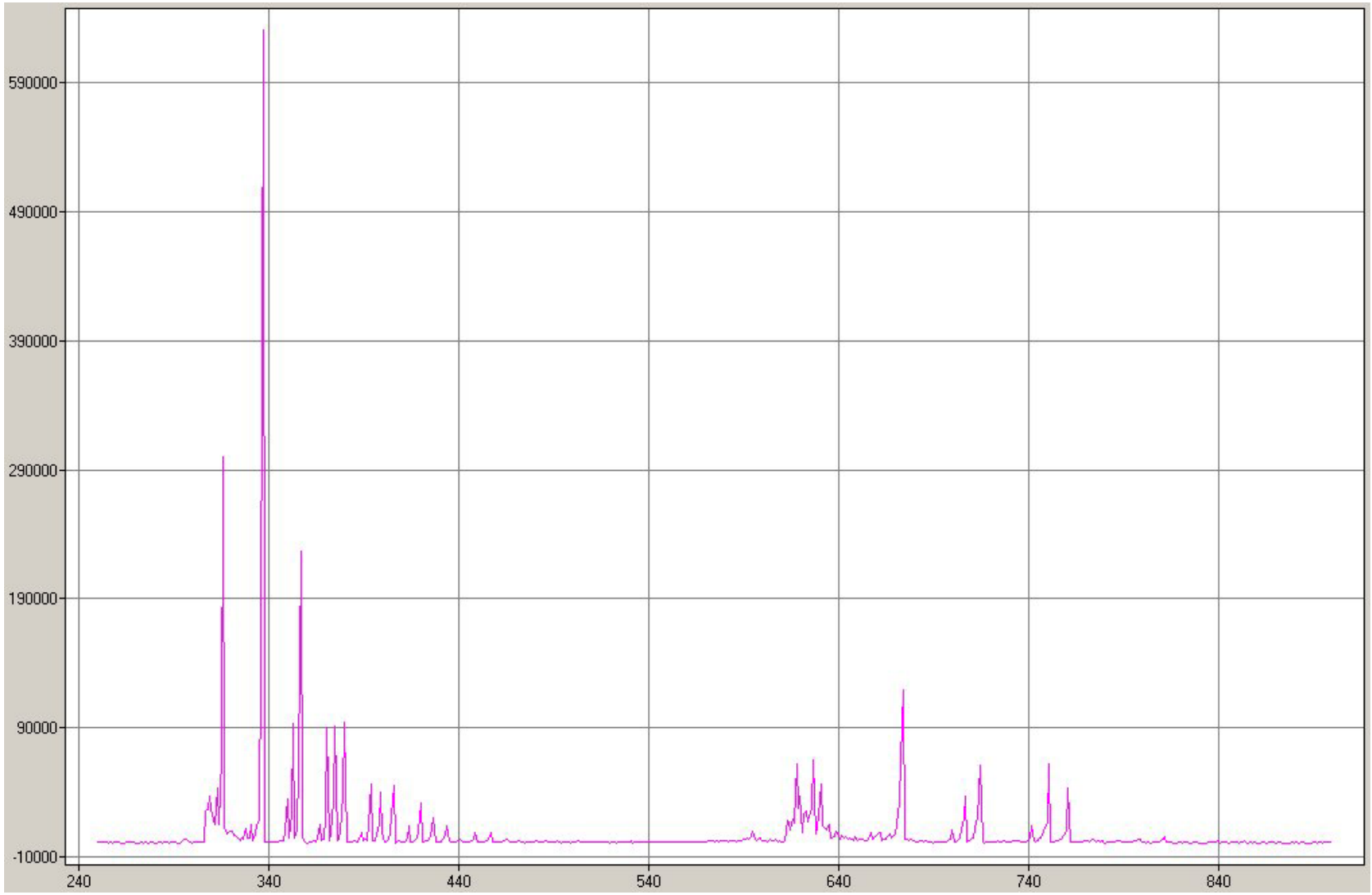

Figure B19. Process Spectrum at 2.0 Torr / 500Watts (t=3 minutes).

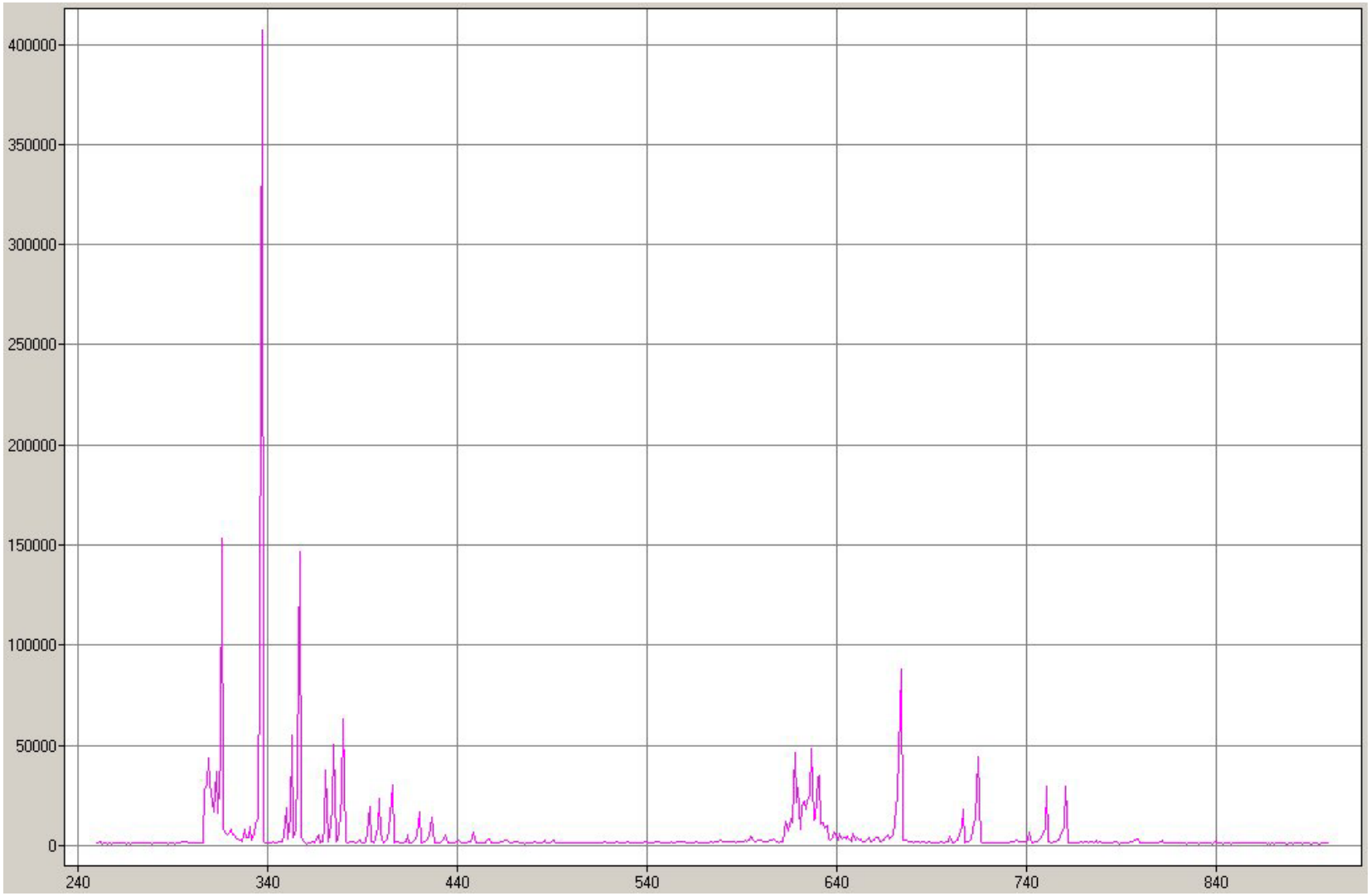

Figure B20. Process Spectrum at 2.0 Torr / 500Watts (t=6 minutes).

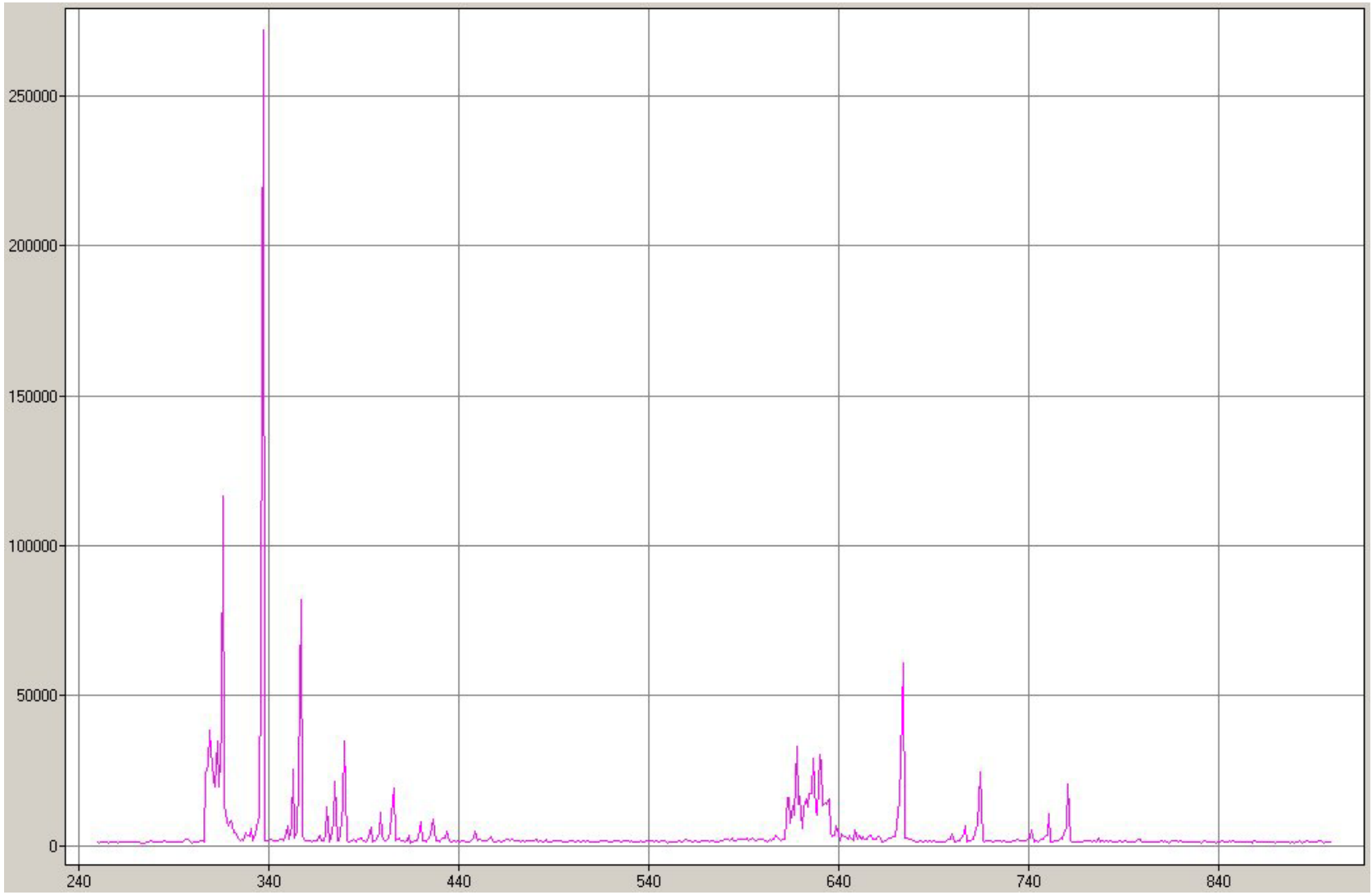

Figure B21. Process Spectrum at 2.0 Torr / 500Watts (t=9 minutes).

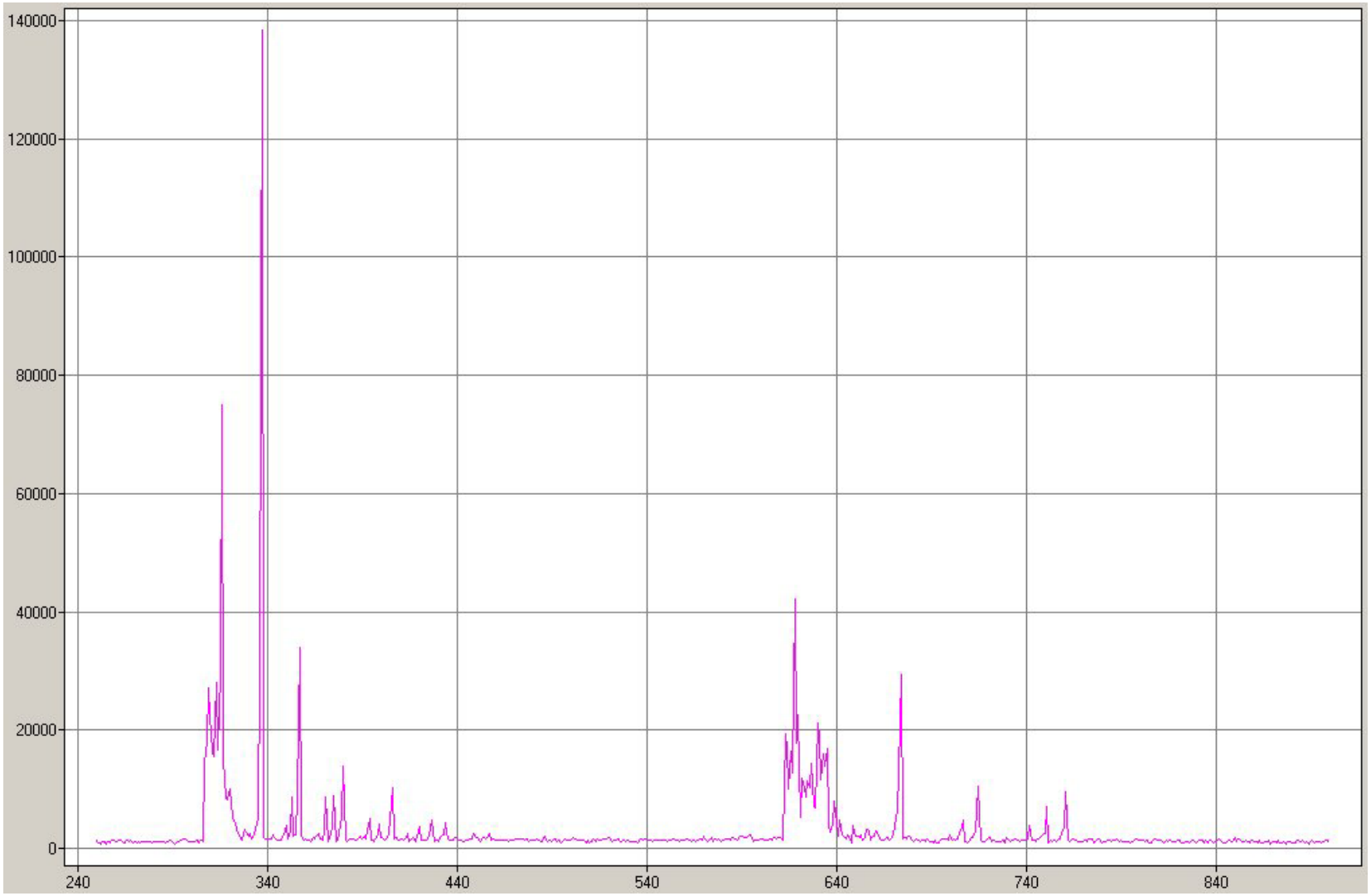

Figure B22. Process Spectrum at 2.0 Torr / 500Watts (t=12 minutes).

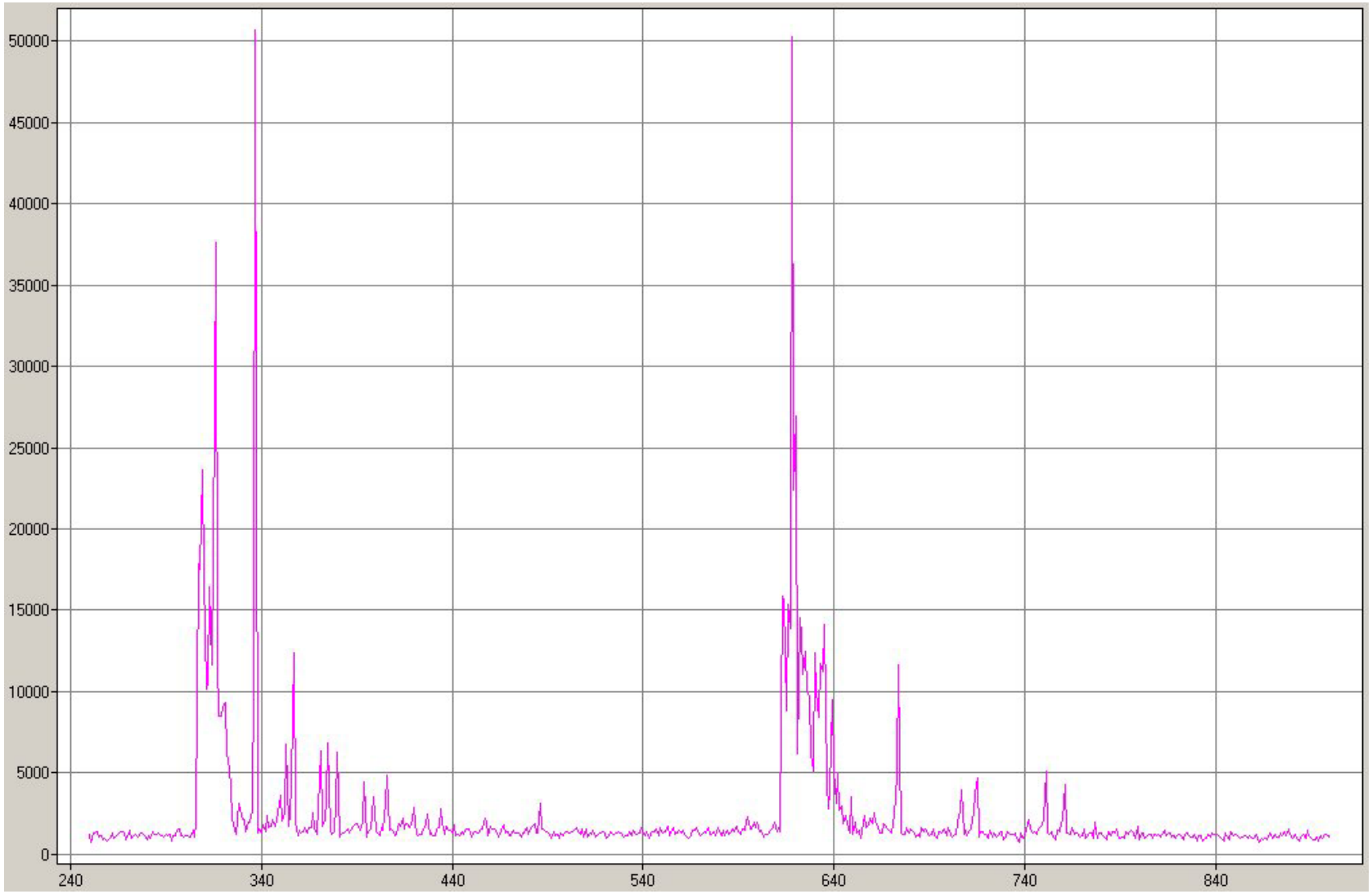

Figure B23. Process Spectrum at 2.0 Torr / 500Watts (t=15 minutes).

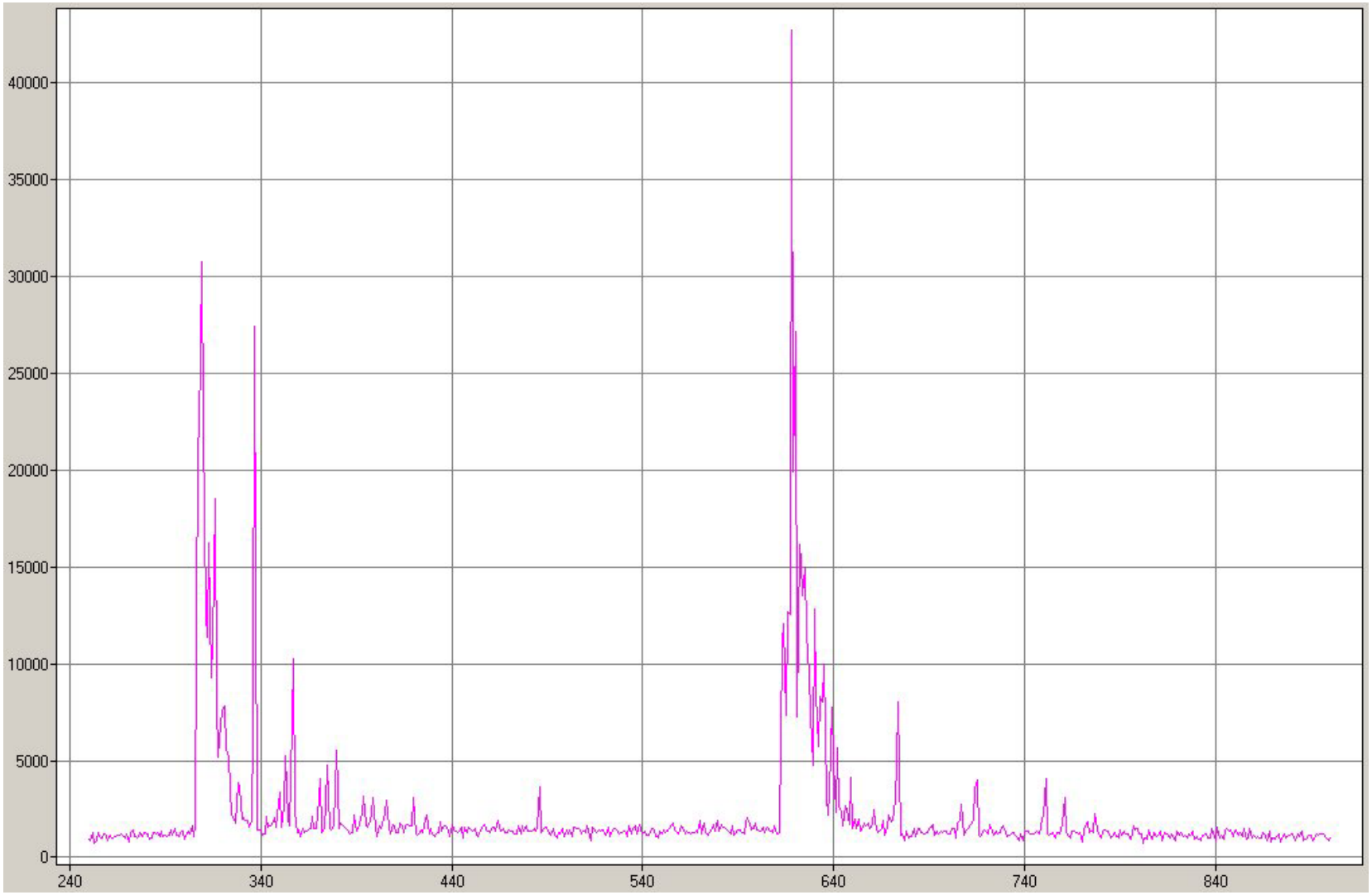

Figure B24. Process Spectrum at 2.0 Torr / 500Watts (t=18 minutes).